STUDY OF THE ORIGIN OF SALINITY IN THE UNSATURATED SOIL ZONE USING CHLORIDE PROFILES AND STABLE ISOTOPE AT EKUMFI AKWAKROM AND EKUMFI ASOKWA MANKESSIM MUNICIPALITY OF THE CENTRAL REGION OF GHANA

This thesis is submitted to the University of Ghana, Legon

BY

ISAAC APPIAH OTOO (10362238)

B.Sc. (Physics), 2008

In partial fulfilment of the Requirement for the award of

MASTER OF PHILOSOPHY

In

Nuclear Earth Science Degree

JULY, 2013

DECLARATION

This is to certify that the work presented in this thesis was carried out entirely by myself, and all assistance have been duly acknowledged. And it does not contain any material previously published or written by another person except where due reference is made in the text; and has never been presented either in part or in whole for a degree in any other University.

SIGNED…… DATE……
ISAAC APPIAH OTOO
(STUDENT)

SIGNED……... DATE……
DR. T.T. AKITI
(PRINCIPAL SUPERVISOR)

SIGNED……... DATE……
PROF. S.K.D. OSAE
(CO – SUPERVISOR)

SIGNED…… DATE……
MR. S.Y. GANYAGLO
(CO – SUPERVISOR)

DEDICATION

This research is dedicated to my cherished parents Mr J.K. Otoo and Madam Christiana Effah, and my lovely siblings: Richard, Douglas, Titus and Priscilla.

ACKNOWLEDGEMENTS

I am most grateful to the Almighty God who by His Grace and love has brought me this far in my studies.

Very special thanks go to my supervisors, Dr. Thomas, T. Akiti; Prof. Shiloh, D.K. Osae, and Mr. Samuel, Y. Ganyaglo, for their infinite patience, thorough scientific supervision, encouragement and invaluable guidance. I pray for God's blessings for you.

My special thanks also go to Prof. Yaw Serfoa – Armah, Director of Graduate School of Nuclear and Allied Sciences, God richly bless you. Prof. S.B. Dampare Deputy Director and his family, I say God richly bless you for your special contributions, encouragement and support to my education, and special appreciation to the entire staff of Department of Nuclear Science and Applications.

I will like to register my gratitude to Dr. Dennis, K. Adotey for his important contributions and ideas, as well as data interpretation advices, Dr. Dickson Adomako, Head of Chemistry Department for the opportunity to given me the use of the laboratory facility, I say God bless you.

I thank my family for their constant support and ceaseless prayers for me. I also want to show my appreciation to Mr. Kwame Gyamfi a brother and friend; and also to all the staff of Chemistry Department, National Nuclear Research Institute (NNRI), Ghana Atomic Energy Commission, most especially Ms. Cynthia Laar, Mr. Abbas Gibrilla, Mr. Courage Egbi Davidson, Mr. David Saka, Mr. Felix Aidoo and Mr. Musa Salifu.

Fundamental technical support was offered to me by: Mr. Nash Owusu Bentil, Mr. George Cis Crabbe of the Inorganic laboratory, Mr. Godfred Ayanu, Ms. Eunice Agyeman and Ms. Ruby Torto of Isotope laboratory.

I also register my appreciation to my colleagues in the Nuclear Earth Sciences Programme who helped in diverse ways: Mr. Maximillian – Robert Serlom Doku and Mr. Salam Adams Djasbaka. God richly bless you.

Finally, I would like to mention all those who supported me during this extenuating but fascinating (interior) journey: Mr. Akwasi Nyantekyi Asubonten, Mr. Emmanuel Agyei Abloh, Mr. Charles Yao Ansri, Mr. Wisdom Ayomi, Ms. Patience Nyarko, Ms. Mordling Ntriwaa Agyei and Ms. Bernice Antwi for their assistance, support and warm friendship.

I am grateful to all my friends at Graduate School of Nuclear and Allied Sciences and everyone who in one way or the other rendered support to me.

To all sundry, I say Ayekoo and I pray that may the Lord God Almighty open the windows of heaven and pour out so much blessing on you that you will not have room enough for it. I love you all.

TABLE OF CONTENTS

LIST OF TABLES

LIST OF FIGURES

ABSTRACT

This research was carried out to investigate the origin of salinity in the unsaturated soil zone with emphasis on chloride profile and stale isotopes in the Ekumfi Akwakrom and Ekumfi Asokwa in Mankessim Municipality of the Central Region of Ghana, which has been reported to have high saline groundwaters. A total of 159 samples were analysed, which comprises: fifty – six (56) rainwater samples, fifty – three (53) soil from the unsaturated zone, two (2) groundwaters, forty – two (42) water extracted from soil and six (6) water from unsaturated zone. Samples of soil, rainwater, groundwater and water from unsaturated zone were analysed for physical parameters, major ions, trace elements, nutrients and stable isotopes composition. Chloride concentrations varied as the depth increases along the profile, showing accumulation of Cl in the unsaturated zone at depth of 80 cm and 120 cm. Stable isotope of the rainwater, water extracted from soil, water from unsaturated zone and groundwater in the study area indicates that, rainfall is the only source of recharge to the groundwater in the area. The chloride mass balance (CMB) approach was used to estimate recharge rate in the flushed portion of profiles in the study area and is 65.56 mm/yr., (mean for 9 profiles), any heavy/intense rainfall can result in downward movement of salts that had accumulated near the surface of the soil. The high chloride concentration found in groundwaters in the coastal aquifers is as a result of dissolution of soluble salts ($\boldsymbol{Cl^-}$) accumulated in the unsaturated zone at a depth of 80 .0 cm and 120.0 cm and not direct sea water intrusion. Movement of water through the unsaturated zone dissolves these salts without any isotopic fractionation and discharges them into the groundwater system leading to groundwater salinization in the study area.

CHAPTER ONE

INTRODUCTION

1.1 Background

One of the most obvious phenomena of water quality degradation, particularly in arid and semi – arid zones, is salinization of groundwater and soil resources (Vengosh, 2003). Salinization is a long – term phenomenon, and during the last century many aquifers have become unsuitable for human consumption owing to high levels of salinity (high chloride content), most especially Ekumfi Akwakrom and Ekumfi Asokwa in the Mankessim Municipality of the Central Region of Ghana. Increase demand for water has created tremendous pressures on water resources that have resulted in increasing salinization of groundwater systems at Ekumfi Akwakrom and Ekumfi Asokwa. An understanding of the origin of groundwater salinity and salinization mechanisms is very important for future developments; including the design and drilling of new boreholes and hand – dug wells.

Salinity is measured by soluble salts (high chloride concentration) and high electrical conductivity in soil or water. The main sources of salt in soil and groundwater are; the primary minerals in the exposed layer of the earth's crust, direct seawater intrusion depending on the hydraulic connection between the rocks and sea, aerosol deposition from sea spray, long residence time of groundwater as the water moves from the recharge area to the discharge area, evaporative discharge, shallow water table, deposition of marine sediment, connate saline groundwater and dissolution of soluble salts in the

unsaturated zone. The released salts are transported away from their source of origin through surface or groundwater systems.

Salt concentrations in the soil and the aquifer are based on: (i) salt is a natural occurring element in soil and water; and (ii) water serves as the vehicle by which salt is transported in and out of both soil root zone and aquifer (Sharma and Prihar, 1973). Studies (Gardner and Fireman, 1958; Sharma and Prihar, 1973; Allison et al., 1983) have shown that, in arid regions when the water table is within 1 to 2 m of the soil surface, significant evaporation can occur from the soil surface and root zone which will lead to salinization of groundwater. The rise in groundwater levels may induce salinization in the unsaturated zone or accumulation of salts, through the combination of capillary rise, evaporation and transpiration. And any rise in water table heights may mobilise previously suspended unsaturated zone salts, further exacerbating the build – up of soil salts (Werner and Lockington 2004).

However, water percolation through the unsaturated zone does not leach out the entire soluble salts. The incomplete leaching of the unsaturated zone by the percolating water releases soluble salts into the groundwater during every recharge event as a result of the rise of the water table in the unsaturated zone; this process results in high groundwater chloride and electrical conductivity (Amiaz, et al, 2011). An understanding of water movement in the unsaturated zone is essential for describing movement of these salts from the surface deposition into the groundwater and for describing transport of chemical weathering products (Gazis and Xiahong, 2004).

1.2 Problem Statement

Water supply in many rural settlements in the Mankessim and its environs, including Ekumfi Akwakrom and Ekumfi Asokwa, has been based on rainwater, sources of surface water, such as streams, rivers, boreholes and hand dug wells. However, rainfall is quite erratic in the study area and also surface waters are polluted and are the source of water borne and water related diseases, such as guinea worm, bilharzia and typhoid fever.

Groundwater is generally better of quality than surface water, unless it is contaminated. However, a problem to water development in the Ekumfi Akwakrom and Ekumfi Asokwa is high salinity (i.e. high chloride concentration) in groundwater system. Especially, the quality of shallow hand – dug wells in the study area is of concern as many wells have been abandoned due to salinization as a result of high chloride content and high electrical conductivity (Armah, 2004; Ganyaglo (personal communication, 2012)). However, in these investigations, no concrete or baseline facts have being established about the origin of these salts in particularly the high chloride concentration in these boreholes and hand – dug wells, but were attributed to factors such as: direct seawater intrusion, shallow water table, and aerosol deposition in the soil.

Therefore, it has become imperative to critically examine the chemistry of the soil, water from the unsaturated zone and groundwater in evaluating the origin of this high salinity. Because, salts in groundwater become concentrated as the water with dissolved salts moves from the unsaturated zone to the saturated zone. Detailed studies on the possible effect of the unsaturated zone on the high saline content in groundwater at Ekumfi

Akwakrom and Ekumfi Asokwa areas is lacking, because studies on groundwater quality in the study area has been limited only to saturated zone and little emphasis has been placed on the study of the unsaturated zone. It behoves on this study to investigate the unsaturated soil zone to find out the possible source of the high salinity in boreholes and hand – dug wells.

Chloride distribution patterns in the soil and water from the unsaturated zone could serve as tool in understanding the origin of salinity (high chloride content) in the groundwaters in the study area, taking into consideration the various physical and chemical processes/changes occurring in the unsaturated zone profile. Geochemistry and stable isotopes compositions will be used to investigate the effect of evaporation on soil water in the study area and chloride profiles within the unsaturated zone will also be investigated to find out its variations within the profile with respect to depth.

1.3 Hypotheses

In order to determine the origin of salinity (high chloride concentration) and its contribution to groundwater salinization, chloride concentrations and stable isotope compositions would be studied along a given profile in the unsaturated zone with depth. Four (4) hypotheses will be tested to know whether:

1) the source of salinity in the study area is as a result of direct seawater intrusion.

2) the source of salinity is as a result of sea aerosol deposition.

3) the source of salinity occur as a result of ancient sea water flooding.

4) the source of salinity occur as a result of dissolution of soluble salts in the unsaturated zone.

1.4 The Objectives of the Study

The primary objective for this study is to investigate the concentration of salts in the unsaturated soil zone that is liable to groundwater salinization in the groundwater system in the study area.

The specific objectives of the study are:

- To investigate the relationship between rainfall, water from the unsaturated zone and groundwater with the use of stable isotopes.
- To investigate the recharge events in the unsaturated zone in the study area.
- To investigate the origin of salts in the unsaturated soil zone using chloride profiles and stable isotopes and their contribution to salinization.
- To investigate chloride distribution pattern along profiles in the unsaturated zone.

1.5 Significance of the Studies

Groundwater salinization is potentially of great concern, because in many semi – arid regions such as Ekumfi Akwakrom and Ekumfi Asokwa, groundwater is the only available fresh water resource. And once is contaminated, is difficult to remediate,

because of long groundwater residence times and limited options for removal of salt on a large scale. For these reasons, the quality of the groundwater needs to be sustained.

The analysis of soils and water for chloride concentration along the individual profiles together with the determination of physico – chemical, trace and major elements, stable isotopes in the profiles. Findings in this study will provide basic data for delineating the possible sources of salinity and hence for understanding the salinization processes in other areas along the coast, and also it will serve as a guide to improve water sustainability, and add to literature. This evaluation is crucial for management and future exploitation of any aquifer that are saline.

.

CHAPTER TWO

LITERATURE REVIEW

This chapter discusses some of the relevant literature from several authors of importance to the current study. The topics of discussion in this chapter include: the unsaturated zone, salinity issues; chloride, groundwater salinization, and stable isotopes as well as similar works previously done in Ghana on salinity and unsaturated zone studies.

2.1. The Unsaturated Zone (UZ)

Soils are normally defined as the biologically active layer at the surface of the earth's crust that is made up of a heterogeneous mixture of solid, liquid, and gaseous material, as well as containing diverse community of living organisms (Jury and Horton, 2004). While pores between solid grains are fully filled with water in the saturated zone, pores in the unsaturated zone are partially filled with water, with the remaining part of the pore space occupied by the gaseous phase.

Water typically enters the unsaturated zone in the form of rainfall, or by means of industrial and municipal spills. Some of the rainwater may be intercepted on the leaves of vegetation. If rainfall is larger than the infiltration capacity of the soil, water will be removed by surface runoff, or will accumulate at the soil surface until the water evaporates back to the atmosphere or infiltrates into the soil (Mallants et al., 2011), and the processes of evaporation and transpiration are often combined into the single process

of evapotranspiration. Water that is not returned to the atmosphere by evapotranspiration may percolate to the deeper unsaturated zone and eventually reach the groundwater table.

The unsaturated zone (UZ) is found to be effective in protecting groundwater from most heavy metal contaminants by adsorption onto the surface of the soils zone. Groundwater hydrologists according to Nielsen, et al., 1986 hold two traditional views of the unsaturated zone. One is that it serves as a buffer for runoff and erosion through its potential to absorb water infiltrating from rainfall. The other view is that it serves as a source of water that reaches the water table at a rate equal to the difference between infiltration and evapotranspiration. Both viewpoints generally ignore those properties of the unsaturated zone that impinges on the quality of the water, in turn has a direct influence on the retention and transmission of water in the unsaturated zone.

Most of the water which eventually recharges the groundwater must first pass through the unsaturated zone. Plants utilize water from the unsaturated zone. Capillary water may be drawn from the pores by the plant's roots until the capillary forces can no longer be exceeded. The remaining capillary water can only be displaced through evaporation. Research into the characteristics and dynamics of flow within the unsaturated zone is very active. Varieties of human activities may impact the unsaturated zone. These include agriculture, subsurface pipeline and tank emplacement, and waste disposal. The nature of the unsaturated zone and its ability to isolate the waste from human activities is a subject that needs detailed investigation.

Depth of the unsaturated zone varies greatly depending on the area one is working. In the humid area, the unsaturated zone can be few centimetres (cm) thick and disappearing when the water table is high. In the arid area, the unsaturated zone can be several hundred centimetres (cm) thick (Chapelle, 2001).

In the unsaturated zone, total potential (the gradient) and unsaturated hydraulic conductivity determine the movement of water within the unsaturated zone according to Richard's equation (Jury, 1991). And in the similar manner, as the gradient and saturated hydraulic conductivity determine the movement of water in the saturated zone according to Darcy's Law. Unlike saturated hydraulic conductivity, unsaturated hydraulic conductivity changes are nonlinear with water content. The unsaturated hydraulic conductivity of a dry material is likely to be several orders of magnitude less than that of a wet soil. If the hydraulic conductivity of unsaturated material is known or can be estimated as a function of water content or water potential, then the downward flux of water can be estimated (Nimmo, 2002).

2.2. Salinity

Salinity is the concentration of dissolved salts, high electrical conductivity in soil or water as a unit of volume or weight basis (Ghassemi et al., 1995). The major ions present in a soil solution are the anions chloride (Cl^-), sulphate (SO_4^{2-}), bicarbonate (HCO_3^-), carbonate (CO_3^{2-}) and nitrate (NO_3^-), and the cations sodium (Na^+), calcium (Ca^{2+}), magnesium (Mg^{2+}), and potassium (K^+) (Tanji, 1990). Salinity is expressed in terms of

electrical conductivity (EC), in units of milliohms per centimetre (mmhos/cm), micromhos per centimetre (µmhos/cm), or deciSiemens per meter (dS/m).

The electrical conductivity (EC) of water sample is proportional to the concentration of the dissolved ions in the sample; hence EC is a simple indicator of total salt concentration. Specific salts reported on a laboratory analysis often are expressed in terms of mg/L for water samples and mg/kg for soil/sediments; these represent mass concentration of each component in the water and soil sample.

Soluble salts most commonly present are chlorides and sulphates of sodium, calcium and magnesium. Sodium and chloride are by far the most dominant ions, particularly in highly saline soils, although calcium and magnesium are usually present in sufficient quantities to meet the nutritional needs of crops (Fipps, 2003).

In field conditions, saline soils can be recognized by the spotty growth of crops and often by the presence of white salt crusts on the surface. Increased succulence often results from salinity, particularly if the concentration of chloride ions in the soil solution is high. Plants in salt – affected soils often have the same appearance as plants growing under moisture stress (drought) conditions although the wilting of plants is far less prevalent because the osmotic potential of the soil solution usually changes gradually and plants adjust their internal salt content sufficiently to maintain turgor and avoid wilting (Szabolcs, 1994).

As water with dissolved salts moves from the more humid to the arid zones, the salts in it are concentrated and the concentration may become high enough and result in

precipitation of salts of low solubility. Apart from this precipitation, the chemical constituents of water may undergo further changes through processes of exchange, adsorption, differential mobility and the net result of these processes invariably is to increase the concentration in respect of chloride and sodium ions in the groundwater and in the soils (Walworth, 2006). Salinization problems can be more severe when the salinity of groundwater is high as in the case of arid regions.

2.2.1. Causes of salinity

There are three major types of salinity based on soil and groundwater processes, these are: (a) groundwater associated salinity, (b) transient salinity and (c) irrigation salinity (Rengasamy, 2006). Groundwater associated salinity, commonly known as dry land salinity, occurs in discharge areas of the landscape where water exits from groundwater to the soil surface bringing salts dissolved with it. In landscapes where the water table is deep and drainage is poor, salts, which are introduced by rain, weathering and Aeolian deposits, are stored within the soil profile. The concentration of salts often fluctuates with season and rainfall and salt accumulation in soil layers is a common feature in sodic soils regions. This type of salinity is termed ‘‘transient salinity’’ (Szabolcs, 1994).

Salts, derived from rainfall and soil weathering reactions, accumulate in the unsaturated zones in the soil profile. After wet season, when the water evaporates quickly, salt accumulation in the sodic subsoil layers is exacerbated. The development of transient salinity can be strong in low rainfall environments because of the low rates of leaching in sodic clays, low rainfall in dry land areas and high transpiration by vegetation and high evaporation during summer (Scanlon et al., 2007).

2.3 Chloride

The element chlorine is the most abundant of the halogens. Others in this group of elements are fluorine, bromine, and iodine. The geochemical behaviour of chlorine reflects the volatility of the element. Compounds of chlorine with common metallic elements, alkali metals, and alkaline earth metals are readily soluble in water.

Although chlorine can occur in various oxidation states ranging from $Cl^{1-}$to Cl^{7+}, the chloride (Cl^-) is the only one of major significance in water exposed to the atmosphere (Kuroda,1956) and is one of the first elements removed from minerals by weathering process as soils are formed. Most of the world's chloride (Cl^-) are either found in oceans or in salt deposits left by evaporation of old inland seas (Flowers, 1988). The Chloride (Cl^-) content of the soil is not an intrinsic property of the soil but is a result of soil management, because of its mobility in the soil and the fact that it moves with the water in the soil (Gouhua et al., 2000).

A significant fact illustrating the geochemical behaviour of Cl^- is that, more than three – fourth of the total amount present in the Earth's outer crust, atmosphere, and hydrosphere is in solution in the ocean as Cl^- ions. Chloride forms ion pairs or complex ions with some of the cations present in natural waters, but these complexes are not strong enough to be of significance in the chemistry of freshwaters. They may be of more significance in seawater and brine.

2.3.1 Sources of Chloride

Chloride is present in rock types and their concentrations are lower than any of the other major constituents of natural water. Among the chloride – bearing minerals occurring in igneous rock are the sodalite, $Na_8[Cl(AlSiO_4)_6]$, and the phosphate mineral apatite. Minerals in which chloride is an essential component are not very common, and chloride is more likely to be present as an impurity. For example, Kuroda and Sandell (1953) suggested that chloride may replace hydroxide in biotite and hornblende and may be in solid solution in glassy rocks such as obsidian. Igneous rocks cannot yield very high concentrations of chloride to normally circulating natural water. Considerably, more important sources are associated with sedimentary rocks, particularly the evaporites.

Chloride is mostly present either as sodium chloride crystals or as a solution of sodium and chloride ions (White et al., 1963). The performance of chloride in the hydrosphere can be represented by a cycle. Chloride is present in rain owing primarily to physical processes that entrain marine solutes in air at the surface of the sea. Some of the entrained chloride also reaches the land and its fresh water by dry fallout.

2.3.2. Geochemistry of Chloride

The chemical behaviour of chloride in natural water and soil is tame and subdued compared with other major ions. Kaufman and Orlob 91956) found that chloride ions moved with the water through most soils with less retardation or loss than any other tracers – including tritium that had actually been incorporated into the water molecules.

This conservative behaviour should not be expected where movement is through compacted clay or shale.

Chloride ions may retain in solution through most of the processes that tend to separate out other ions (Flowers, 1988). The differential permeability of clay and shale may be a major factor in the behaviour and composition of saline groundwater associated with fine – grained sediments. For example, chloride held back while water molecules passed through clayey layer might accumulate until high concentrations were reached (Chapman and Pratt, 1961).

Chloride profiles in unsaturated zone in semi – arid regions provide an archive of past environmental changes, including climate variability and/or land use change (Jolly et al., 1989; Walker et al., 1988; Cook et al., 1992). Results from chloride profiles have also been corroborated with data from stable isotope profiles (Sharma and Hughes, 1985; Fontes et al., 1986). Chloride profiles have been used in a variety of settings to evaluate moisture fluxes in the unsaturated zone (Allison et al., 1985; Phillips et al., 1988).

2.4 Groundwater Salinization

Groundwater salinization is a widespread phenomenon in the world which can cause health problems; decrease agriculture yields, jeopardizes livelihoods, and changes or even destroys ecosystems. Fresh groundwater stored in coastal aquifers constitutes an important water resource for rural and urban areas. Excessive extraction of groundwater in coastal settings can leads to salinization of the aquifers through encroachment of seawater. Seawater intrusion is a major environmental problem in areas where there is

over – exploitation of coastal aquifers and reduced rainfall and low recharge to coastal fresh water aquifers can lead to intrusion of seawater (Marie and Vengosh, 2001).

In certain circumstances, the unsaturated soil zone above water table may become salty damaged due to transport and concentration of saline water under capillary rise and evapotranspiration. The predominant precursor to dry land salinity and similar soil salinization phenomenon is an increase in water table elevations resulting from changes to the hydrologic cycle, namely increases in groundwater recharge (Pavelic et al., 1997).

The rise in groundwater levels may induce salinization in the unsaturated zone or an accumulation of salts on the ground surface. Any rise in water table heights, may also mobilise previously suspended soluble salts in the unsaturated zone, further exacerbating the build – up of soil salts.

Evaporative losses at the ground surface are expected to drive soil salinization (Cramer and Hobbs, 2002) and as such, an evaporative boundary condition is adopted at the upper model limit. While it is understood that transpiration losses will contribute to the process of unsaturated zone transport, surface evaporation from bare soil and evapotranspiration are assumed equivalent for the purposes of this study. Cook and Rassam (2002) also adopted this assumption in an investigation of high water table drainage.

Fresh groundwater is often young and tends to be actively recharged. In contrast, a large part of saline groundwater on earth but certainly not all of it is present in a more or less stagnant condition at greater depths and may have been there already for many thousands

or even millions of years. Continuous dissolution over geological times of the reservoirs containing this groundwater may have enriched the mineral content in the groundwater. So groundwater salinity increases with increasing depth. The contents of dissolved solids in groundwater vary highly from one location to another on earth, both in terms of specific constituents (halite, anhydrite, carbonates, gypsum, fluoride salts and sulphate salts) and regarding the concentration levels (van Weert et at., 2009).

2.5 Stable Isotope Hydrology

Oxygen and hydrogen stable isotope ratios are the ultimate tracers of the physical processes affecting water because they are properties of water molecule itself. Stable isotope data are conventionally expressed in ‰ (permil) with respect to Vienna Standard Mean Ocean Water (VSMOW) on the delta scale (Craig, 1961 and Gonfiantini, 1986). The stable isotope ratios of deuterium (^{2}H) to hydrogen (^{1}H) and of oxygen – 18 (^{18}O) to oxygen – 16 (^{16}O) of water have been used as natural tracers in many studies in order to explore hydrological processes (Mazor, 2004).

The difference in the ratio of two isotopes of the same element in species or phases A (R_A) and B (R_B) can be described by fractionation factor $\boldsymbol{\alpha}$

$$\boldsymbol{\alpha = \frac{R_A}{R_B}} \qquad \textbf{2.1}$$

Since the changes in isotopic values are generally very small, values are typically given as parts per thousand (permil ‰) deviations from a standard; e.g. for example, for ^{18}O,

$$\delta^{18}O_{sample} = \frac{(^{18}O/^{16}O)_{sample} - (^{18}O/^{16}O)_{standard}}{(^{18}O/^{16}O)_{standard}} \times 10^{3}. \qquad \textbf{2.2}$$

When the isotopic composition of two phases in equilibrium are measured, their difference can be related to the fractionation factor as

$$\delta^{18}O_A - \delta^{18}O_B \approx (\alpha - 1) \times 10^3 \qquad 2.3$$

The fractionation factor between two phases are obtained by measuring the difference in isotopic composition between the phases in equilibrium. Heavy isotopes will favour species in which the element has the stiffest bonds. Often equilibrium is not maintained between chemical species or phase and the source reservoir. In this case, the isotopic composition of the source evolves according to Rayleigh distillation, in which small increment of the species is formed in equilibrium with the source, but is immediately removed from further interaction, and does not remain in equilibrium with the changing source (Kendall and McDonnell, 1998).

Craig (1961) proposed that the relationship between ^{18}O and ^{2}H isotopes in rainfall over most of the earth's surface could be approximated by the equation 2.4

$$\delta^2 H = 8\delta^{18}O + 10 \qquad 2.4$$

The commonly – observed slope of ~8, particularly for temperate zone stations, is less than that predicted by the action of an equilibrium fractionating process during evaporation from the ocean. This indicates that, non – equilibrium (kinetic) fractionation and mixing are important factors in the development of the isotopic content of atmospheric water vapour. This is not unexpected, given the amount of atmospheric activity occurring during the creation of vapour masses (Mook et al., 2000).

The intercept value of 10 is an average figure and is related to humidity conditions above the ocean – atmosphere boundary layer in the moisture source area (Gonfiantini, 1986). By contrast, the condensation of atmospheric vapour is much more of an equilibrium process. Condensation occurs when the temperature of a particular air mass falls below its dew point, where humidity reaches 100%, as a result of adiabatic expansion and/or heat radiation. At this point raindrops form, will be enriched in the heavier isotopes of ^{18}O and ^{2}H while the remaining vapour will be depleted by an amount dictated by the mass balance of the rainfall – vapour system. In reality this tends to be a continuous process of the Rayleigh distillation type (Clark and Fritz, 1997).

The consequence is that any process resulting in temperature loss in a moist air mass leads to progressively more isotopically – depleted rainfall. This can take the form of the 'continental effect' (movement of the air mass over land), the 'altitude effect' (passage of the air mass over upland barriers) and the amount effect (Rozanski et al., 1993). For most part, $\delta^{18}O$ and $\delta^{2}H$ are highly correlated in rainfall and some variations can also occur as a result of atmospheric conditions. A useful index of this is the deuterium excess or d – value defined by Dansgaard, 1964, defined as:

$$\boldsymbol{d = \delta^{2}H - 8\delta^{18}O} \qquad \textbf{2.5}$$

The d – value is considered to be largely controlled by conditions of atmospheric humidity during the vapour forming process. For Global Meteoric Water Line (GMWL) in Eqn. (2.4), d has a value of 10 ‰ vs VSMOW. Many temperate – zone collection stations have d – values around this value, though, it sometimes fluctuates seasonally

mainly owing to changes in humidity in the moisture source area (Merlivat and Jouzel, 1979).

Stable isotope ratios of rainfall are strongly correlated with air temperature, a distinct seasonal pattern of rainfall more enriched in heavy isotopes during summer and more depleted in winter is found in humid climates. In the absence of kinetic fractionation this variability determines the atmospheric boundary condition for hydrological stable isotope studies at the plot scale (Mazor, 2004).

The propagation and attenuation of seasonal isotope signal with increasing soil depth also allows an investigation of vertical water movement in the unsaturated zone. The water isotopes in soil water fractionate only slightly in humid climates. An enrichment of heavy isotopes in the subsurface may occur in the uppermost part of the soil column due to evaporation (Windhorst et al., 2012).

2.5.1 Rainfall

Rainfall is a component of the hydrologic cycle in which water condenses and produces rains that reach the land surface. Isotopic compositions of the parent cloud and temperature at which condensation occurs determine the isotopic composition of rainfall (Barnes and Turner, 1998). The isotopic compositions of each parent cloud that generates rainfall will vary depending directly on; temperature, the distance the air mass has travelled from its source area, the change in altitude over topographic features, differences in latitude and seasonal variations (Clark and Fritz, 1997). Mostly, due to Rayleigh's processes which occurs while condensation takes place from the water vapour

source, heavier isotopes ^{2}H and ^{18}O are enriched in the liquid or solid phase and the lighter isotopes remain in the vapour phase because of mass differences which will allow heavier isotope forms to precipitate first (Araguas – Araguas et al., 2000).

As moisture is transported from higher altitude to lower altitude, more evaporation and re – evaporation processes takes place, causing more enrichment in ^{2}H and ^{18}O compositions in the lowlands and more depleted compositions in the mountains (Bowen, 1986). Isotope compositions vary with distance inland as the heavier isotope forms precipitate first, leaving the vapour enriched in the lighter isotope forms with increasing distance from the origin of the vapour source (Mazor, 2004). Evaporation also occurs with seasonal changes, as rainfall is more susceptible to fractionation processes with the increase in temperature during summer than winter (Barnes and Turner, 1998). These isotope composition variations give an input signal characterized by Local Meteoric Water Lines (LMWL) particular to each region, thus permitting the tracing of recharge sources (Mook, 2000).

2.5.2 Evaporation from the Soil

Evaporation from soils and to a lesser extent from shallow water table has been recognised as an important component of the water balance. Excessive water table evaporation leads to salinization of soils because of the salts left behind, lowering their usefulness. Evaporation can only occur where a vapour pressure gradient is maintained between the evaporating surface and the overlying atmopshere (Mazor, 1991). This needs energy to convert water into vapour. This energy is provided by the evaporating water

and indirectly from solar radiation and heat from the atmosphere (Mook, 2000) and is often limited by the availability of water. For a well – watered vegetated surface or a wet soil, evaporation is normally close to an open water surface and is indicated as potential evapotranspiration (Barnes and Allison 1988).

Salt accumulations in soils can be attributed to evaporation of aqueous solutions, transported upward from the water table through the capillary fringe to an evaporation front that is a few centimetres below the ground surface. Salts in the sediment of shallow depths are depleted in chloride and enriched in carbonate relative to deeper samples. Surficial sediments exposed on the margins of saline lakes, and other arid and semi – arid settings accumulate salts through evaporation of shallow groundwater (Salama et al. 1999; Reynolds et al. 2007).

Several studies have examined the processes responsible for salinization of soil as a result of transport of water and dissolved salts through the capillary fringe to an evaporative surface (Qayyum and Kemper 1962; Hassan and Ghaibeh 1977; Shimojima et al. 1996; Rose et al. 2005). White, efflorescent salts coating sediment surfaces in semi – arid settings are a visible reminder of these processes (Breit et al., 2009). Evaporative concentration also occurs in the subsurface at depth of transition from liquid water to vapour – dominated transport the zone of evaporation front (Rose et al., 2005).

Salinization of soil is a major problem in semi – arid areas with shallow water table, which is influenced by climate, soil type, crop; and management practice, depth of water table and salinity of water table. Shallow water table conditions are quite extensive in

arid and semi – arid (Jalili et al., 2011). Young et al., (2007) reported that the upward flux is limited by the atmospheric evaporative potential when the water table is shallow. Gardner (1958) also described the contribution of the vapour phase to overall evaporation and concluded that subsurface vapour movement would seldom exceed 20 % of maximum liquid transport and would usually be much less. Jalili et al., 2011 reinforced this conclusion by finding that liquid water movement deeper in the soil limits total evaporation on daily or greater time scales (Saravanapavan and Salvucci, 2000).

2.5.3 Salinization of soil due to evaporation effect

Soil salinization is the first stage of environmental destruction caused by salinity (high chloride content). The accumulation of soluble salts in soil occurs when evaporation exceeds rainfall, and salts are not leached but remained in the upper soil layers in low – lying areas. Natural soil salinization, called primary salinization, occurs in arid and semi – arid climatic zones and secondary salinization is the term used to describe soil salinized as a consequence of direct human activities (Fitzpatrick et al., 2000). Salinization of soil can also results from combination of evaporation, salt rainfall and dissolution, salt transport, and ion exchange (Jalili et al., 2011).

Excessive salinity in soil leads to toxicity in crops, reduction in soil fertility, and reduction of availability of water to plants by reducing the osmostic potential of the soil solution and significant change in the hydraulic properties of soil (Hillel, 1982). In shallow groundwater conditions, water and dissolved salts move by capillary action to the

soil surface from the water table and when the water evaporates at the surface, the salts are left behind.

The source of salt in salinized environment can be derived from (i) mixing of meteoric water with saline water such as seawater, connate fluids, and hydrothermal waters trapped within or outside the aquifer; (ii) dissolution of evaporites left behind after the last seawater or brine retreat; (iii) weathering of the aquifer minerals; (iv) accumulation of salts derived from long term deposition of atmospheric fallout; (v) sewage (domestic or industrial) contamination; and (vi) salinization by agricultural return flows. Each of these sources has a unique and distinctive chemical and isotopic composition.

The integration of geochemical and isotopic tracers can be used to resolve multiple sources. The application of hydrogen and oxygen stable isotopes to the study of soil moisture evaporation dates back to the 1960s. Zimmermann et al., (1967) were the first to describe deuterium isotope concentration in the saturated uniform sandy soil water on the condition that, soil evaporation in steady state has a constant temperature. They showed that, the maximum deuterium isotope concentration occurs near the ground surface and decreases exponentially with increasing soil depth.

Moreover, Barnes and Allison (1983) also studied the motion model between hydrogen and oxygen stable isotopes in evaporation of unsaturated soil under steady – state conditions and constant temperature. They found that, the hydrogen and oxygen stable isotopes concentration increased with soil depth until at the evaporation front and then decreased exponentially, being similar to the above hydrogen and oxygen stable isotopic

profile line, and that isotopic depletion might appear below the evaporation front under steady – state conditions and in constant temperature. However, in the field, the soil evaporation is not steady – state in most cases (YongQin et al, 2011).

In unsaturated zone, soils are either evaporating under steady state conditions with the water table at depth, or evaporating under non – steady state conditions, water vapour is lost from a region known as the evaporating front which is well defined in light textured soils but may be more diffused in soils of higher clay content (Allison, 1998). Beneath the evaporating front, water and isotope movement is mainly in the liquid phase, while above it, vapour transport dominates. For this reason, the stable isotope profile, beneath the evaporating front, at least, is under isothermal conditions (Allison, 1998).

The integration of geochemical and isotopic tracers can be used to help resolve these multiple sources. The use of the stable isotopes of oxygen and hydrogen for tracing the origin of salinity is straightforward in the case of river salinization, but it is more problematic in groundwater studies. In many cases, the original $\delta^{18}O$ and $\delta^{2}H$ values of the saline sources are completely modified by mixing (dilution) with meteoric water (Jalili et al., 2011).

2.5.4 Water Quality

Water quality, as described by Appelo et al., (1993) is its suitability for human consumption, domestic use and irrigation. Groundwater system in any area varies in chemistry mainly due to chemical alteration of the host environment of the meteoric

water recharging the aquifer system (Hem, 1989). The quality of groundwater is very crucial for the sustainability of life. Groundwater quality depends on its physical, chemical, and biological qualities. A number of factors influence water quality and according to Gibbs (1970), the possible factors that control water chemistry are weathering of rocks, atmospheric precipitation, evaporation and crystallization.

The influence of soils on water quality is very complex and can be attributed to the processes controlling the exchange of chemicals between the soil and water. The chemical quality of groundwater depends on the characteristics of the soil and rock media through which it passes en route to the groundwater zone of saturation (Foster et al., 2000). It is also dependent on the length of time the water is stored in the ground (residence time).

2.6 Previous Works on Salinity and Unsaturated Zone in Ghana

Armah (2004) used geophysical techniques, hydrochemistry and stable isotope composition of water to determine the source of high salinity in the groundwaters along the coastal areas by studying the saturated zone. He established that the electrical conductivity of the groundwaters are > 5000 µS/cm. His findings could not, however, establish the overriding processes that account for the saline waters in the coastal aquifers. Ganyaglo (personal comm. 2012), also found electrical conductivity to be between 423 µS/cm and17000 µS/cm and the Cl concentration to be between 949.99

mg/L and 4798.5 mg/L in the boreholes in these communities. These works by the two researchers were limited only to the saturated zone.

In Ghana, the studies on unsaturated zone by Alfa (2008) on the impact of the unsaturated zone heterogeneity and land use/cover on groundwater recharges in the Densu Basin have been one of the first few works to be carried out on the unsaturated zone. This was followed by Bam et al., (2011) also carried out research on the investigation of the vertical distribution of some major and trace elements in the soil and water from the unsaturated zone in the Densu Basin. They concluded that, the vertical profile of the unsaturated zone solution chemistry of the Densu river basin has some direct impact on the groundwater chemistry and this were controlled by the weathering of silicate bearing minerals. Courage (2011) also carried out an investigation on the leachate migration in unsaturated zone and concluded that leachate produced by waste disposal sites contains substances which are likely to contaminate groundwater in such areas and the impact of contaminants from such sites on groundwater can be quantified by monitoring the concentration of potential contaminants and soil properties at specific points in the unsaturated zone. Extensively over the years, more works has been done in the unsaturated zone, however, no report or literature exists on the origin of salinity in the unsaturated soil zone.

CHAPTER THREE

MATERIALS AND METHOD

This chapter describes the location of the study area, the geology of the area and discusses methods of sample collection and the methods used for sample analyses.

3.1.1 Location and Description of Study Area

The study area is Ekumfi Akwakrom and Ekumfi Asokwa; both located in the Mankessim municipality at the Mfantsiman West of the Central Region of Ghana and are located between latitudes 05°15''45.108 N and 05°15''40.248 N and longitudes 0°58''46.488 W and 0°58''59.880 W, as shown in Fig 3.1.

The study areas are in typical farming communities and are bounded at the northern part about 2 km from the main Accra to Cape Coast highway and at the southern is about 6 km from the Gulf of Guinea.

The study area was chosen because of high electrical conductivity > 4000 µS/m and chloride concentration (~ 17000 mg/L) found in the hand dug wells in the communities (Ganyaglo, personal communication, 2012).

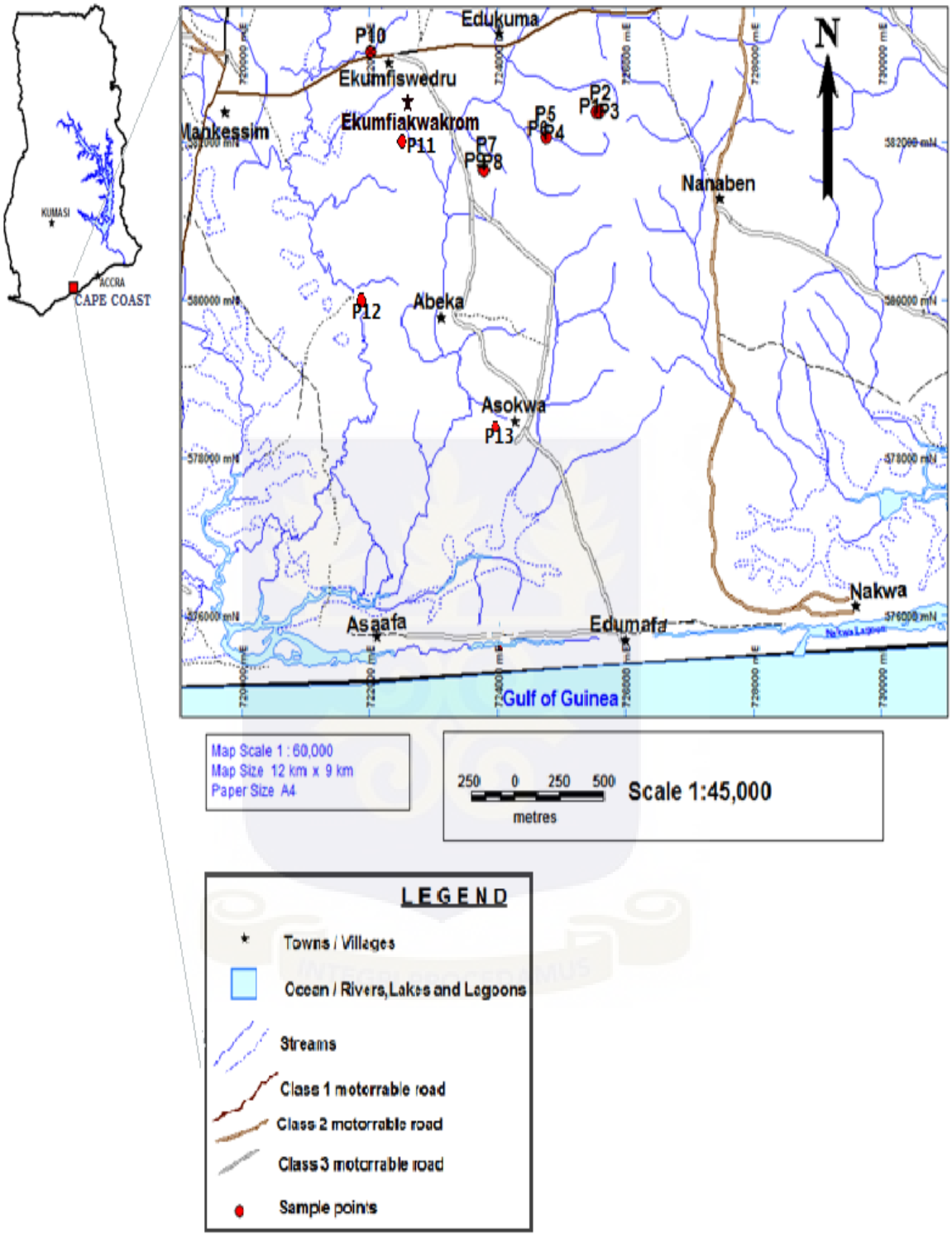

Fig. 3.1: Map Ghana showing the study area and sampling points

3.1.1 Climate

The climate of Ekumfi Akwakrom and Ekumfi Asokwa falls mainly within the Wet Semi-equatorial climate. This climate has two rainfall maxima; however, the mean annual rainfall is between about 74 cm and 89 cm. The first rainy season is from March to June, with the heaviest rainfall in June. The second rainy season is from September to October (Benneh and Dickson, 2004). Temperatures are almost the same as in the south-west equatorial region (26 ^{o}C in August and 30 ^{o}C between March and April). Monthly relative humidity is higher in the rainy seasons than during the rest of the year. The highest average monthly humidity does not exceed 75 % and the lowest is about 60 % (Benneh and Dickson, 2004). The annual temperature of the study area ranges between 24.1°C in June and 27.4°C in August. February and March are normally the hottest months while mean daily temperature is lowest between December and January. Mean relative humidity is high within a twenty – four hour period with lowest relative humidity in January and highest in August (Benneh et al., 1990).

3.1.2 Relief and Drainage

Ekumfi Akwakrom and Ekumfi Asokwa has a low relief with an average height of less than 35 m above sea level and a gently plain with the highest point being less than 86.9 m above sea level (Benneh and Dickson, 2004). The study area is within the coastal plain. The land is not flat but rather undulating. Various types of rock are found here, but the most widespread are the cape coast granites which also form most of the hills. The drainage system in the area is fairly dense and belongs to the Nakwa river basin, which eventually joins the Gulf of Guinean (Dickson and Benneh, 1985).

3.1.3 Vegetation

The study area is found in the Coastal scrub and grassland vegetation. Reports from early European visitors to the coast indicate that the area used to carry a luxuriant vegetation- probably a drier and more open variety of the moist semi-deciduous forest. The original vegetation has been greatly modified by man in the last three centuries or so. Today, it consists of dense scrub without grass (Benneh and Dickson, 2004). Two vegetative zones (the Guinea Savannah and Moist semi-deciduous forest) occur in the area.

The dominant vegetative zones in the district and study area are shrubs and grasslands.

3.1.4 Geology of the study area

The study area occurs within Paleoproterozoic terrain which forms one of the four litho – stratigraphic complexes of Ghana as shown in Fig 3.2. The Paleoproterozoic terrain of Ghana is made up of the Birimian Supergroup, Tarkwaian Group, Plutonic Suite and the Eburnean Suite. The terrain is believed to have occurred between 2195 Ma and 2072 Ma (Kesse, 1985). This is made up of metavolcanics and metasediments intruded by granitoids during the later stages of Eburnean orogeny at or after the end of Bririmian deposition which is somehow older than 2000 Ma of age (Taylor et al., 1992).

A major part of the Paleoproterozoic terrain of Ghana is underlain by Supercrustal and intrusive rocks of the Birimian Supergroup displacing a characteristic pattern of north – eastern trending, parallel, approximately evenly – spaced ‘volcanic belts’ and intervening ‘sedimentary basins’ called the Volcano – Plutonic Group and the Sedimentary – Volcano – Sedimentary Group, respectively.

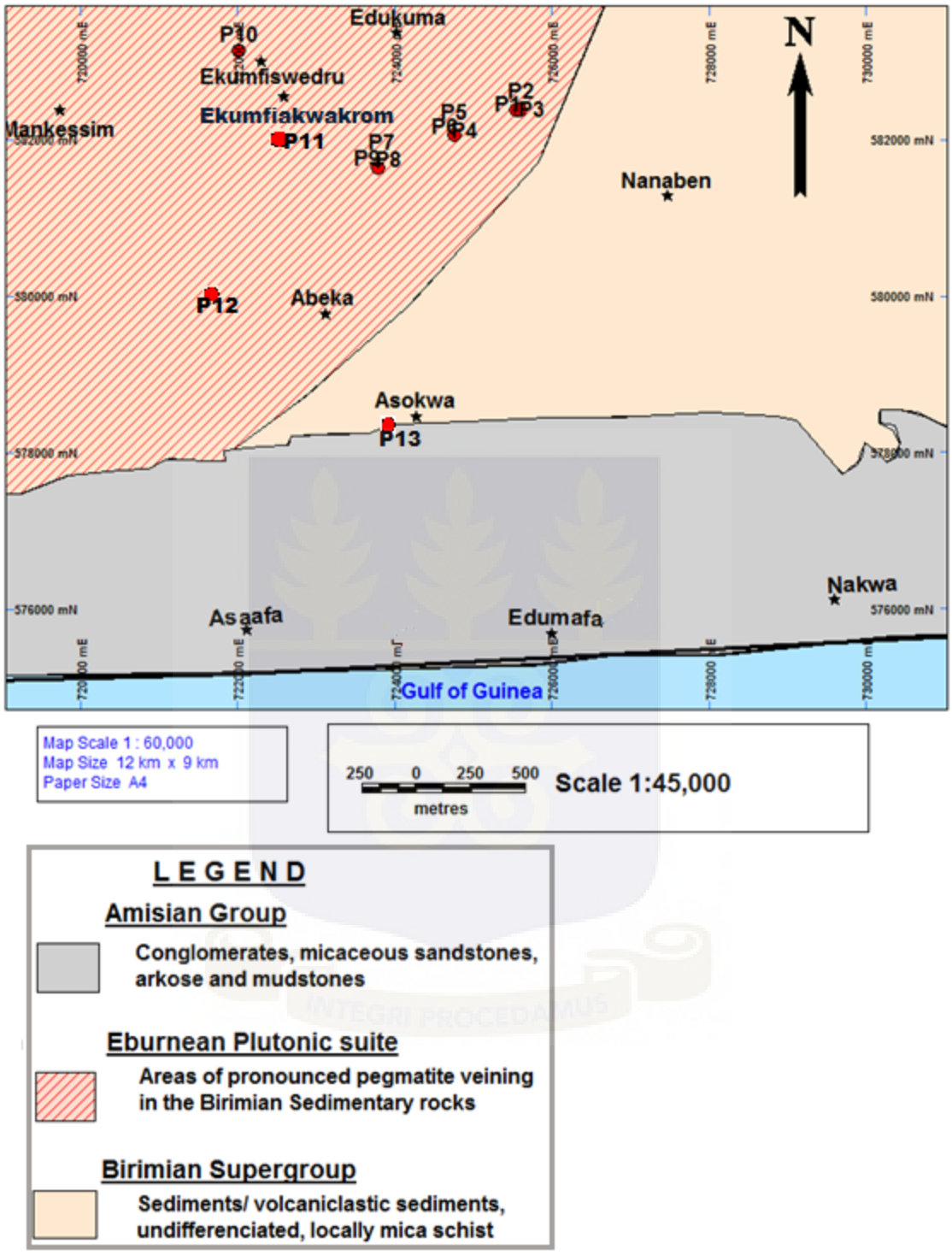

Fig 3.2: Geological map of the study area showing the major types of rock

Rocks of the former are lithologically and genetically diverse. However, most 'volcanic belts' are dominantly made – up of low – grade metamorphic tholeiitic basalts with intercalated volcanicastics as well as minor andersitic and felsic flow rocks and locally chemical sediments (Kesse, 1985).

Starting between 2120 Ma and 2115 Ma, the extensional tectonic regime was followed by (probably slightly diachronous) crustal shortening and associated regional metamorphism, defining the Eburnean tectono – thermal event, which folded and metamorphosed the previously formed Paleoproterozoic rocks and is responsible for, inter alia, the formation of high – strain zones at the Birimian belt/basin boundaries (Kesse, 1985). Preferentially, the Birimian basins and locally some Birimian volcano – plutonic belts were intruded by extensive, syn and late – kinematic, frequently peraluminous granitoids intruded of the Eburnean Plutonic Suite, which display crystallization ages between 2116 Ma and 2088 Ma and probably originated from partial melting of only slightly older Birimian basin sediments. Isotopic evidence for a contribution of significantly older continental (Archean) crust to these Eburnean plutons is minimal and is restricted to the Winneba type granitoids plutons, which occur locally in South – Eastern Ghana. The latest manifestation of Eburnean plutonism is pegmatitic veining with an age of 2072 Ma (Geological Survey Department. 2009).

The Birimian formation is greatly intruded by large masses of granites and basic intrusive of uncertain age. They are two types, Cape Coast and Winneba granites and Dixcove granites. The Cape Coast and Winneba types are often well foliated, as well as magmatic

and are potassium – rich, which come in the form of muscovite – biotite granite and granodiorites, porphyroclastic biotite gneiss, aplites and pegmatites (Kesse, 1985).

The Cape Coast granites complex generally comprised of granite – magmatic complex known as G1 granitoids and believes to be formed from the reworking of the Archean basement and emplaced synchronously with early Proterozoic folding (Kesse, 1985). These are well foliated often magmatic, potash – rich granitoids which are in the form of muscovite biotite granite and granodiorites, porphyroblastic biotite gneiss, aplites and pegmatites. Granitoids are characterized by the presence of many enclaves of schist's and gneisses, which are generally associated with Birimian metasediments and their internal structures, are always concordant with those of their host rocks (Taylor et al., 1992).

3.2. Sampling

3.2.1 Sampling Containers

All polyethylene containers (bottles) with the exception of containers for stable isotopes were immersed for at least 48 hours in a 10 % (v/v) HNO_3 solution and thoroughly rinsed with double – distilled water before use.

3.2.2. Field work

3.2.2.1 Collection of water samples

Three different types of water samples were collected (rainwater, groundwater, and water from the unsaturated soil zone), for analysis of physico – chemical parameters, trace elements, major ions and nutrients.

3.2.2.2 Collection of Rainwater

Fifty – six (56) rain water samples were collected from rain gauges sited at Saltpond Meteorological Station, for chloride and stable isotopes analysis.

3.2.2.3 Collection of Groundwater

The Global Positioning System (GPS) reading for the sampling points was taken and recorded together with the date of sampling in the field before collection of the samples. All the groundwater samples were collected in pre – conditioned polyethylene bottles (250 mL). At the sampling sites, prior to the collection of the water samples, the boreholes were pumped out for about twenty (20) minutes if it had not been pumped for the day to make sure that water is sampled directly from the aquifer. The sampling bottles were rinsed three (3) times with the water to be sampled, followed by filling the bottle with water to the brim (Donkor et al., 2006; Serfor – Armah et al., 2004).

At each sampling point, three (3) water samples were taken; for the determination of trace metals, major ions and stable isotopes analysis. The sample for trace metal was acidified with two (2) drops of 1 % HNO_3 just after the collection of the water sample, this prevent the adsorption of the metals to the walls of the container.

The water samples were stored in thermo – insulated container with ice packs. However, samples for stable isotope analysis were also stored in a thermo – insulated container without ice to prevent condensation of the lighter isotopes. The samples were transported to the laboratory at the Ghana Atomic Energy Commission (GAEC) for analysis.

3.2.2.4 Collection of water from the Unsaturated Zone

Water from the unsaturated zone collection was done by first drilling of boreholes, followed by installation of piezometers and subsequently followed by sampling of water from the unsaturated zone. The detailed procedures (drilling to collection) are as follows:

3.2.2.4.1 Drilling of Profiles

A hand auger was used in the profiling. In all nine (9) profiles were done and they were all installed with piezometers. Soil samples (about 500 g) were taken at every 20 cm intervals to the maximum depth depending on the geological conditions. The soil samples were placed in hermetically – closed polyethylene bags which were immediately zipped up at the mouth, well labelled well labelled and kept in a thermo – insulated container, for the determination of physical parameters, trace element, major ions, nutrients and isotopes studies in the study areas. Soil identification and classification were carried out on the undisturbed cores in the field with the help of a hydrogeologist. In all, 53 soil samples were collected and the samples were transported to the laboratory for analyses.

3.2.2.4.2 Installations of piezometers

Slots of two inches (2'') P.V.C pipes with end caps (piezometers) were inserted into the drills and installed as shown in Fig. 3.3 as wells for sampling for physical, hydrochemical and isotopic analyses to determine the mechanism and extent of solute transport in the soil. Screens were made on the piezometers at the lower part to allow percolation of

water but the cuts were small enough to exclude significant intake of soil (Izbicki et al., 2000).

Fig. 3.3 Installed piezometers in the study area

3.2.2.4.3 Collection of water from unsaturated zone

Water from the unsaturated zone (piezometers) was pumped dry to purge it of stagnant water and to obtain fresh water samples for analysis. This was done using a peristaltic pump 12 V DC with tube specification of min.2.0 and max.2.2. At each sampling site, the polyethylene sampling bottles were rinsed at least three times with the sample before sampling was done.

The samples were taken in triplicate for major ions, trace elements and stable isotopes. Samples for trace element analysis were preserved with three drops of nitric acid at a pH of 4. Samples for stable isotopes analysis were neither acidified nor filtered but were

directly filled in 50 mL pre – conditioned bottles to the brim and tightly capped to prevent evaporation.

Each sample was well coded and labelled with information on sample identification number, date and time of sampling. Samples for anions and cations were ice – packed in order to, as much as possible, preserve them in their natural state; but samples for stable isotopes were not put in ice and the samples are transported to the Ghana Atomic Energy Commission laboratories for preparations and analyses.

3.2.2.5 Measurement of Physico - Chemical parameters of groundwater and water from unsaturated zone in the field

3.2.2.5.1 Conductivity, Salinity and Total Dissolved Solids (TDS)

Conductivity, TDS and salinity were measured in the field using a multi – function HACH Sension 5 conductivity meter. The conductivity meter was first calibrated using the following standard solutions; 0.01 M KCl (Conductivity: 1413 μScm^{-1}) and 0.1 M KCl (Conductivity: 12880 μScm^{-1}).

This was followed by simultaneous measurement of the conductivity, TDS and salinity of the water samples.

3.2.2.5.2 pH and Redox potential (Eh)

Measurement of pH, Eh and temperature were measured on the field just after sample collection, using the multi – function HACH Sension 5 pH meter.

For pH measurements, the pH meter was calibrated using standard buffer solutions at pH of 4.01, 7.0 and 9.21, respectively. After calibration, the pH of the water samples collected was measured. The calibration of the pH meter was verified after measurement of two water samples.

The Eh was determined using the assigned programme on the pH meter.

After each reading, the electrode was rinsed with double distilled water and small portion of the next sample to be determined.

3.2.2.6. Determination of alkalinity and bicarbonate of water samples using the potentiometric method

The alkalinity of the water samples (groundwater and unsaturated zone) was determined in the field.

Twenty five (25 mL) aliquot of the water sample was measured with a measuring cylinder and transferred into 250 mL conical flask and titrated against 0.02 M HCl solution using phenolphthalein and methyl orange as indicator till the colour changes from yellow to pale yellow colour signifying the end point. Three replicate titrations were done and the mean (titre) value calculated. The volume of water sample, HCl (average titre) and the molarity of the acid were used to compute the alkalinity using the following equation

$$\boldsymbol{Alkalinity}\left(\boldsymbol{mg}\frac{\boldsymbol{CaCO_3}}{\boldsymbol{L}}\right)=\frac{\boldsymbol{A\times M\times 50000}}{\boldsymbol{Volume\ (V) of\ sample}} \qquad \textbf{3.1}$$

where A is the averaged titre value in mL and M is the molarity of the acid (HCl solution).

The bicarbonate concentration was calculated using equation 3.9

$$[HCO_3^-] = (1.2191817) \times Alkalinity \qquad 3.2$$

3.3. Laboratory Work and Analysis

Analysis of samples includes; determination of physico – chemical parameters, determination of major ions, trace elements, nutrients and extraction of water from soils for stable isotope composition analysis were conducted as follows:

3.3.1. Measurement Electrical Conductivity (EC), Total Dissolve Solids, salinity, pH, Eh and Temperature of soil samples

3.3.1.1 Conductivity, Total Dissolved Solids (TDS) and Salinity for soil samples

3.3.1.2 Calibrations

Conductivity, TDS and salinity were also measured in the laboratory for soil using a multi – function HACH Sension 5 conductivity meter which measures conductivity, salinity and TDS simultaneously. The conductivity meter was first calibrated using the following standard solutions; 0.01 M KCl (Conductivity: 1413 μScm^{-1}) and 0.1 M KCl (Conductivity: 12880 μScm^{-1}).

3.3.1.3 Soil samples

Eighty (80) g of the soil samples was placed in a 300 mL titration flask with 160 mL and leached distilled water in a ratio of 1:2. The flask and its contents were shaken for 10

minutes (IAEA, 2009). Then the supernatant liquid was poured into 250 mL polyethylene plastic containers which have been preconditioned and the conductivity, TDS and salinity, were measured using HACH Sension 5 conductivity meter. The measure of total dissolved solids (TDS) is a good indicator of the mineralised character of the water.

This was followed by measurement of the conductivity, salinity and TDS of the soil samples.

After each reading, the electrode was rinsed with double distilled water and small portion of the next sample to be determined.

3.3.1.4. pH, Eh and Temperature

3.3.1.5. Calibrations and measurement

For measurements, the pH meter was calibrated using standard buffer solutions at pH of 4.01, 7.0 and 9.21, respectively.

Eighty (80) g of the soil samples was placed in a 300 mL titration flask with 160 ml of distilled water in a ratio of 1:2. The flask and its contents were shaken for 10 minutes (IAEA, 2009). Then the supernatant liquid was poured into 250 mL polyethylene plastic containers which have been preconditioned and the pH, Eh and temperature were measured using the HACH Sension 5 pH meter.

After each reading, the electrode was rinsed with double distilled water and small portion of the next sample to be determined.

3.3.2. Determination of alkalinity and bicarbonate of leached soil

Alkalinity was determined by two methods namely the potentiometric and the methyl orange indicator method. The choice of the method is depended on the pH of the water sample. The methyl orange indicator method was used for samples of pH < 4.5 and for pH > 4.5 the potentiometric method was used.

3.3.2.1 Soil samples

Twenty – five (25) mL aliquot of the leached filtered water sample was measured with a measuring cylinder and transferred into 250 mL conical flask and titrated against 0.02 M HCl solution till a pH of 4.5. Three replicate titrations were done and the mean (titre) value calculated. The volume of water sample, HCl (average titre) and the molarity of the acid were used to compute the alkalinity using the following equation

$$\boldsymbol{Alkalinity}\left(\boldsymbol{mg}\frac{\boldsymbol{CaCO_3}}{\boldsymbol{L}}\right)=\frac{\boldsymbol{A\times M\times 50000}}{\boldsymbol{Volume\ (V) of\ sample}} \qquad \textbf{3.3}$$

where A is the averaged titre value in mL and M is the molarity of the acid (HCl solution).

The bicarbonate concentration was calculated using equation 3.9

$$[\boldsymbol{HCO_3^-}]=(\mathbf{1.2191817})\times\boldsymbol{Alkalinity} \qquad \textbf{3.4}$$

3.3.3. Determination of soil water content

The standard method of soil water content measurement involves taking a physical sample of the soil, weighing it before any water is lost, and drying it in an oven and

reweighed again. The mass of water lost on drying is a direct measure of the soil water content. This measure is normalized either by dividing by the oven – dry mass of the soil sample, in which case the units are (g g^{-1}), or by converting the mass of water to a volume thus by dividing the mass of water by the density of water and dividing this volume of water by the volume of the sample, in which case the units are (m^3 m^{-3}) (IAEA, 2008).

The measurement of water content is by measuring the mass of water (M_w, g) lost on drying in a convective oven at a specified temperature (usually 105ºC) until mass remains constant which is usually 24 h or longer. Samples containing more than a few percent organic matter may lose mass due to volatilization of organic matter at temperatures higher than 50 ºC.

Gravimetric – moisture content was determined for this study by drying at least 80 g of soil at 105 °C for 48 hr. Three independent weights were taken namely; weight of wet samples (M_w), weight of empty aluminium cans (Mc) and weight of oven dry soil (M_d). The water content was then obtained by dividing the differences of the masses of the wet and dry soils by the mass of the dry soil sample. The percentage water content was obtained by multiplying the ratio by 100. This gives the gravimetric water content.

The mass basis water content (θ_m, g g^{-1}) of the soil was determined using eqn. 3.11

$$\boldsymbol{\theta_m} = \frac{\boldsymbol{mass\ of\ water}}{\boldsymbol{mass\ of\ soil\ solids}} = \frac{\boldsymbol{M_w}}{\boldsymbol{M_d}} = \frac{\boldsymbol{M_w - M_d}}{\boldsymbol{M_d}} \times 100\% \qquad \textbf{3.11}$$

where M_d is the mass of the soil after drying and M_w is the mass of the soil sample before any water is lost. If the volume of the sample (V_s, m^3) is known, then the volumetric

water content (θ_v, m^3m^{-3}) can be calculated by converting the mass of water lost on drying to a volume and then dividing by the sample volume given by eqn. 3.12,

$$\boldsymbol{\theta_v} = \frac{\boldsymbol{volume\ of\ water}}{\boldsymbol{total\ soil\ volume}} = \frac{\left(\frac{\boldsymbol{M_w}}{\boldsymbol{\rho_w}}\right)}{\boldsymbol{V_s}} = \frac{\boldsymbol{V_w}}{\boldsymbol{V_s}} \times 100\% \qquad \textbf{3.12}$$

where ρ_w is the density of water (1 gm^{-3}), θ_v and θ_m are related by the soil bulk density (ρ_b), which is the oven – dry weight of soil per unit volume of field soil as in eqn. 3.13

$$\boldsymbol{\rho_b} = \frac{\boldsymbol{M_d}}{\boldsymbol{V_s}} \qquad \textbf{3.13}$$

3.3.4. Determination of bulk density and total porosity

3.3.4.1 Bulk density

Bulk density (Bd) is the dry mass of the sample divided by the volume of the sample. Bulk density (Bd) is expressed in the unit of gcm^{-3} (Jury, 1991). The method involves sampling a soil core from a desired depth in its natural condition using core sampler ad determining the mass of solids and water content of the core, by weighing the wet core, drying it to constant weight in an oven at 105 ºC, and reweighing after cooling (after 24 hours of drying). Bulk density is then, calculated from the measurement of bulk volume, using the core length and the diameter of the cutting edge of the sampler.

3.3.4.1.1 Equipment

Core sampler (aluminium can), vernier calliper, plastic ruler (0.0 cm to 30.0 cm), oven (50 to 150 ºC), spatula, and weighing balance (± 0.001 g).

3.3.4.1.2 Experimental procedure

The core sampler cans were first weighed to determine their masses (Mc) and properly labelled. These were driven into the into the soil core deep enough to fill the sampler can, the extra soil was trimmed off. The soil sample and cans were weighed to determine the mass of the wet soil (Mw).

The height (h cm) of the soil in the cans were measured and recorded with a plastic ruler and the diameter (d cm) of the cans was determined using vernier calliper. The soil samples were dried in an oven at 105 ^{o}C to determine the water content (Md).

The bulk densities (Bd) were calculated as follows:

$$\boldsymbol{mass\ of\ oven\ dry\ soil\ M_s = M_d - M_c} \qquad \textbf{3.14}$$

Volume of soil (**V cm^{-3}**) is $\boldsymbol{V = \pi \frac{d^2}{4} h}$ **3.15**

$$\boldsymbol{Bulk\ density\ (Bd) = \frac{mass\ of\ oven\ dry\ soil}{volume\ of\ soil}} \qquad \textbf{3.16}$$

$$\boldsymbol{Bd = \frac{M_d - M_c}{V}} \qquad \textbf{3.17}$$

$$\boldsymbol{Bd = \frac{4(M_d - M_c)}{\pi d^2 h}} \qquad \textbf{3.18}$$

3.3.4.1.3 Determination of total porosity

The porosity of a porous medium (such as rock or sediment) describes the fraction of void space in the material where the void may contain for example air or water. It is defined by the ratio:

$$\boldsymbol{n = \frac{V_V}{V_T}}, \qquad \textbf{3.19}$$

where $\boldsymbol{V_V}$ is the volume of void – space and $\boldsymbol{V_T}$ is the total or bulk volume of material, including the solid and void components.

Porosity is a fraction between 0 and 1 and may also be represented in percent terms by multiplying the fraction by 100. The corresponding porosities were also determined as:

$$\boldsymbol{Total\ Porosity\ (n) = \left[1 - \frac{Bd}{Pd}\right]} \qquad \textbf{3.20}$$

where Bd is the bulk density, n is the porosity and Pd is the particle size distribution (Blake and Hartge, 1986).

3.3.5 Determination of major cations in the soil and water samples (Unsaturated zone and groundwater)

Five (5) g of the oven – dried, homogenised soil sample was leached with 100 ml of deionised water. The samples were manually shaken and allowed to stand for two days and the supernatant was filtered through 0.45 µm filters, which were used for the determination of Na^+, K^+, Ca^{2+} and Mg^{2+} in the soil.

3.3.5.1 Determination of Sodium (Na) and Potassium (K)

The levels of sodium (Na) and Potassium (K) in the leached water samples were determined by the flame emission photometric method, using the Sherwood 420 Flame Photometer (Sherwood, UK).

3.3.5.1.1 Reagents

Suppressor solution – A 100 mg/L lithium (Li) solution was prepared by dissolving 6.941 g $Li_2SO_4.H_2O$ in double – distilled water and diluting to 1000 mL volumetric flask.

The suppressor solution is important because Na, K and Li are in group one of the periodic table. The addition of Li is to suppress the other group one elements (Rb, Cs and Fr) present in the water samples with the exception of Na and K.

3.3.5.1.2 Standards

Mixed Na/K calibration standard – A 100 mg/L mixed Na and K calibration standard was prepared by pipetting 1 mL of commercially – available stock Na standard and 1 mL of commercially – available stock K standard into a 10 mL volumetric flask and diluting to the mark.

3.3.5.1.3 Calibration

2 mL of the suppressor solution was added to 5 mL of the mixed Na and K standard and thoroughly mixed by swirling. The combined solution was aspirated into the liquefied petroleum gas LPG – fed flame of the Sherwood 420 Flame photometer. The

concentrations of Na and K were read at their respective wavelengths (Na: 589 nm and K: 766.5 nm). This was followed by the analysis of the blank solution and subsequently the water samples.

3.3.5.1.4 Analysis

A blank solution made of thoroughly mixed double – distilled water – suppressor solution (5:2) was aspirated into the LPG – fed flame of the Sherwood 420 Flame Photometer. After analysis of the blank, the Na and K contents of the filtered leached soil water samples were determined. The procedure for the analysis of Na and K in the soil and water samples (unsaturated zone and groundwater) was as follows:

5 mL of the filtered leached soil water sample was measured and transferred into 10 mL test tube followed by addition of 2 mL of suppressor solution. The mixture was homogenized by shaking for about 1 minute. The homogenized solution was aspirated into the flame of the photometer. The contents of Na and K were read and recorded.

The above procedure was also repeated for Na and K in the water samples (unsaturated zone and groundwater).

3.3.5.2 Estimation of Calcium Ca^{2+} in the soil and water samples (unsaturated zone and groundwater)

The most widely used method for the determination of Ca^{2+} is by complexometric titration involving ethylene diamine tetra – acetic acid (EDTA). The classical indicator

employed for Ca^{2+} titration is ammonium purpurate (murexide) powder. Murexide at a pH 11 is purple in colour in the absence of Ca^{2+} but in the presence of Ca^{2+} ions it forms a pink complex.

3.3.5.2.1 Reagent

3.3.5.2.1.1 Murexide indicator

200 mg of murexide was mixed with 100 g solid NaCl, the mixture were grinded to 40 to 50 meshes and was used as indicator.

3.3.5.2.1.2 Standard EDTA titrant 0.01 M

A 0.01 M EDTA solution was prepared by dissolving 1.179 g of disodium salt of ethylene diamine tetra – acetic acid dihydrate (analytical reagent grade) and 780 mg magnesium sulphate ($MgSO_4.7H_2O$) in 50 mL double – distilled water. The solution was added to 16.9 g NH_4Cl and 142 mL concentrated NH_4OH by mixing and diluted to 250 mL with double – distilled water.

3.3.5.2.2 Experimental procedure for calcium determination

For the purpose of this study, blank solution of distilled water was first titrated to serve as correction for the sample. 25 mL of the extract from the soil was taken into a 250 ml conical flask, followed by 1.5 mL of NaOH solution and approximately 50 mg of murexide indicator powder was added to the sample solution before titration. The solution was titrated against 0.01 M EDTA solution till the colour changed from pink to

purple. In the final stage of the titration, EDTA solution was added drop – wise as the colour change was not instantaneous and the end point was compared to the blank solution.

The above procedure was also repeated for calcium in the water samples (unsaturated zone and groundwater).

The concentrations of Ca was calculated by using eqn. 3.5

$$\boldsymbol{mg\ of\ Ca/L = (V_2 - V_3) \times 0.01 \times \frac{V_2}{V_1} \times \frac{100}{W}} \qquad \textbf{3.5}$$

where:

V_1 = Volume of the aliquot used in analysis

V_2 = Titre – value for the sample

V_3 = Titre – value for the blank sample

W = Weight of the soil taken (5 g)

3.3.5.3. Magnesium determination in the soil and water (unsaturated zone and groundwater samples)

The magnesium (Mg) concentration in the both soil and water samples (groundwater and unsaturated zone) was determined using the FAAS.

1 ml of each of the samples (leached filtered soil water, groundwater and water from the unsaturated zone) was pipetted into different test tubes and 9 ml of Lanthanum solution of concentration 10000 mg/L was added to each sample to serve as ion suppressants in order to bring out the precipitates in the solution which were used for the determination of Mg in the soil.

3.3.5.4 Determination of Chloride by the Argentometric Method

Argentometric Method (APHA 1992, 4500-Cl- B) was used in determining the chloride content in the soil and water samples (rain water, groundwater and unsaturated zone). Titration is a process by which the concentration of an unknown substance in solution is determined by adding measured amounts of a standard solution that reacts with the unknown. Then the concentration of the unknown can be calculated using the stoichiometry of the reaction and the number of moles of standard solution needed to reach the end point.

3.3.5.4.1 Apparatus

Burette of volume 50 mL, pipette of volume 20 mL and conical flask of volume 250 mL

3.3.5.4.2 Reagent

3.3.5.4.2.1 Potassium chromate indicator solution.

A 50 mL potassium chromate indicator was prepared by dissolving 2.5 g of K_2CrO_4 in 250 mL volumetric flask with double – distilled water and allowed to stand for 12 hours. The supernatant was filtered and diluted to 50 mL mark with double – distilled water.

3.3.5.4.2.1 Silver nitrate titrant solution, 0.0141 M.

A 0.0141 M silver nitrate ($AgNO_3$) solution was prepared by dissolving 2.395 g $AgNO_3$ in double – distilled water and diluted to make 1000 mL. The solution was standardised against NaCl solution and stored in amber coloured bottle in cool place away from light.

3.3.5.4.3 Determination of Chloride in soils, groundwater and water from unsaturated zone

To determine chloride content in the soil, double – deionized water was added to the 80 g of oven – dried soil sample in 2:1 ratio and it was vigorously shaken and allowed to stand for two days. The supernatant was filtered through 0.45 µm filters and chloride was then analysed by titration (Scanlon, 1991).

The procedure for the analysis of Cl in the soil and water samples (unsaturated zone and groundwater) was as follows:

25 mL of the sample (water and filtrate) were taken and titrated against silver nitrate standard of concentrations of 0.0141 M, with chromate as an indicator. The titrimetric method uses chromate ions as an indicator in the titration of chloride ions with silver nitrate standard solution was used in this method. After all the chloride has been precipitated as white silver chloride, the first excess of titrant results in the formation of a silver chromate precipitate, which signals the end point.

The above procedure was also repeated for chloride in the water samples (unsaturated zone and groundwater).

The reactions involves

$$Ag^{+} + Cl^{-} \leftrightarrow AgCl(s) \qquad \textbf{3.6}$$

$$2Ag^{+} + CrO_4^{2-} \leftrightarrow Ag_2CrO_4(s) \qquad \textbf{3.7}$$

The amount of chloride in the unknown samples was determined by using eqn. 3.8, and the stoichiometry and moles consumed at the end point are known.

$$\boldsymbol{mg/L = \frac{(A-B)\times N\times 35.45\times 1000}{mL\ of\ sample}} \qquad \textbf{3.8}$$

where A is the average titre, B is the titre value for the blank solution; N is the molarity of $AgNO_3$ (0.0141 M).

3.3.5.5 Determination of Phosphate (PO_4^{3-}), Sulphate (SO_4^{2-}) and Nitrate (NO_3^-) in soil and water samples (unsaturated zone and groundwater)

The phosphate, sulphate and nitrate concentrations in soil samples were determined according to the official methods in the Association of Official Analytical Chemists (Anon, 2007). Phosphate was determined by Official method 4500 – P E (Ascorbic acid method). The Official method 4500 – SO_4^{2-} E (Turbidimetric method) was used for the determination of sulphate. Nitrate was determined using AOAC Official method 973.50.

3.3.5.5.1 Determination of Phosphate

3.3.5.5.1.1 Principle

Ammonium molybdate and potassium antimonyl tartrate react in acid medium with orthophosphate to form an antimonyl – phosphomolybdate complex, which is reduced to intensely coloured molybdenum blue by ascorbic acid. The absorbance of the molybdenum blue is measured at a wavelength of 880 nm on a UV – visible spectrophotometer.

3.3.5.5.1.2 Instrumentation

A Shimadzu UV – 1201 UV – visible Spectrophotometer (Japan) with 1 cm matching quartz cells was used for absorbance measurements.

3.3.5.5.1.3 Chemical and Reagents

Ammonium heptamolybdate,$[(NH_4)_6Mo_7O_{24} \cdot 4H_2O]$ potassium antimonyl tartrate $[K(SbO)C_4H_4O_6 \cdot 5H_2O]$, sulphuric acid (96% H_2SO_4), and Ascorbic acid.

3.3.5.5.1.4 Potassium antimonyl tartrate $[\boldsymbol{K(SbO)C_4H_4O_6 \cdot 5H_2O}]$

500 mL of potassium antimonyl tartrate solution was prepared by dissolving 1.375 g of $\left[K(SbO)C_4H_4O_6 \cdot {}^{1}/_{2}\, H_2O\right]$ in about 400 mL double – distilled water and diluting to 500 mL. The solution was stored in a glass – stoppered bottle.

3.3.5.5.1.5 Ammonium molybdate $[\boldsymbol{(NH_4)_6Mo_7O_{24} \cdot 4H_2O}]$

A 500 mL ammonium molybdate $[(NH_4)_6Mo_7O_{24} \cdot 4H_2O]$ solution was prepared by dissolving 20 g ammonium molybdate in excess of aqueous ammonia and evaporating the solution at room temperature with double – distilled water and diluting to the 500 mL mark.

3.3.5.5.1.6 Ascorbic Acid

A 0.1 M solution of ascorbic acid solution was prepared by dissolving 1.76 g of ascorbic acid in double – distilled water and diluting to the 100 mL mark. Since ascorbic acid

solutions are not stable for long period of time at room temperature, they were always freshly prepared.

3.3.5.5.1.7 Combined Reagent

The combined reagent is an acidic (H_2SO_4) solution of potassium antimony tartrate, ammonium molybdate and ascorbic acid.

A 100 mL combined reagent was prepared by adding 50 mL of 5 M H_2SO_4 to a mixture of 5 mL potassium antimony tartrate, 15 mL ammonium molybdate and 30 mL ascorbic acid. After the addition of the reagents, it was allowed to attain a room temperature, followed by thoroughly mixing. The combined reagent was stored in a plastic bottle. The combined reagent was always prepared fresh because it is stable for only four (4) hours.

3.3.5.5.2 Phosphate standard

A stock standard phosphate solution (50 mg/L) was prepared by dissolving 219.5 g of oven – dried potassium dihydrogen phosphate (KH_2PO_4), in double – distilled water to make 1000 mL of solution. Working solutions of concentrations 0.2, 0.4, 0.6, 0.8 and 1.0 mg/L were prepared by appropriate dilution of the stock.

3.3.5.5.2.1 Calibration of UV – Visible spectrophotometer

In order to construct a calibration curve, 10 mL aliquot of the calibrant solutions were transferred into separate 20 mL test tubes. To each test tube, 2 mL of the combined reagent was added to each test tube and left to stand for about 5 minutes. During this period, the blue colour of antimonyl – phosphomolybdate complex was developed in

each test tube. Appropriate aliquot of each blue – coloured calibrant solution was transferred into a 1 mL cuvette; the cuvette was inserted into the spectrophotometer and the absorbance measured at a wavelength of 880 nm against a reagent blank.

A calibration graph of absorbance against concentration of PO_4^{3-} in each calibrant solution was plotted. The concentration of PO_4^{3-} in the water sample was deduced from the calibration graph.

3.3.5.5.2.2 Measurement of phosphate ($\boldsymbol{PO_4^{3-}}$) in soil samples, water from unsaturated zone and groundwater

The procedure for the analysis of $\boldsymbol{PO_4^{3-}}$ in the soil and water samples (unsaturated zone and groundwater) was as follows:

10 mL aliquot of the filtered soil water samples was transferred into a 20 mL test tube and the same procedure as used for the establishment of the calibration graph was followed to obtain the absorbance of each water sample at a wavelength of 880 nm on the UV – Visible Spectrophotometer. The concentration of PO_4^{3-} in the soil samples was obtained from the calibration graph.

The above procedure was repeated for phosphate in the water samples (unsaturated zone, and groundwater).

3.3.5.5.3 Determination of Sulphate SO_4^{2-} in soil samples, water from unsaturated zone and groundwater

3.3.3.5.2.1 Principle

The method is based on the reaction of phosphate ion SO_4^{2-} with barium chloride ($BaCl_2$) under acidic conditions to precipitate barium sulphate ($BaSO_4$). The absorbance of white $BaSO_4$ suspension is measured at a wavelength of 420 nm on the UV – Visible Spectrophotometer.

3.3.5.5.2.2 Instrumentation

A Shimadzu UV – 1201 UV – visible Spectrophotometer (Japan) with 1 cm matching quartz cells was used for absorbance measurements.

3.3.5.5.2.3 Chemicals

Barium chloride ($BaCl_2$, 99.999 %), sodium chloride (NaCl), Hydrochloric acid (HCl), sodium sulphate (Na_2SO_4) and glycerol.

3.3.5.5.2.4 Reagents

Acid salt solution:

60 g NaCl was dissolved in 5 mL of 37 % HCl and diluted with double – distilled water in a 250 mL volumetric flask.

3.3.5.5.2.5 Sulphate standard

A stock standard of sulphate solution (100 mg/L) was prepared by dissolving 0.1479 g of anhydrous Na_2SO_4 in double – distilled water to make 1000 mL of solution. Working

solutions of concentrations 15, 20, 25, 30 and 35 mg/L were prepared by appropriate dilution of the stock.

3.3.5.5.2.6 Calibration

10 mL of the standard SO_4^{2-} calibrants solutions were quantitatively transferred into separate test tubes. To each test tube, 1 mL of the acid salt solution, 0.5 mL glycerol solution (conc.) and 0.5 g of $BaCl_2$ were added. The resulting cloudy solution was shaken for 50 seconds and left to stand for 5 minutes. Appropriate aliquot of the cloudy solution was transferred into 1 cm cell and the absorbance of the coloured solution measured at a wavelength of 420 nm on the UV – Visible Spectrophotometer. The absorbance of each calibrant solution was plotted against concentration of the calibrants. A straight line graph was obtained. The concentration of the water samples were deduced from the graph after measurement of the absorbance for each sample at a wavelength of 420 nm on the UV – Visible Spectrophotometer.

3.3.5.5.2.7 Measurement of $\boldsymbol{SO_4^{2-}}$ in the samples

The procedure for the analysis of $\boldsymbol{SO_4^{2-}}$ in the soil and water samples (unsaturated zone and groundwater) is as follows:

10 mL aliquot of the filtered soil water sample was transferred into a 20 mL test tube and the same procedure as used for the establishment of the calibration graph was followed to obtain the absorbance of each of the water sample at a wavelength of 420 nm on the UV – Visible Spectrophotometer. The concentration of SO_4^{2-} in each of the water sample was obtained from the calibration graph.

The above procedure was repeated for sulphate in the water samples (unsaturated zone and groundwater).

3.3.5.5.3 Determination of Nitrate NO_3^- in soil samples

3.3.5.5.3.1 Principle

The method is based on the reaction of nitrate ion with brucine sulphate in H_2SO_4 solution at a temperature of 100 ℃. The yellow colour of the resulting complex is measured at a wavelength of 410 nm.

3.3.5.5.3.2 Standards

A stock standard nitration solution of concentration 100 mg/L was prepared by dissolving 0.7218 g of KNO_3 (pre – oven dried at 105 ℃ for 24 hours) in double – distilled water to make 1000 mL of solution. The stock solution was preserved with 2 mL $CHCl_3$. Working calibrant solutions of concentrations 0.2, 0.4, 0.6, 0.8 and 1.0 mg/L were prepared by appropriate dilution of the stock.

3.3.5.5.3.3 Reagent

Brucine – sulfanilic acid reagent

1 g of brucine sulphate $[(C_{23}H_{26}N_2O_4)_2 \cdot H_2SO_4 \cdot 7H_2O]$ and 0.1 g of sulphanilic acid $(NH_2C_6H_4SO_3H \cdot H_2O)$ were dissolved on 70 mL hot double – distilled water. 3 mL conc. HCl was added; the resulting solution was cooled and diluted to the 100 mL mark with double – distilled water. The reagent was stored in a dark bottle at 5℃.

3.3.5.5.3.4 Calibration

5 mL of each of the calibrant solution was pipetted into separate 20 mL test tube. To each test tube, 1 mL of 30 % of NaCl was added, followed by addition of 5 mL of 6.5 M H_2SO_4.

The test tube was shaken to ensure thoroughly mixing of the reagents. 0.5 mL of the brucine – sulfanilic acid was added to the content of each test tube except the blank. The test tube was then packed on a rack and lowered into a water bath at 95 ℃ for 25 minutes. At the end of the 25 minutes, the rack together with the test tube was removed from the water bath and immersed in ice. An appropriate aliquot of the yellow coloured calibrant solutions was transferred into 1 cm cell. The cell was placed into the spectrophotometer and the absorbance of the solution measured at a wavelength of 410 nm. A graph of absorbance of standards against concentration of standards was plotted.

3.3.5.5.3.5 Measurement of nitrate (NO_3^-) in soil samples and water samples (unsaturated zone and groundwater)

The procedure for the analysis of NO_3^- in the soil and water samples (unsaturated zone and groundwater) was as follows:

5 mL aliquot of the water samples were transferred into separate 20 mL test tube and the same procedure as was used for the establishment of the calibration graph was followed to obtain the absorbance of each of the water sample at a wavelength of 410 nm on the UV – Visible spectrophotometer. The concentration of NO_3^- in each of the sample was deduced from the calibration graph. The concentration was calculated from the relation:

$$C_{NO_3^-} = C_{calibration} \times D_f \qquad 3.9$$

where $C_{NO_3^-}$ is the nitrate concentration, $C_{calibration}$ is the concentration from the calibration graph and D_f is the dilution factor.

The above procedure was repeated for sulphate in the water samples (unsaturated zone and groundwater).

3.3.6 Determination of trace elements in the soil samples and water samples (groundwater and unsaturated zone)

Flame Atomic Absorption Spectrometry (FAAS) was used for the determination of Cd, Fe, Cr, V, Mn, Pb, Ni, Zn, Co, As and Cu.

3.3.6.1 Instrumentation

Fast Sequential Atomic Absorptions Spectrometer (VARIAN, AA 250 FS, Australia) was used for atomic absorption measurement. The AAS was equipped with a deuterium background corrector.

3.3.6.2 Experimental procedure

3.3.6.2.1 a. Digestion of soil samples

Digestion of soil sample was done according to the procedure described by Hoening et al., (1998). The procedure was as follows:

1.5 g of soil sample was weighed into a previously acid washed labelled 100 mL polytetraflouroethylene (PTFE) Teflon bombs. 6 mL of concentrated nitric acid (HNO_3, 65

%), 3 ml of concentrated hydrochloric acid (HCl, 35 %) and 0.25 ml of hydrogen peroxide (H_2O_2, 30 %) were added to the samples in a fume chamber. The samples were then loaded on the microwave carousel. The vessel caps were secured tightly using a wrench. The complete assembly was microwave – irradiated for 26 minutes using milestone microwave labstation ETHOS 900, INSTR: MLS – 1200 MEGA. The soil samples were digested using a four step digestion procedure as shown in the Table 3.1. After digestion, the Teflon bombs mounted on the microwave carousel were cooled in a water bath to reduce internal pressure and allow volatilized material to re- stabilize. The digestate was made up to 20 mL with double distilled water and assayed for the presence of Cd, Fe, Cr, V, Mn, Pb, Ni, Zn, Co, As and Cu using VARIAN AA 240FS – Atomic Absorption Spectrometer in an acetylene- air flame.

Table 3.1: Microwave digestion programme used for digestion of water samples

Digestion Step	Time (min)	Power (W)	Pressure (bar)	Temperature 1 (^oC)	Temperature 2 (^oC)
1	05:00	250.0	100.0	400.0	500.0
2	01:00	0.0	100.0	400.0	500.0
3	10:00	250.0	100.0	400.0	500.0
4	05:00	450.0	100.0	400.0	500.0

Temperature 1 and 2 represents the initial and final temperatures respectively

3.3.6.2.1 b. Digestion of water samples (unsaturated zone and groundwater)

6ml of concentrated nitric acid (HNO_3, 65 %), 3 ml of concentrated hydrochloric acid (HCl, 35 %) and 0.25 ml of hydrogen peroxide (H_2O_2,30 %) was added 5 mL water in

Teflon digestion tubes sample in a fume chamber. The samples were then loaded on the microwave carousel. The vessel caps were secured tightly using a wrench. The complete assembly was microwave irradiated for 26 minutes using milestone microwave labstation ETHOS 900, INSTR: MLS-1200 MEGA .The water was digested using a four step digestion procedure as shown in the Table. After digestion, the Teflon bombs mounted on the microwave carousel were cooled in a water bath to reduce internal pressure and allow volatilized material to re- stabilize. The digestate was made up to 20 ml with double distilled water and assayed for the presence of Fe, Cr, Mn, Ni, Co, As and Cu using VARIAN AA 240FS – Atomic Absorption Spectrometer in an acetylene- air flame.

3.3.6.3.2 Atomic Absorption

The VARIAN, AA 250 FS, Australia, working conditions used for the FAAS of Cd, Fe, Cr, V, Mn, Pb, Ni, Zn, Co, As and Cu were as follows: The air – acetylene flame atomizer was made up of air as oxidant (flow rate: 13.50 L/min) and acetylene as fuel (flow rate: 2 L/min).

The lamp current and wavelength of the hollow cathode lamps and the spectral slit width used for Cd, Fe, Cr, V, Mn, Pb, Ni, Zn, Co, As and Cu determinations are shown in Table 3.2. For vanadium (V) determination, nitrous – oxide was used as oxidant.

Table 3.2: FAAS conditions used for the determination of Cd, Fe, Cr, V, Mn, Pb, Ni, Zn, Co, As and Cu

Element	Wavelength (nm)	Lamp current (mA)	Slit width (nm)
Zn	213.9	5.0	1.0
Pb	217.0	5.0	1.0
Cu	324.7	4.0	0.5
Fe	248.3	5.0	0.2
Mn	279.5	5.0	0.2
Cr	357.9	7.0	0.2
V	318.5	20.0	0.2
As	193.7	10.0	0.5
Co	240.7	7.0	0.2
Ni	232.0	4.0	0.2
Cd	228.8	4.0	0.5

3.3.6.3.3 Calibration of atomic absorption spectrometer

The AAS was calibrated with the calibration standards for the element being determined. The absorbances obtained were used to plot calibration graphs for each element and these graphs are shown in Appendix X for the various elements analysed. Three standard solutions (of the same element) of increasing concentrations were used to establish the reliability of readings since the equipment is already fixed to a programmable computer that reads out concentration and absorbance directly. The calibration function was established by plotting absorbance (% absorption) for a set of calibration solutions against the concentration analyte. Linearity of the calibration curves were checked before

samples were aspirated. “Resloping” was carried out with standards during readings to account for instrumental drift.

After the calibration, each element was determined by measurement of the absorbances of the samples aspirated into the absorption cell.

3.3.6.3.4 Calculation of concentration

The concentration of each analyte in the water samples were calculated from the calibration curve for the analyte. In cases of dilution of a sample, the concentration deduced from the calibration curve was multiplied by the dilution factor to give the actual concentration of the analyte in the sample.

Analyses were done at AAS laboratory, Department of Chemistry, National Nuclear Research institute, Ghana Atomic Energy Commission, Accra Ghana.

Final concentrations of the selected elements were the determined from the relation:

$$\textbf{Final concentration} = \frac{\textbf{Conc(DF)xNominal Volume}}{\textbf{Sample weight in grams}} \qquad \textbf{3.10}$$

where Conc = AAS reading,

DF = dilution factor (Ratio of final volume of dilution to volume of aliquot taken).

Nominal volume = 20 mL

3.3.7. Extraction of water from soils for stable isotopes

Extraction of water from the soils was achieved by using the vacuum distillation method. The scheme for the extraction is presented in Fig 3.4. The experimental set – up is shown in Figures 3.5 and 3.6.

3.3.7.1 Equipment

- Hotplate with temperature regulator for heating water in to the required temperature (70 °C to 85 °C).
- 500 mL Pyrex round bottomed flask use to contain the soil for extraction
- Dewar for holding liquid nitrogen (LN_2)
- Dewar stands for increasing or decreasing the height of the Dewar's during the extraction
- SinkuKiko DA60 vacuum pump for sucking gases/air from vacuum glasses
- Connecting tubes connects the 500 mL Pyrex glass to the condensing cylindrical glasses
- Cylindrical condensing glasses serves as moisture collection trap
- Retort stand to hold glassware (500 mL Pyrex round bottom flask and condensing cylindrical glasses)
- Pressure control valves
- Pressure tubes
- Thermometer for checking the temperature of water

3.3.7.2 Extraction procedure

Cryogenic extraction is the standard method used to extract water from soils for analysis of either hydrogen or oxygen isotopic ratios.

A vacuum moisture extraction system consisting of two parallel units with cryogenic collection of the extracted water from the unsaturated core samples was used. This was connected to a wide mouth 500 mL Pyrex round bottomed flask at the entry of the extraction system containing about 250 g of each soil sample for extraction.

At the beginning of each extraction, the exterior of sample vial was kept dry and the system evacuated with a rotary vacuum pump (SinkuKiko DA60) to avoid condensation of any available gas shown in Figure 3.4.

Fig 3.4: Soil moisture extraction system without moisture trap and showing system being degasing.

The round bottomed flask containing the soil sample was gradually heated in a water bath and the temperature was maintained between 70 °C to 85 °C throughout the extraction

period. This was to reduce the risk of removing any immobile water in the clay lattice which can be a source of error in the isotope composition of the extracted water. Periodic additions of cold water were added to the water bath kept the water level constant throughout the extraction period and also to maintain constant temperature.

It is imperative that the water is completely extracted from the samples in order to avoid fractionation. The heavier isotopic molecules $\boldsymbol{H_2}^{18}O$ are extracted from the samples later than the $\boldsymbol{H_2}^{16}O$ water. Extraction was done between 5 to 7 hours in order to avoid any isotopic fractionation as much as possible (Araguás-Araguás et al., 1995, IAEA 2009, Adomako, 2010).

The Dewar of liquid nitrogen was placed on the collection tube in order to freeze out the water vapour emanating from the sample. The moisture was then trapped and collected into a cylindrical condensing glasses using liquid nitrogen (LN_2) at -196° C as shown in Figure 3.5.

Fig 3.5: Soil moisture extraction system with moisture trap

It was ensured that only the very bottom tip of the tube was immersed in LN_2. The LN_2 vial was periodically raised few centimetres with the help of the Dewar stand to trap the moisture as it condenses.

It is easy to determine when all of the moisture has been extracted from the sample, because there will be no further moisture condensation on the vacuum line walls. At this point, the heating mantle was turned off and removed. At the completion of the distillation, the boiling water and liquid nitrogen were removed from the collection tube and the extraction tube, respectively. The thawed water was poured into clean air tight glass bottles and tightly sealed to avoid evaporation. The samples were labelled and made ready for stable isotopes analysis. The total number of samples soil extracted was 42.

3.3.8 Determination of the stable isotopes of water

3.3.8.1 Instrumentation

Determination of the composition of the isotopes (δ^2H and$\delta^{18}O$) in the water samples was accomplished by using the Los Gatos DLT – 100 Liquid – water Stable Isotope Analyzer [off – axis integrated cavity output spectroscopy (OA – ICOS) via laser absorption]. The equipment is made up of a laser analysis system, an internal computer, a CTC LC – PAL liquid auto sampler, a small membrane vacuum pump and a room air intake line that passes air through a Drierite column for moisture removal. The auto sampler and the DLT – 100 are connected by a ~ 1 m long polytetraflouroethylene (PTFE) transfer line. A 1.2 μL microliter syringe (Model 7701.2N, Hamilton) was used to inject 0.75 μL of sample through PTFE septum in the auto sampler.

3.3.8.2 Reference Material

The validity of the isotopic composition analysis (δ^2H and$\delta^{18}O$) using the liquid – water stable isotope analyzer was checked by International Atomic Energy Agency (IAEA) reference material, LS1 [(Water) (δ^2H_{VSMOW} and$\delta^{18}O_{VSMOW}$)].

3.3.8.3 Standard

Three secondary standards were used for the analysis: two calibration standards [prepared from IAEA reference material, LS1 ([(Water) (δ^2H_{VSMOW} and$\delta^{18}O_{VSMOW}$)], and a control standard (‘‘in – house’’ prepared).

Calibration standard 1: STD_1 (LS1) – enriched: $\delta^2H = 2.10 \pm 0.3\ Hg$ and $\delta^{18}O = 0.24 \pm 0.03$

Calibration standard 2: STD_2 (KWK3) – depleted: $\delta^2H = -76.50 \pm 1.0$ and $\delta^{18}O = -11.13 \pm 0.1$

Calibration standard 1: STD_1 (ER) – control: $\delta^2H = -24.34 \pm 0.6$ and $\delta^{18}O = -4.78 \pm 0.8$

3.3.8.4 Experimental procedure

The experimental procedure was according to the methods prescribed in the IAEA training course series 35 [IAEA laser spectroscopic analysis of liquid samples for stable hydrogen and oxygen isotopes], (IAEA, 2009). The procedure is as follows:

1 mL aliquot of each standard (in – house, working and control) and 1 mL aliquot of the water sample were quantitatively transferred into 1.5 mL auto – sampler glass using the

1000 μL Eppendorf disposable tip pipette. The 1.5 mL auto – sampler glass vial were then capped with PTFE septum caps. This was followed by the arrangement of the samples on the CTC LC PAL auto – sampler. The arrangement of the samples and the standards is also according the procedure described below (IAEA, 2009):

A dummy sample (de – ionized water) was placed in the first position to prime the flow line. The dummy vial was followed by the three secondary standards (two calibration standards and a control standard); five water samples, followed by another set of three standards. This array of standards and water samples were repeated up to a maximum six times (30 water samples) for a single run. Each standard and water sample was individually measured six injections lasting for 25 minutes. Measurement for each batch of 30 samples lasted for 12.5 hours. The measurement results for the last four of the six injections from each vial were averaged. The measured and the known d values of calibration standards before and after each batch of five water samples were used for a linear regression to convert absolute isotope ratios to d values.

The instrument is prone to give erratic results during the start of a run, the dummy sample used allowed the system to stabilize before the first standards were run on the liquid – water Analyzer. The arrangement of the vials in the CTC LC PAL auto – sampler was designed to overcome the effects of instrumental drift which can be significant during a daily run. The first two injections were disregarded because they are often less stable and the injections with the most potential for carrying a memory effect of the previous sample (IAEA, 2009).

3.3.9 Recharge rate of soil water into groundwater

Recharge is the addition of water to an aquifer, generally from rainfall events that infiltrates downward through the unsaturated zone.

Qualitative estimates of relative recharge rates can be determined using chloride concentrations in groundwater or unsaturated zone pore water if rainfall and dry fallout are the only sources of chloride to the subsurface. In this case, chloride concentrations are inversely related to recharge rates.

The recharge rate (R_d) in the profiles were estimated using Eqn. 3.11

$$R_d = \frac{PC_p}{C_{uz}} \qquad \textbf{3.11}$$

where C_p is the mean chloride concentration in rainfall (mg/L), P is the annual rainfall amount (mm/year) and C_{uz} is the mean chloride concentration in the unsaturated zone (mg/kg) (Edmunds et al., 1988, Marei et al., 2010).

The mean (C_P) is calculated according to the following equation:

$$C_P = \frac{P_1 \times C_1 + \cdots P_n \times C_n}{P_1 + \cdots .. + P_n}, \qquad \textbf{3.12}$$

where P_1 is the first rainfall event (mm) and C_1 is the corresponding chloride concentration in the rainfall (mg/L), for 1 to n events.

Ion concentrations are also expressed as mg/L of pore water (mg/kg divided by gravimetric water content and multiplied by water density):

$$\text{mg/L} = \frac{mg/kg}{\theta}\rho, \qquad \textbf{3.13}$$

where ρ is the density of water Mg/cm^{-3}, θ is the water content

3.3.10 Quality Assurance/Quality Control (QA/QC)

Quality Assurance usually consists of quality control and quality assessment.

Quality control refers to the set of procedures undertaken by the laboratory for continuous monitoring of operations and results in order to ensure that the results are good enough to be released (Ibe and Kullenberg, 1995).

Quality Assurance is defined as the total sum of activities employed by a laboratory to ensure that the data it produces meet the quality desired for decision making (Ibe and Kullenberg, 1995).

The following QA/QC guidelines were taken during sampling and analysis to produce acceptable results.

- All the glassware and sampling containers were soaked in nitric acid (10%) for three (3) days and rinsed with deionised water before use. This was to ensure that the sample bottles were free from contamination, which could affect the concentrations of various ions in the groundwater samples
- In sampling from the hand pumps, purging was done for five (5) minutes to flush the stagnant water retained in pipes. In the case of dug wells, it was properly checked and confirmed that the dug well was being used daily. This was to ensure that stale and stagnant water was not sampled.
- The drilling blade of the hand auger was cleaned after each sample was taken so as to prevent contamination of the next sample.
- The collected samples were properly labelled with sample type, time and date of collection, location and environmental characteristics. Samples that require

preservation and special treatment for transportation to prevent their deterioration were treated promptly.

- All reagents used during analysis were of analytical grade.
- Every instrument used was calibrated with standard chemical solutions prepared from commercially available chemicals and validated with Standard Reference Materials (SRM) and Certified Reference Materials (CRM). The SRM were analysed repeatedly at predetermined intervals to confirm that the method remained in a state of statistical control.
- In the vacuum extraction set – up, the flasks were cleansed with deionised water after each extraction. This was to prevent contamination of the next sample.

CHAPTER FOUR

RESULTS AND DISCUSSION

In this chapter, soil physical parameters, trace metals of Fe, Cu, Mn, As, Ni, Cr, Co, Cd, V, Pb and Zn and major cations ions such as; Ca, Na, K, Mg obtained from the analyses of soil, water from unsaturated zone and groundwater are discussed. The concentrations of chloride with depth for individual profiles in the study area, stable isotopes of water from unsaturated zone, groundwater and soil extracts are also discussed together with recharge/drainage system in the study area. Tables obtained from the analysis has been grouped in Appendices I to IX.

4.1 Soil Physico – Chemical Parameters

The physical parameters of the soil samples are presented in Appendix III. pH, Eh, electrical conductivity, porosity and moisture content are important to determine the origin of salinity in the soil and groundwater.

The soil pH ranged from 5.3 to 7.8 units with a mean value of 6.5. The soil can be classified as slightly acidic – neutral acidic Fig 4.1, (Borggaard and Elberling, 2004). This can be attributed to the uptake of protons by mineral weathering and ion – exchange reactions occurring within the soil. At intermediate values of pH, carbonic and organic acids can readily attack and cause the dissolution of carbonates, silicates and aluminosilicates minerals in processes of chemical weathering, which increasingly consumes H^+ and CO_2, increasing alkalinity.

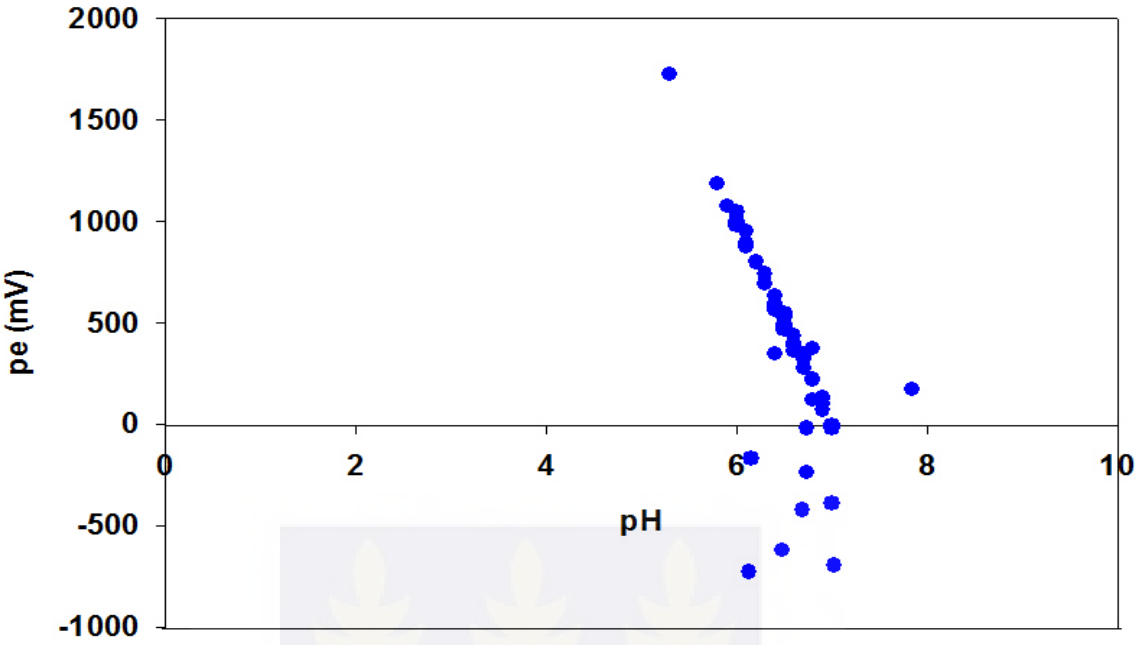

Fig 4.1: pe – pH diagram for the study area (soil and water) samples

This pH variation has major impact on many other unsaturated zone water parameters, such as trace element solubility and bicarbonate concentrations. Metal cation adsorption at mineral and organic surfaces is favoured at higher pH. Fulvic and humic acids dissolve leading to increased complexation by these ligands for some of the trace metals (e.g., Pb, Cu, and Cr).

Soil pH controls the movement of the trace elements from one soil compartment to another, since trace elements can be held in the lattice of secondary minerals. For instance, Maskall and Thornton (1998) found increases in the proportion of readily mobile form of Pb and Zn as pH fell below 7, and Cattlet et al., (2002) also observed a decrease of the Zn^{2+} activity in the soil solution as pH increased.

Soil acidity can increase as basic cations such as Na^+, Ca^{2+}, and K^+ are leached from the soil, as is common in humid regions and is also a product of microbial mediated reactions, such as nitrification, or of chemical reactions, such as the exposure of sulphide minerals to air and water. This condition, according to Alloway (1995), supports the dissolution of metals such as Fe and Mn. The dissolution of these metal oxides allows co – precipitated metals of the hydrous oxides of the metals to be released into solution.

Redox potential, Eh, is a measure of the tendency of chemical species to acquire electrons and thereby to be reduced. The soil Eh ranged from – 1.2 (pe = - 20.34) to + 101.7 (pe = + 1723.73) mV units whilst the mean Eh is + 30.84 mV (pe = + 522.74) mV (Appendix III) and Fig 4.1, which indicate that area is anaerobic. This is a numerical index of the intensity of oxidising or reducing conditions within a system, where positive potentials indicate that the system is relatively oxidising whilst negative potentials indicate that it is relatively reducing. By contrast, in anaerobic systems, Eh measurements may be stable and meaningful only if species of Fe, and Mn dominate the redox chemistry and these were evident in the study area (Appendix I).

Electrical conductivity is a measure of total dissolved solids. Electrical conductivity values in the soil ranged from 35.1 µS/cm to 1276 µS/cm with the mean of 261.99 µS/cm whilst the total dissolved solids (TDS) ranged from 17.6 mg/L to 636.0 mg/L with mean of 130.83 mg/L (Appendix III).

Electrical conductivity values for water from the unsaturated zone ranged from 193.2 µS/cm to 987.5 µS/cm with the mean of 441.7 µS/cm whilst total dissolved solids (TDS)

ranged from 96.6 mg/L to 494 mg/L and the mean of 220.03 mg/L. The electrical conductivity for the groundwater is from 1965 µS/cm to 17000 µS/cm with mean value of 9482.5 µS/cm whilst total dissolved solids (TDS) also ranged from 983 mg/L to 8490 mg/L and the mean being 4736.5 mg/L (Appendix VIII). The high EC and TDS in the study area suggest that, the percolating water is dissolving the accumulated soluble salts (Cl) in the unsaturated zone as the water moves from the unsaturated zone to the saturated zone.

Porosity influences soil hydraulic conductivity and shows how water can move through pore spaces in the soil. More open area for the flow of water shows higher hydraulic conductivity. However, the relationship between the two indicators is mainly useful for the comparison between soil textures. The porosity in the study area ranges from 0.49 to 0.62 with the mean of 0.56 (Appendix III). This can be attributed to the soil type in the study area; about 85 % of the soil type is clay as the depth increases along the profiles.

Clayey soil has high porosity, but its hydraulic conductivity is low (Appendix IV). This has the ability to hold large volume of water without releasing it and this accounts for the reason why the study area is considered as anaerobic. The pore sizes and their connectivity determine whether a soil has high or low permeability. Water flows easily through soil with large pores with good connectivity between them. Small pores would have lower permeability, and because water flow through the soil would be more slowly. Porosity of subsurface soil is lower than in surface soil due to compaction by gravity.

Another variable to consider as a possible reason for the variation in solute concentration is the change in moisture content. The soil moisture content in the study area ranged from 8.91 to 26.9 % with the mean value of 17.46 % (Appendix III). These variations can be attributed to the presence of perched water or water trapped in the soil from rainfall at certain depths in the unsaturated zone, since majority of the soil samples were clayey as the depth increases (Appendix IV) which are highly porous but low permeability.

Larger moisture content restricts gas diffusion and decreases the partial pressure of O_2 and increases the partial pressure of CO_2 due to biological activity. A large partial pressure of CO_2 would promote chemical weathering, which constitutes one of the major sources of base cations in soils (Appendix II). The liberation of base cations through chemical weathering increases the alkalinity of water in the unsaturated zone and these variations are evident in the study area which shows an increase in Na^+, Ca^{2+}, K^+ along the profiles.

Soil texture has strong influence on water percolation, because coarse textured soils with high porosity are generally well drained and water tends to move more vertically than in finer textured soils with higher clay content. Soils with high clay content generally have lower rates of hydraulic conductivity and greater water holding capacities. Metals such as iron, nickel, and manganese are normally associated with very fine clay particle size formed by weathering within the soil (Appendix IV) and most of these metals are derived from the native rock, rather than being added contaminants.

4.2 Major Ions in the Soil

The major ions analysed in the soil and water samples were sodium, potassium, calcium, magnesium, chloride, and nutrients (sulphate, phosphate and nitrate). Their concentrations with respect to varying depth in the individual profile are shown in Appendices II and IV.

Potassium, sodium (Na) and calcium (Ca) are the major cations whilst sulphate (SO_4^{2-}) and chloride (Cl) are the major anions in soils at different depths. They constitute major soluble ions in soils in the unsaturated zone and shows varying trend with depth, as shown in Appendix II. Stronger evaporation results in higher total of these salts content near the land surface.

Potassium (K) concentration in the soil varied between 2.0 mg/kg and 1244.0 mg/kg, with a mean of 375.96 mg/kg in the study (Appendix II). The high concentration of K in the soils may be due to primary minerals such as aluminosilicates, K – feldspars, biotite, and muscovite micas found in the study area Fig 3.2, because the soils contain their weathered products. In the natural recycle potassium is leached into the soil by rains during the dormant season or made available by the gradual decay of organic material.

The concentration of sodium (Na) in the soil ranged from 208 mg/kg to 13080 mg/kg, with the mean of 1526 mg/kg (Appendix II). The source of sodium in the unsaturated zone may be due to readily soluble sodium salts deposited in the soil as results of aerosol or left in the soil by saline water that entered in the past (paleo). It can also be as a results

of evaporites (halites) that were deposited from water that became concentrated owing to evaporation in the unsaturated zone. The increase of pH could cause a significant increase of the sodium. This suggests that increasing the pH (5.3 – 7.8) enhances the preference of Na^+ to be adsorbed on clay colloids (Appendix II and III). It also suggests that, increase of Na with pH is the main factor determining the clay deflocculation at a given and salinity levels. Sodium tends to remain in solution rather than adsorbed onto the soil surface.

The concentration of calcium (Ca) in the soil ranged from 100.2 mg/kg to 721.44 mg/kg with a mean of 330.09 mg/kg (Appendix II). Calcium can be derived from oceanic and inland dust sources, together with periodic material from fires. Calcium is an essential constituent of many igneous rock minerals, especially of the chain silicates pyroxene and amphibole, and the feldspars. Calcium is readily dissolved from rocks rich in calcium minerals, particularly as carbonates and sulphates. Conversely, Ca^{2+} does not remain completely soluble and might be high in soil solution because of dissolution of soil minerals and usually precipitates in the presence of carbonates minerals, bicarbonates and/or sulphates in solution.

Magnesium is essential in plant and animal nutrition. Concentrations of magnesium varied from 6.0 mg/kg to 155.30 mg/kg, whilst the mean is 43.25 mg/kg in the study area, (Appendix II). The major source of magnesium in soil comes as a result of olivine, the pyroxenes, the amphiboles, and the dark – coloured micas, along with various less common species. Magnesium occurs in significant amounts in most limestones. The

dissolution of this material obviously brings magnesium into solution and its concentration tends to increase along the flow path of a groundwater, until a rather high Mg to Ca ratio is reached. The cation – exchange behaviour of magnesium is similar to that of calcium. Both ions are strongly adsorbed by clay minerals and other surfaces having exchange sites.

Phosphate concentration varied from 0.03 mg/kg to 38.74 mg/kg with a mean value of 7.01 mg/kg in the study area (Appendix II). The main natural source of phosphate in many soils is the breakdown of organic matter. However, phosphate minerals often do not last long in readily available form and tend to quickly combine with other minerals in the soil. At high pH (alkaline soils), phosphorus is often present as calcium phosphates. In an acidic soil, phosphorus readily reacts with aluminium and iron to form aluminium and iron phosphates. Therefore, phosphorus is often present in the soil at lower concentration but relatively unavailable to plants due low pH < 7. Phosphate is a negatively charged ion and is held to a limited extent by exchanged sites on clays.

Sulphate can be derived from atmospheric deposition sources (wet and dry fallout), anthropogenic sources such as fertilizers in typical farming communities and sedimentary lithogenic sources (gypsum, anhydrite, and pyrite). Sulphate concentration varied from 18 mg/kg to 5992.86 mg/kg with a mean of 1156.19 mg/kg in the study area (Appendix II). High sulphate values may be due to naturally occurring atmospheric sulphate derived from marine sources (sea spray) or from volcanic sources (from post emission oxidation of SO_2 and H_2S) deposited in the soil and sulphate minerals that has accumulated in the

unsaturated zone. The sulphate ion is negatively charged and is only held loosely on soil exchange sites which are highly soluble in water and therefore unless sulphate is used by plants it can leach down into the soil through the unsaturated zone to the saturated zone.

The exchangeable K and Na contents in the soil exchange phase increase as the ratio of Mg to Ca increases. Potassium and Na are more competitive against Mg than against Ca in the soil, as Ca adsorption is preferred over that of Mg. The degree of adsorption of preference for Na and K over that of Mg in soils, as compared with that of Ca, depends apparently on the nature of the exchangeable complex.

The sequence of order of major cation ions concentration in the soil showed that, sodium was the highest concentration followed by potassium, calcium and with magnesium been the least shown in the soil in the study area (Na > K > Ca > Mg). For the nutrients, sulphates have the highest value with nitrate being the least in the soil samples.

4.3 Trace Element in the Soil

The trace elements studied in the study area were Fe, Mn, Cu, As, V, Pb, Cr, Ni, Zn, and Co. The concentrations of the individual element in the soil can be found in Appendix I.

The range of Iron (Fe) concentration in the soil was from 15.24 mg/kg to 195.62 mg/kg with the mean concentration of 148.89 mg/kg (Appendix I). The variations in Fe can be attributed to natural variability such as weathering. Because weathered soils are enriched

with Fe which are heavily insoluble oxides due to leaching out of the soil by the downward movement of rainwater in the soil (Borgaard et al., 2004). The increment observed at the shallow depth near the surface can also be due to the fact that Fe is able to form oxides which are resistive to leaching from the surface.

Measured concentration of manganese (Mn) in the soil varied from 3.05 mg/kg to 76.46 mg/kg (Appendix I). Manganese normally occurs in rocks; however, humans enhance manganese concentrations in the environment by industrial activities and through the burning of fossil fuels (Nayaka et al., 2009). Manganese derived from human sources such as application of manganese pesticides can enter soils and groundwaters. Manganese forms heavily insoluble oxides which cannot be leached out by water under condition of rainfall hence its accumulation in the soil.

The concentration of copper ranged from 0.09 mg/kg to 5.75 mg/kg, with a mean value of 3.53 mg/kg in the soil (Appendix I). Copper occurs naturally in the environment and spreads through natural and artificial phenomena (Nayaka et al., 2009). Natural sources can be: decaying vegetation, potash from ashes and sea aerosol. Phosphate fertilizer production is another means of artificial phenomena that generate copper into environment. Most of the colloidal materials of soils (oxides of Mn, Al, and Fe, silicate clays and humus) adsorb Cu^{2+} strongly, and increasingly so as the pH is raised (McBride, 1994). Furthermore, Cu has a much lower mobility in reducing conditions.

The range of Arsenic (As) concentration in the soil is from <0.001 mg/kg to 167.33 mg/kg with a mean concentration of 67.25 mg/kg (Appendix I). Arsenic is found as a result of cycling vegetation, atmospheric deposition and adsorption by soil organic matter and as a result of agrochemicals (Alloway, 1995). Also, organic forms of As are often linked to methylation reactions by microorganisms, which leads to the formation of several possible compounds and is linked to the supply of anthropogenic compounds (e.g., fertilizers and pesticides). Arsenate (As(V)) and arsenite (As (III)) are the main forms of As in soils, with As(V) dominating in anaerobic soils, whereas As(III) predominate in slightly reduced soils, with increasing mobility under alkaline conditions (Sadiq, 1997). The soil at the study area is considered as anaerobic with Eh (+ 101.7 to – 1.2 mV) (Appendix III) and the changes in oxidation states linked to the variation in pH and Eh have slow kinetics in an aqueous system, which explains why the species found in interstitial water do not always follow to the expected distribution.

The range of concentration of Vanadium (V) in the study area was from 0.2 mg/kg to 4.8 mg/kg, with a mean concentration of 1.56 mg/kg (Appendix I). Vanadium is redox – sensitive elements, where their oxidation state as well as their solubility depends upon the redox conditions. Vanadium enrichment is also associated with heavy chemical industry such as oil refinery and paint manufacturing companies, however, Ekumfi Akwakrom and Ekumfi Asokwa are not close to any industry and concentration found in the study area is as a result of their association with the geology of the area (Fig 3.2). As a general result, vanadium solubility is driven both by pH, being greater in alkaline and lower in acid conditions, and by redox conditions. Vanadate anions adsorbed to both Mn and Fe

oxyhydroxides (Wehrli and Stumm, 1989) and bind on oxides and silicates most effectively at low pH (Appendix III), following the pattern of phosphate and other oxyanions.

The concentration of lead (Pb) varied from <0.001 mg/kg to 8.53 mg/kg, with a mean of 2.12 mg/kg in the study area. The low concentration along depth is due to the fact that Lead is the least mobile of the trace metals in soils and is particularly affected by reducing conditions. Higher pH and alkalinity promote Pb precipitation or co – precipitation as the carbonate. However, from (Appendix III), the pH of the study area is not high (slightly acidic to neutral) to promote this precipitation, hence is least detectable. Lead is also strongly chalcophilic and becomes very insoluble in reduced soils because of its precipitation by sulphide generated by sulphate reduction; however, the redox potential calculated does not seem to suggest these conditions for the soil studied (i.e. sulphate reduction), hence lower concentration.

The concentration of chromium (Cr) varied from 4.46 mg/kg to 120.33 mg/kg, with a mean value of 37.56 mg/kg. In general, chromium, as other oxyanion – forming elements tends to become less strongly sorbed as the pH increases (Dzombak and Morel, 1990). Chromium levels in soil vary according to area and degree of contamination from anthropogenic chromium sources (WHO, 2000). Besides, Cr can be mobilized as stable Cr(VI) oxyanion species under oxidizing conditions, but forms cationic Cr(III) species in reducing environment and hence behaves like other trace cations (i.e. is relatively immobile at near neutral pH values) (McGrath, 1995).

The measured concentration of Nickel (Ni) varied from 0.25 mg/kg to 34.37 mg/kg, with a mean of 11.71 mg/kg in the study area. Nickel occurs naturally in soils as a result of the weathering of the parent rock (McGrath, 1995). The highest concentrations are found in basic igneous rocks. Soil pH is the most important factor controlling nickel solubility, sorption and mobility with the clay; the solubility and mobility of nickel increases with decreasing pH (Kabata – Pendias and Mukherjee, 2007; McGrath, 1995). Many nickel compounds are soluble at a pH less than 6.5 (IPCS, 1991).

The concentration of Zinc (Zn) varied from 0.05 mg/kg to 2.00 mg/kg, with a mean value of 1.19 mg/kg in the study area. Zinc is an element commonly found in the Earth's crust ad has both natural and anthropogenic sources. However, Zn from anthropogenic sources is greater than those from natural sources. The primary anthropogenic sources of zinc in the environment (air, water, soil) are related to mining and metallurgic operations involving zinc and use of commercial products containing zinc, but no such activity goes on in the study area, hence the low concentration found is natural environment. Zinc does not volatilize from water but is deposited primarily in sediments through adsorption and precipitation.

The measured concentration of Cobalt (Co) varied from 0.27 mg/kg to 3.45 mg/kg, with a mean of 1.99 mg/kg in the study area. Cobalt is a compound which occurs in nature. Some natural sources of cobalt in the environment are soil, dust, and seawater. Cobalt is released from burning of coal and oil, and from car and truck exhaust. Natural sources include erosion (wind-blown continental dusts), weathering of rocks, soil, seawater

aerosol spray, forest fires, and continental and some marine biogenic emissions (Dalvi and Robbins 1978).

High background concentrations of trace elements, both natural and anthropogenic, could result in mobilization and release of trace elements into the unsaturated zone and groundwaters system. Soil factors such as organic matter, type and amount of clay, and pH influence the quantity of trace elements available for mobilization and release or sorption in a soil.

4.4 Chloride Profiles in the Unsaturated Zone

Chloride (Cl^-) from atmospheric deposition (including dry – fall and rainfall) moves into the soil with infiltrating rainfall and evaporation causes chloride to accumulate in the soil because chloride is not taken up by plants and is non – volatile. Chloride is extremely soluble and is not found in the solid phase but moves conservatively in water throughout the unsaturated zone. Chloride is mobile, non – reactive and not significantly adsorbed onto mineral surfaces, and is therefore often used as a tracer of water movement in soil.

It was assumed that chloride in the study area is derived from aerosol deposition from the sea which includes both dry – fall and rainfall, and no other source or sinks are available in the study area, whilst it was also assumed that the area receives equal amount of chloride deposition from the sea, based on the analysis of the rainwater samples from the area. An average of 11.10 mg/L of chloride concentration for three (3) years (2010 to

2012) has been deposited in the soil. The mean annual chloride and rainfall for individual years is shown in Figure 4.2 and (Appendix VII).

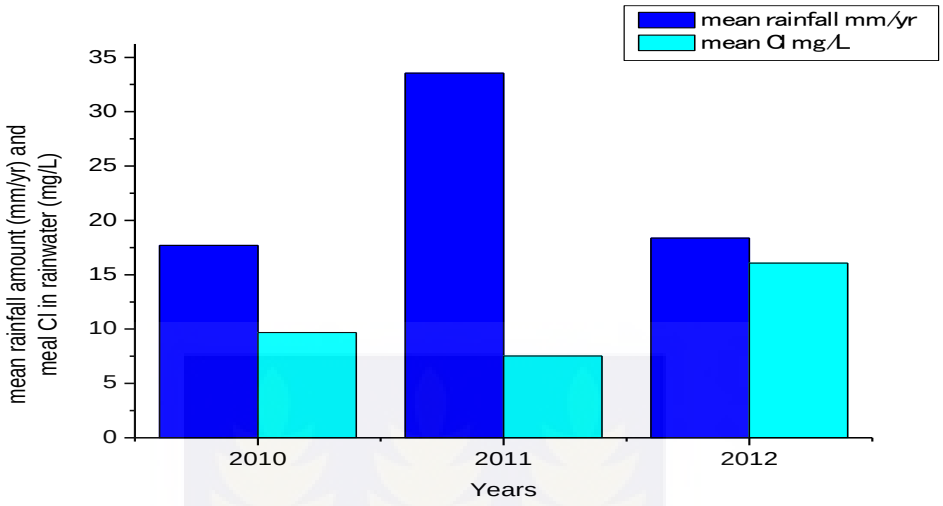

Fig 4.2: Mean rainfall and chloride concentration from 2010 to 2012 years

Nine (9) profiles (P) were drilled and the soil sampled for Cl^- analysis as described in section 3.2.2. The profiles was distributed as (1) upstream (P1 to P3), (2) intermediate (P4 to P6) and (3) lower/downstream (P7 to P9) as shown in Figure 3.1.

Chloride concentrations within the profiles display a wide variability in their maximum chloride concentrations, in the study area. The mean chloride concentration for the nine (9) profiles in the unsaturated zone in the study area is 96.95 mg/kg. The minimum and maximum values recorded are 24.99 mg/kg and 449.86 mg/kg, respectively, these are shown in Figure 4.3 and Appendix II. The individual profile shows a variation in Cl^- concentration and these are discussed below together with other physical parameters along each profile.

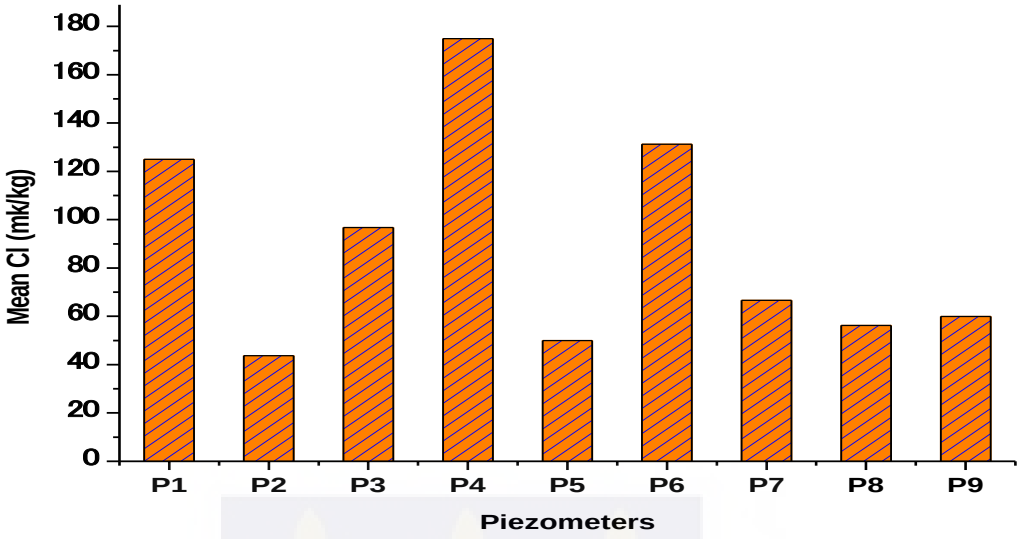

Fig 4.3: Mean Cl concentrations in mg/kg for the individual soil profiles in the study area

Profile 1 (Fig. 4.4) is located upstream of the study area. The maximum depth drilled was 60.0 cm because of the impermeable clay and pebbles at that depth (Appendix IV). The mean Cl^- concentration measured is 124.96 mg/kg, as shown in Fig. 4.3; whilst the range is from 24.99 mg/kg to 249.92 mg/kg.

The chloride profiles can be broken up into two periods; a period of low deposition with Cl^- concentration of 24.99 mg/kg and a period of high deposition which is characterised with a Cl^- peak of 249.92 mg/kg at 40.0 cm. The low Cl^- concentration suggests that there were no deposition at a certain period or the amount deposited in the soil was minimal whilst the Cl^- peak suggests a period of high Cl^- deposition, which has being accumulated over years. Below this peak, chloride decreases to a minimum concentration of 99.97 mg/kg which suggests that, either Cl^- has been leached or dissolved in the percolating water.

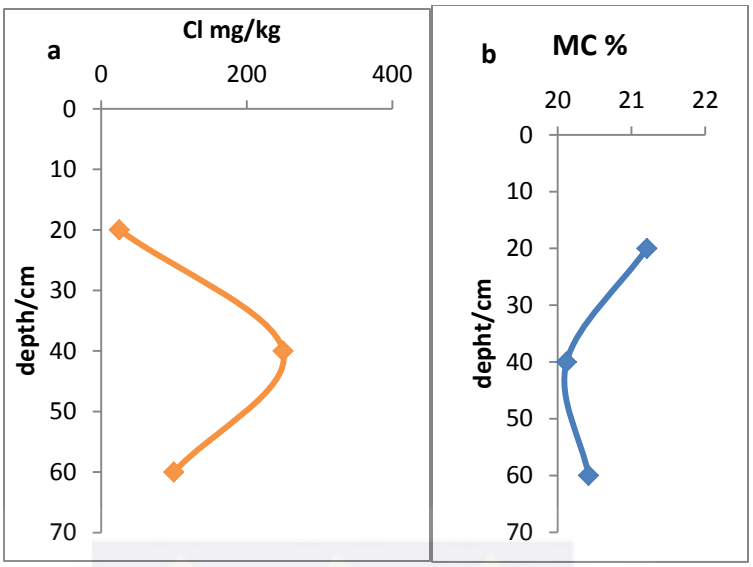

Fig 4.4: Profile 1, variation of (a) Cl concentration and (b) moisture content with depth

The zones of high concentration corresponded to low moisture content within the profile and the zones of low Cl^- concentration corresponded to high moisture content suggesting infiltration of rainwater (Appendix III). The accumulation may come as result of either high evaporation occurring during that period or aerosol deposition by rainfall or dry fallout.

Profile 2 (Fig. 4.5) is located upstream and it is 2.0 m from profile 1 (Fig. 3.1). The maximum depth reached was 80.0 cm below the surface; this is because of the lateritic soil and rocky nature at that depth, (Appendix IV).

The profile is characterized by low Cl^- concentrations. The mean Cl^- concentration is 43.74 mg/kg, as shown in Fig 4.3; whereas the range is from 24.94 mg/kg to 49.98 mg/kg (Appendix II).

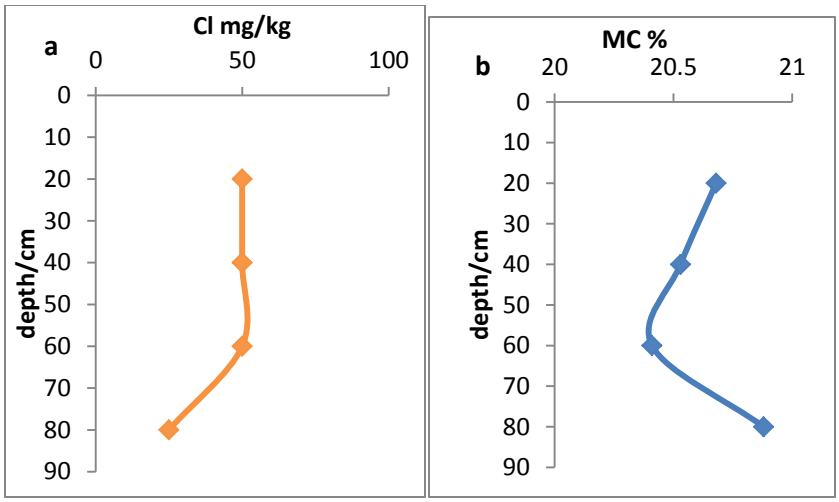

Fig 4.5: Profile 2, variation of (a) Cl concentration and (b) moisture content with depth

The topmost part of the profile (20.0 cm to 60.0 cm) shows low Cl^- deposition of 49.98 mg/kg which remained constant within this depth and decreased to 24.94 after 60.0 cm. This suggests that, Cl^- is non – volatile and is not removed by evaporation or by plant transpiration and no other source has been incorporated into the soil apart from the Cl^- in rainwater. Below 60.0 cm, chloride decreased to minimum concentration of 24.94 mg/kg, which suggests a period of no deposition of Cl^- in the unsaturated zone or the Cl^- zone was missed during drilling.

Profile 3 (Fig. 4.6) is also located upstream and is 2.0 m from profile 2, (Fig. 3.1). The maximum depth reached was 60.0 cm below the surface; this is because of the impermeable rock (pebbles) nature, as shown in Appendix IV. The profile is characterized by high Cl^-concentrations at 20.0 cm and 60.0 cm. The mean Cl^- concentration is 96.64 mg/kg, as shown in Fig 4.3, whilst the range is from 89.99 mg/kg to 99.97 mg/kg in the profile.

The chloride concentration in this profile is similar to that of profile 1 but as a mirror image. At 20.0 cm, the Cl^- concentration is high suggesting a period of deposition and a zone of accumulation of Cl^- as a result of evaporation.

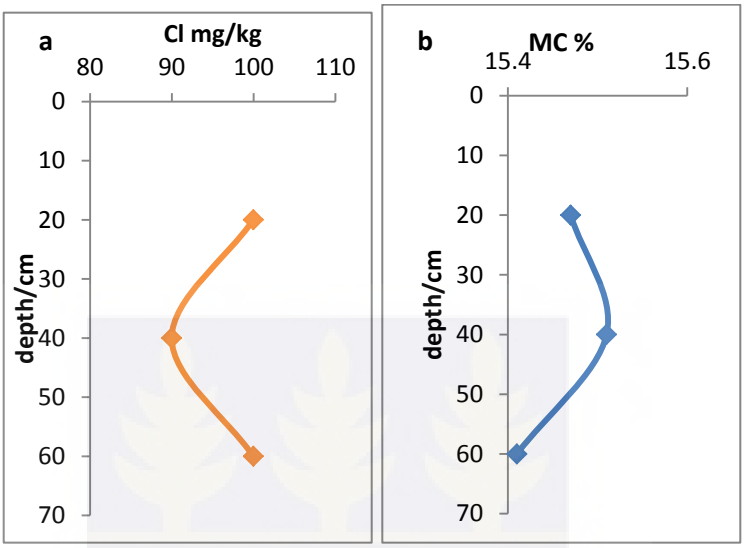

Fig 4.6: Profile 3, variation of (a) Cl concentration and (b) moisture content with depth

Below the 20.0 cm, the Cl^- concentration decreased slightly to 89.99 mg/kg at 40.0 cm and increase again to a concentration of 99.97 mg/kg. The decrease in concentration suggests that, either Cl^- is dissolved by the percolating water as it moves to the groundwater or the Cl^- zone was missed during drilling or it may have been shifted due to morphology. The zones of high concentration corresponded to low moisture content within the profile and the zones of low Cl^- concentration corresponded to high moisture content suggesting infiltration of rainwater (Appendix III).

Profile 4 (Fig 4.7), is located at the intermediate stream and is about 200.0 m from profiles in the upstream Fig 3.1. The maximum depth drilled is 200.0 cm below the

surface; this is because of the impermeable silt which was partly clayey, sandy and partly laterite, as shown in Appendix IV. The profile is characterized by low to high Cl^- concentrations. The mean Cl^-concentration measured is 174.95 mg/kg, as shown in Fig 4.3, whilst the range is from 49.99 mg/kg to 449.86 mg/kg.

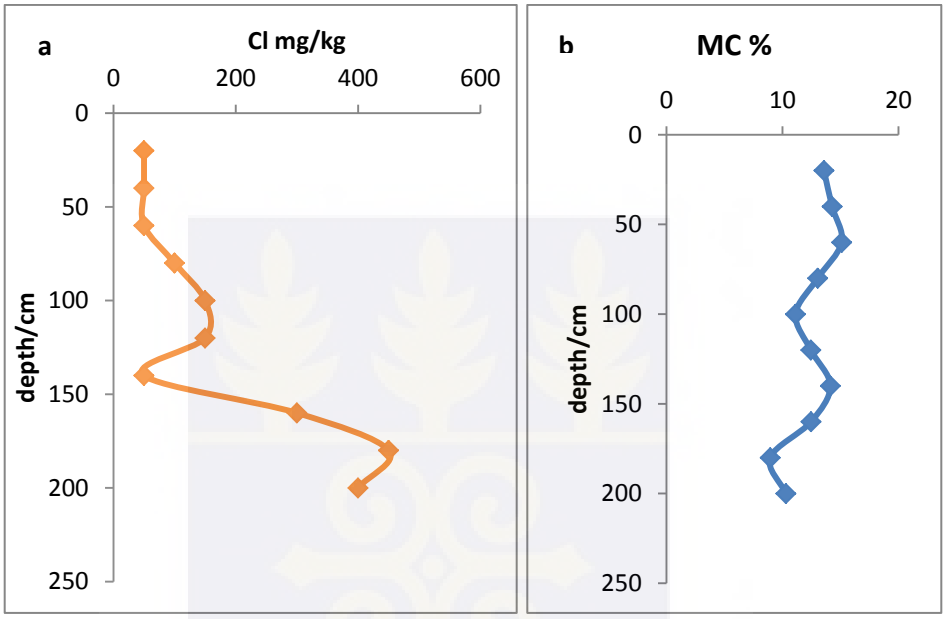

Fig 4.7: Profile 4, variation of (a) Cl concentration and (b) moisture content with depth

The Cl^-concentration between 20.0 cm and 60.0 cm is 49.99 mg/kg, these values suggests that, there were no deposition or accumulation of Cl^- at these depths or Cl^- has been dissolved and leached out in that period, because $Cl^-$is mobile, soluble, non-reactive and not significantly adsorbed onto mineral surfaces. Below this depth, Cl^-concentration increased to 149.95 mg/kg and forming zone of accumulation at 100.0 cm and 120.0 cm. The concentration decreased to the initial Cl^- concentration at depth of 140.0 cm and then finally increased to 449.86 mg/kg at a depth of 180.0 cm.

The profile shows two peaks between 100.0 cm and 120.0 cm; and at 180.0 cm, which suggest zones of accumulations and different period of deposition of Cl^-, because of differences in their concentrations. These peaks also suggest either, dissolution of evaporites left behind after the last seawater or brine retreat or accumulation of salts derived from long term deposition of atmospheric fallout, because Cl^- is mobile, soluble, non – reactive and therefore moves with water in the unsaturated zone. The maximum peak suggests a period of high deposition and accumulation of Cl^- in the unsaturated zone.

The soil texture above 80.0 cm depth is much coarser grained than that below this depth, the transition of from coarse soil to deeper clay corresponds to a marked increase in moisture content (Appendix IV). The zones of high Cl^- concentration correspond to low moisture content within the profile and the zones of low Cl^- concentration correspond to high moisture content (Appendix III).

Profile 5 (Fig 4.8) is located at the intermediate stream, 2.0 m from profile 4, which is characterized by the same amount of Cl^-concentrations within the entire profile. The mean Cl^- concentration is 49.99 mg/kg as shown in (Fig 4.3). This profile is actually marked by a period of no deposition Cl^- by rainfall or dry fallout by wind. The moisture content within the profile was uniform (Appendix III).

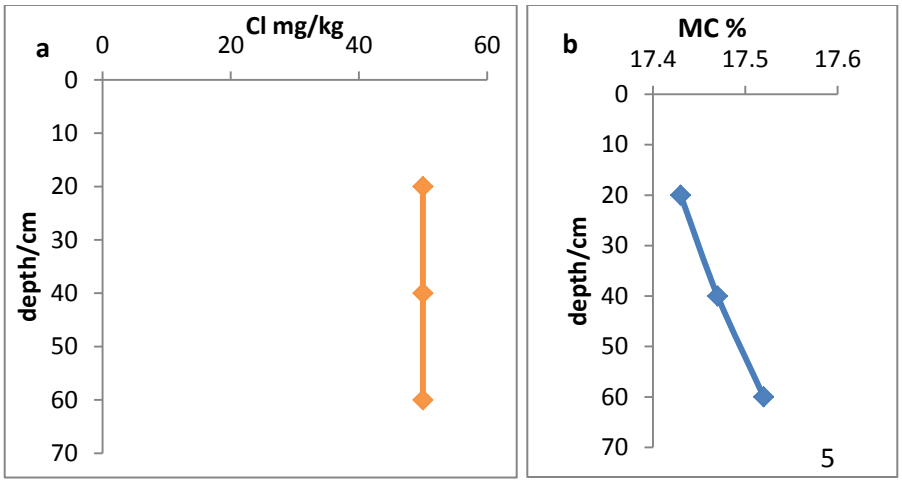

Fig 4.8: Profile 5, variation of (a) Cl concentration and (b) moisture content with depth

Profile 6 (Fig 4.9) is located at intermediate and is 2.0 m from profile 5 (Fig 3.1). The maximum depth drilled is 160.0 cm below the surface; this is because of the impermeable silt which was partly clayey, sandy and partly laterite nature, as shown in Appendix IV. The mean Cl^- concentration is 131.21 mg/kg, as shown in (Fig 4.3), whilst it ranged from 49.99 mg/kg to 249.22 mg/kg within the profile.

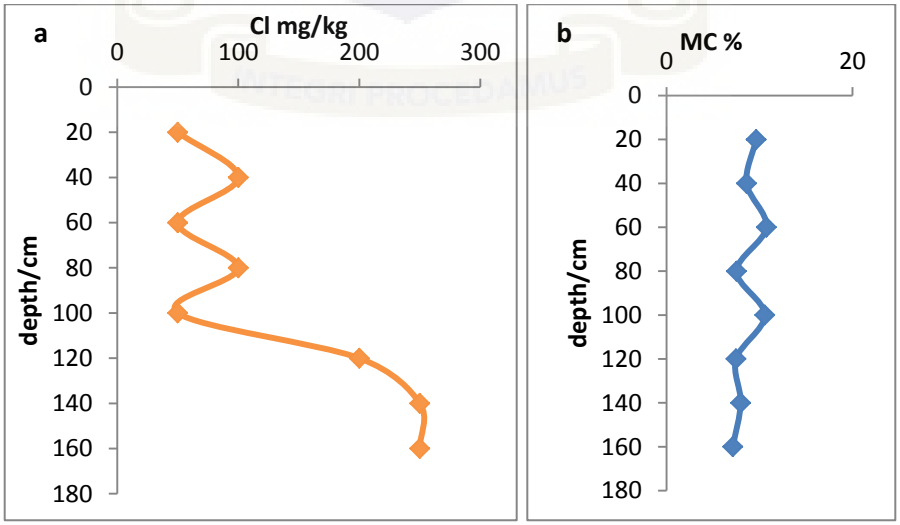

Fig 4.9: Profile 6, variation of (a) Cl concentration and (b) moisture content with depth

The chloride profiles in profile 6 can be broken up into two sections; the top part of the profile (20.0 cm to 100.0 cm) showing increasing and decreasing Cl^- concentration (49.99 to 99.96 mg/kg) characterised with smaller Cl^- peaks, suggesting a minimal or no deposit of Cl^- at these depths and accumulation of Cl^- as a result of evaporation.

Increased chloride concentrations were also observed at depths from 100.0 cm to 160.0 cm within the profile, with the maximum Cl^-concentration of 249.22 mg/kg at 160.0 cm. These suggest dissolution of Cl^- by the percolating water, because Cl^- is mobile, soluble, non – reactive and therefore moves with water in the unsaturated zone and accumulated at (160.0 cm) below the surface and form Cl^- peak. The peak also suggests either, dissolution of evaporites left behind after the last seawater or brine retreat or accumulation of salts derived from long term deposition of atmospheric fallout. The changes in chloride concentrations gradually correspond to changes in moisture content where the chloride peaks occur in the zone of low moisture content (Appendix III).

Profile 7 (Fig 4.10), is located at lower/downstream and it is about 150.0 m from profile 6 (Fig 3.1). The maximum depth reached was 180.0 cm below the surface; this is because of the impermeable silt which was brownish clayey soil and lateritic nature at that depth in which the hand auger could not drill through, (as shown in Appendix IV). The mean Cl^- concentration is 66.65 mg/kg as shown in Fig 4.3, whilst the range was from 49.99 mg/kg to 99.97 mg/kg within the profile.

This profile is actually marked by two events of Cl^-deposition; a period of no or minimal Cl^- deposition and period of maximum deposition.

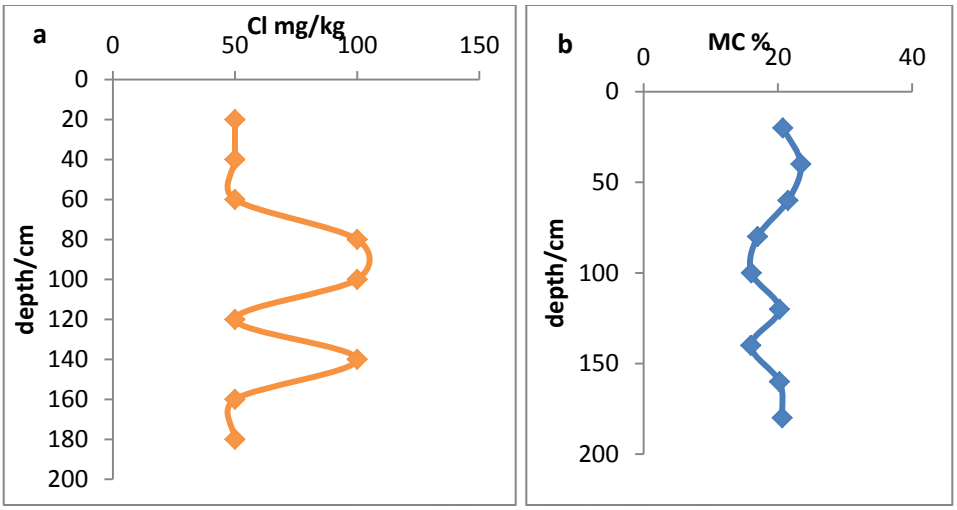

Fig 4.10: Profile 7, variation of (a) Cl concentration and (b) moisture content with depth

The profile also shows two peaks which suggest different period of deposition and accumulations of Cl^-concentration after dissolution of Cl^- by the percolating water, and $Cl^-$is mobile, soluble, non – reactive and therefore moves with the water in the unsaturated zone and accumulated at a certain depths (80.0 and 140.0 cm) below the surface and forming a peak.

These peaks also suggest either, dissolution of evaporites left behind after the last seawater or brine retreat or accumulation of salts derived from long term deposition of atmospheric fallout. The maximum peak suggests a period of high deposition and accumulation of Cl^- in the unsaturated zone.

The soil texture above 80.0 cm depth was much coarser in grained than the soil texture below this depth and transition of from coarser soil to deeper clay corresponds to a marked increase in moisture content (Appendix IV). The zones of high concentration correspond to low moisture content within the profile and the zones of low Cl^- concentration correspond to high moisture content (Appendix III).

Profile 8 (Fig 4.11) is located at lower/downstream and it is about 2.0 m from profile 7 (Fig 3.1). The maximum depth reached was 160.0 cm below the surface; this is because of the impermeable clayey soil and rocky nature pebbles (Appendix IV).

The mean Cl^- concentration was 56.22 mg/kg, (as shown in Fig 4.3), whilst the range was from 49.99 mg/kg to 99.97 mg/kg within the profile.

Profile 8 showed two depositional period of Cl^-concentrations; a period of no or minimal Cl^-deposition and period of maximum deposition. The period of no deposition of Cl^-concentration occurred at 20.0 to 100.0 cm, and 140.0 to 160.0 cm with a concentration of 49.99 mg/kg.

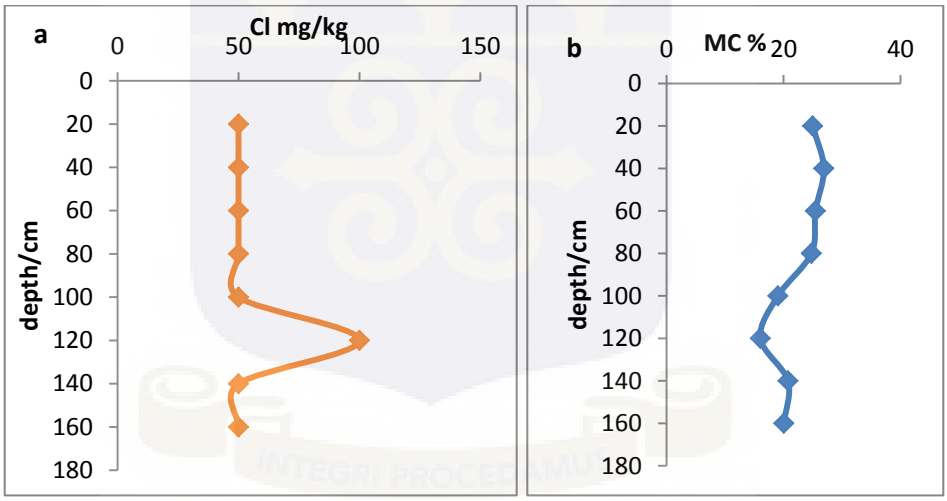

Fig 4.11: Profile 8, variation of (a) Cl concentration and (b) moisture content with depth

The profile also showed a peak of Cl^- concentration which were observed at 120.0 cm depth, suggesting period of deposition and accumulations of Cl^- concentration of 99.97 mg/kg after dissolution of Cl^- by the percolating water, because Cl^- is mobile, soluble, non – reactive and therefore moves with water in the unsaturated zone and accumulated at a depth of 120.0 cm below the surface and forming a peak.

The changes in chloride concentrations gradually correspond to changes in moisture content where the chloride peaks occur in the zone of low moisture content.

Profile 9 (Fig 4.12) is located at lower/downstream and it is 2.0 m from profile 8. The maximum depth drilled was 100.0 cm because of impermeable clay and gravel at that depth (Appendix IV). The mean Cl^- concentration is 59.98 mg/kg as shown in Figure 4.3, whilst the range was from 49.99 mg/kg to 99.97 mg/kg within the profile.

This profile showed two depositions period of Cl^-concentrations; a period of no or less Cl^- deposition and a period of high deposition. The period of no deposition of Cl^- concentration occurred at 20.0 to 40.0 cm, and 80.0 to 100.0 cm with a concentration of 49.99 mg/kg.

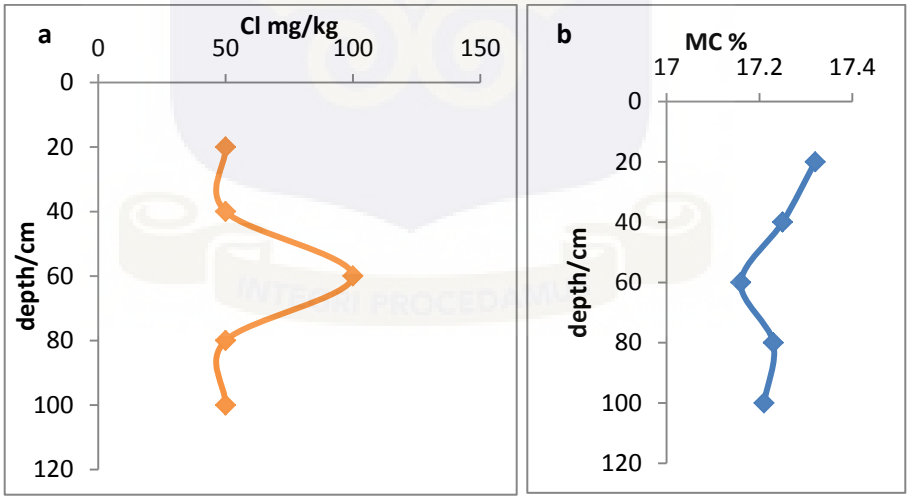

Fig 4.12: Profile 9, variation of (a) Cl concentration and (b) moisture content with depth

The profile also shows a peak which is observed at 60.0 cm depth, suggesting period of deposition and accumulations of Cl^- concentration of 99.97 mg/kg after dissolution of

Cl^- by the percolating water, because, Cl^- is mobile, soluble, non – reactive and therefore moves with water in the unsaturated zone and accumulated at a depth of 60.0 cm below the surface and forming a peak.

The shape of the peak in this profile is similar to profile 8 but at different depth.

The zones of high concentration corresponded to low moisture content within the profile and the zones of low Cl^- concentration corresponded to high moisture content (Appendix III).

Most of the world's chloride is either found in oceans or in salt deposits left by evaporation of old inland seas or accumulation of salts derived from long term deposition of atmospheric fallout. Near the coast, many soils and crops receive more than adequate supply of Cl^- from wind borne sprays of rain. Salts present in the subsoil or deeper formations accumulate from ocean salt carried in rain (aerosols) into a previously highly leached landscape, or the salts are derived from weathering of the mineral constituents. The accumulation of these salts over thousands of years is considerable and the amount of salt stored in the soil profile depends mainly on the soil type and the mean annual rainfall. The salt content is generally higher in clayey soils than in sandy soils, and the salt content changes inversely with average annual rainfall, which is confirmed from (Appendix IV), in which about 70 to 85 % of the soil type is clay.

Chloride in rainfall and dry fallout is transported into the unsaturated zone with infiltrating water and increases through the root zone as a result of evaporation and transpiration, because chloride is non – volatile and is not removed by evaporation or by

plant transpiration. Lower evaporation rates and heavy rainfall allow more chloride to flush through the soil profile and accumulates at certain depths below the surface, as observed in Figures 4.4 to 4.12.

In the upper 40.0 cm of the unsaturated zone, chloride concentrations are very low, reflecting repeated flushing by rainfall or no deposition of Cl^-. Below this depth (40.0 cm), each of the profiles quickly reaches a maximum concentration, ranging from 49.92 to 449.86 mg/kg with the exception of Figure 4.8 which showed the same amount of Cl^- concentration within the entire profile (49.99 mg/kg). This suggests no deposition within that period. Also shown in the figures are both larger and smaller Cl^- peaks which are typical of many chloride profiles in arid regions and may be the result of climatic change.

The chloride concentrations are not constant with depth but vary and each profile shows a distinct chloride peak of high concentration. The changes in chloride concentrations gradually correspond to changes in moisture content, where the chloride peaks occur in the zone of low moisture content. These peaks represent a past period of low percolation rates and high evaporation and transpiration, which was followed by a period of higher percolation rates and lower evapotranspiration that displaced the chloride peaks. The high Cl^- peaks in the Figures (4.4, 4.7, and 4.9 to 4.12) is probably as a result of salt accumulation Cl^- over several years. The combination of low chloride at depth, and significant differences in stored chloride within the individual profiles and the presence of secondary bulges suggest a series of recharging events to which the soil profiles have responded in varying ways.

Groundwater sources become saline due to the excess of evaporation over rainfall and the resultant poor flushing. Salinity is introduced from the accumulations of salts in the soil and on the surface, through the intermediary of floods and recharge waters as in the case of groundwaters in Ekumfi Akwakrom and Ekumfi Asokwa. The groundwaters act as diluting agent and generally one then finds an inverse relation between the discharge rate and the salinity. Dissolution of Cl^- by the slowly movement of groundwaters contributes to these salinity (high Cl^- concentration) build up in the soil zones and in the groundwaters along the coastal aquifers.

Each of these sources has a unique and distinctive chemical and isotopic composition. The integration of geochemical and isotopic tracers can be used to resolve multiple sources.

4.3. Stable Isotope composition in rainwater, groundwater, soil water extract and water from unsaturated zone,

Composition of oxygen – 18 and deuterium of the rainwater, water from the unsaturated zone, groundwater and water extracted from soil are presented in Appendix V and VI. The stable isotope data are expressed as per mil deviations from VSMOW standard.

Rainfall is the source of recharge of the groundwater in the Ekumfi Akwakrom and Ekumfi Asokwa area.

Rainwater samples were collected from the Saltpond Meteorological Station for stable isotopic composition. The isotopic composition of the rain water samples are plotted on

Fig 4.13; while, Fig 4.14 shows a plot of δ^2H ‰ - $\delta^{18}O$ ‰ for groundwater, water extracted from soil and water from unsaturated zone.

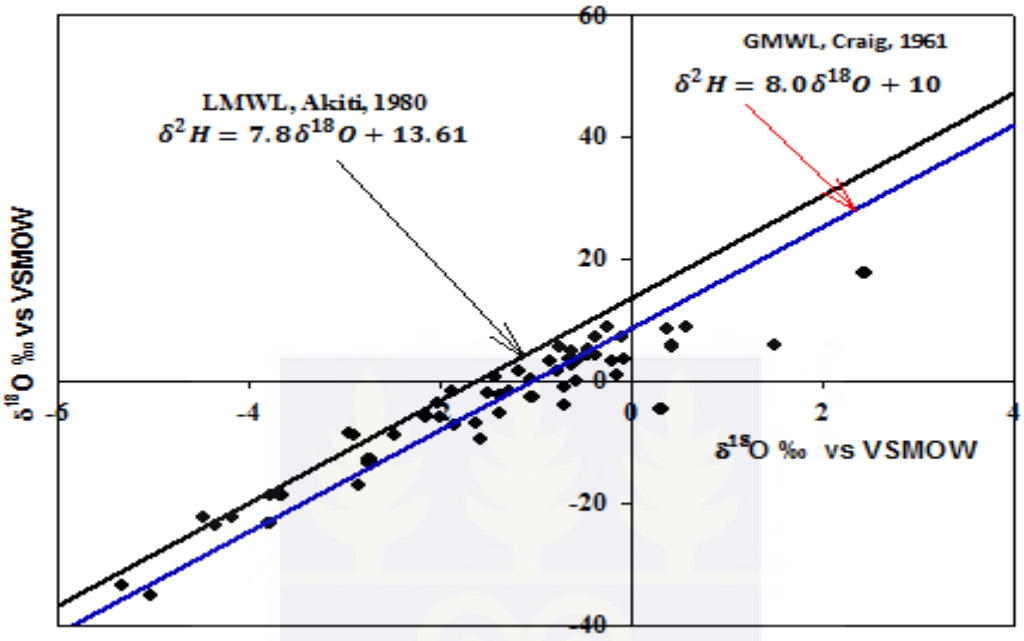

Fig. 4.13: Relationship between δ^2H vs VSMOW and δ^{18}O vs VSMOW in rainwater

From the analysis of the water samples (rainwater, groundwater, water extracted from soil and unsaturated zone), the mean isotopic composition of rainwater for $\delta^{18}O$ ‰ is – 1.47 ‰ vs VSMOW and δ^2H ‰ is – 4.09 ‰ vs VSMOW whereas the range of $\delta^{18}O$ is from + 2.44 ‰ vs VSMOW to – 5.33 ‰ vs VSMOW and + 17.82 ‰ vs VSMOW to – 35.21 ‰ vs VSMOW for δ^2H ‰. The points are scattered around the Global Meteoric Water Line (GMWL) and Local Meteoric Water Line (LMWL).

The mean isotopic composition of water extracted from soil is – 2.85 ‰ vs VSMOW for $\delta^{18}O$ ‰ and – 21.33 ‰ vs VSMOW δ^2H ‰ whilst the range of $\delta^{18}O$ is from + 3.40 ‰ vs VSMOW to – 5.02 ‰ vs VSMOW and – 6.08 ‰ vs VSMOW to – 29.06 ‰ vs VSMOW for δ^2H ‰.

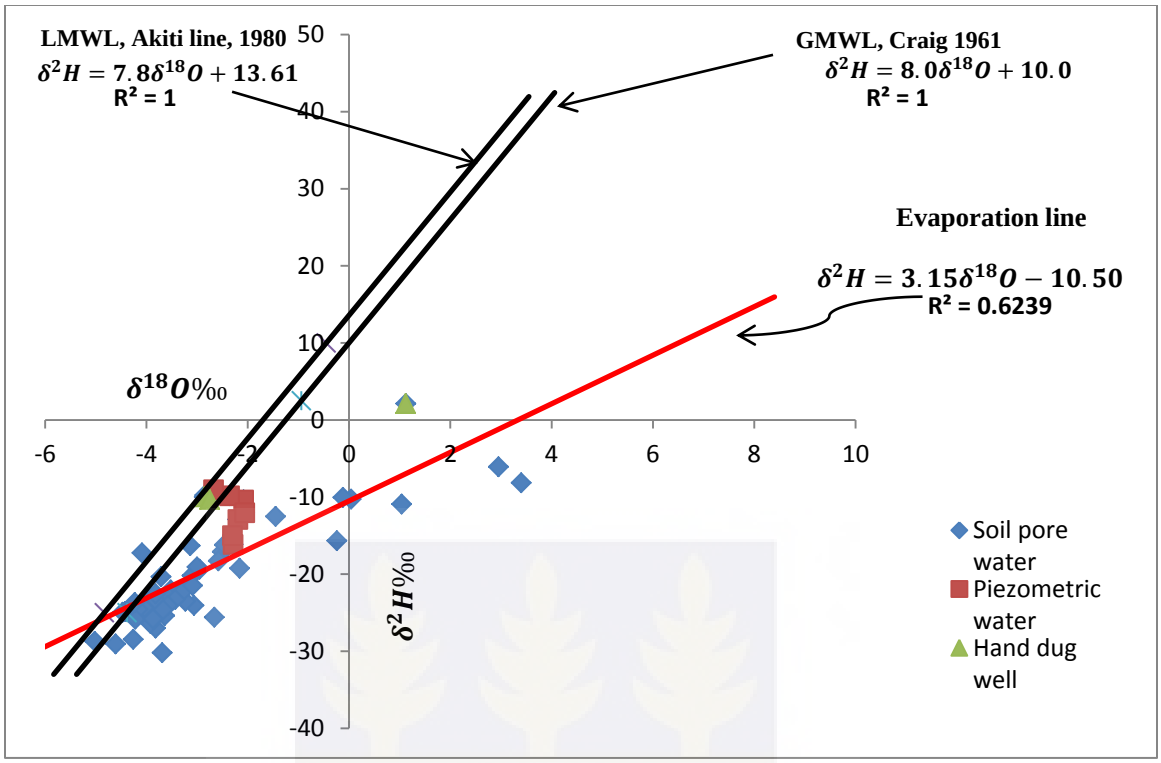

Fig. 4.14: Relationship between δ^2H vs VSMOW and δ^{18}O vs VSMOW water

The mean isotopic composition of water from the unsaturated zone is – 2.28 ‰ vs VSMOW for $\delta^{18}O$ and – 12.19 ‰ vs VSMOW for δ^2H ‰ whilst the range of $\delta^{18}O$ ‰ is from – 2.06 ‰ vs VSMOW to – 2.67 ‰ vs VSMOW and – 9.82 ‰ vs VSMOW to – 16.1 ‰ vs VSMOW for δ^2H ‰.

Figure 4.13 and 4.14 also show the relationships between $\delta^{18}O$ ‰ and δ^2H ‰ compared with the global meteoric water line (GMWL) and local meteoric water line (LMWL).

The isotopic content of rainwater is more enriched with heavier isotopes. The enrichment of the rainwater may be attributed to evaporation and amount effect of the descending raindrops with atmospheric moisture, because smaller/low rainfall tend to have more positive values due to evaporative enrichment as drops fall through dry air and causes enrichment in the heavy isotopes. Also, the positive values of the rainwater and the

deviations from the GMWL line indicate a degree of isotopic enrichment as a result of evaporation.

In this study, the seasonal effect of rainfall was not obvious because the rainfall was not sampled during the entire rainfall event.

Figure 4.14 shows the relationship between groundwater water extracted from soil and water from the unsaturated zone. Some of the samples plotted on and near the local meteoric water line (LMWL), with majority of the samples clustering around the global meteoric water line. Those that were plotted closer or on the (GMWL), in Fig 4.14, are in direct equilibrium with GMWL. Evaporation line (red line) is drawn to account for those that plotted away from the GMWL, which showed little evaporation in the unsaturated zone as compared with the rainwater.

When the mean isotopic composition of the rainwater (– 1.47 ‰ vs VSMOW and – 4.09 ‰ vs VSMOW) for both $\delta^{18}O$ ‰ and $\delta^{2}H$ ‰ respectively is compared to the mean of water extracted from soil (– 2.85 ‰ vs VSMOW and -21.33 ‰ vs VSMOW), for both $\delta^{18}O$ ‰ and $\delta^{2}H$ ‰, it is seen that, rainwater is relatively more enriched than the water extracted from soil and water from unsaturated zone. The enrichment can be attributed to a number of reasons. These are that: (i) rainfall suffered some level of evaporation before infiltrating into the soil, (ii) water extracted from soil and unsaturated zone might have suffered a little evaporation prior to the sampling since sampling was done after the major rainy season, and (iii) mixing of existing waters in the unsaturated zone with recent rainwater, and this is can be attributed to the slower movement of groundwater.

It can be inferred from Appendix III that majority of the soil texture is clay, and this has the ability to hold water for a longer period because of its smaller pores.

The slope of the fitting line of water extracted from soil, groundwater and water from unsaturated zone (the red line in Fig 4.14) is given as:

$$\boldsymbol{\delta^2 H = 4.22\delta^{18}O - 7.10} \ (r^2 = 8.1) \qquad \textbf{4.3}$$

is significantly lower than the Local or Global Meteoric Water Lines. Such a low slope in the δ^2H – δ^{18}O relationship may therefore be due to isotopic fractionations as a result of evaporation from the near surface. This process is a result of semi – arid climatic conditions characterizing the study area.

By comparing isotope composition of rainwater, groundwater; water extracted from soil and water from unsaturated zone, the isotope values suggest that water from the unsaturated zone originated from rainfall but suffered little evaporation during the infiltration process which causes some of the δ^{18}O and δ^2H to depart to the right – side of LMWL in Fig 4.14.

One way of determining the average initial isotopic composition of infiltrating water and the importance of evaporation is to calculate an evaporation trend of the data and plot this line against the meteoric water line on the δ^2H - $\delta^{18}O$ diagram, the red line in Fig 4.14. The evaporative trend line is obtained by calculating a linear regression of the isotopic compositions of water. The point of intersection between the local meteoric water line and the evaporation trend line represents the average isotopic composition of infiltrating water, the red line in (Newman et al., 1997).

4.3.1 Stable isotope composition of water extracted from soil along the profiles

The isotope composition of water in the unsaturated zone is affected by rainfall, evaporation and transpiration which can influence deuterium and oxygen – 18 isotope composition in the unsaturated zone. Generally, the infiltration of water and uptake of water by plant cannot cause the isotope fractionation, whilst evaporation and the amount effect of rainfall can change the isotopic composition of rain and can cause isotope fractionation. Therefore, during periods of heavy rain (rainy season), less evaporation will occur resulting in more depleted values of deuterium and oxygen – 18 isotopic composition.

The extraction of water from the soil was carried out on six (6) out of the nine (9) profiles and the results are discussed here. Figures 4.15 to 4.20 show each profile and (Appendix V) shows the soil characteristics.

The $\delta^{18}O$ ‰ and $\delta^{2}H$ ‰ composition of water samples measured from the soil extracts is expressed in per mil units relative to Vienna Standard Mean Ocean Water (VSMOW).

Vertical profiles of water from the unsaturated zone and $\delta^{18}O$ were investigated to determine the soil water movement with depth (cm) in the study period (Figs. 4.15 to 4.20).

Profile 2 (Fig 4.15) is located upstream (Fig 3.1). The isotopic composition for the profile ranged from – 4.61 ‰ vs VSMOW to + 2.95 ‰ vs VSMOW for $\delta^{18}O$ and – 29.06 ‰ vs VSMOW to ‰ – 6.08 vs VSMOW for $\delta^{2}H$, whilst the mean for both $\delta^{18}O$ and $\delta^{2}H$ for the profile was – 2.06 ‰ vs VSMOW and – 20.31 ‰ vs VSMOW, respectively. The

profile shows isotopic enrichment (+ 2.95 ‰) for $\delta^{18}O$ at the top (0.0 to 30.0 cm); which signifies high evaporation near the surface, because there was little vegetation cover.

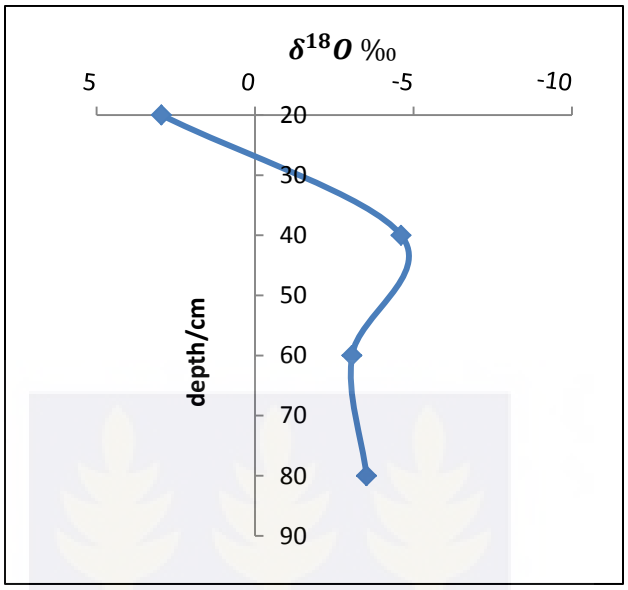

Fig. 4.15: Profile 2, vertical variation of $\delta^{18}O$ ‰ vs VSMOW of extracted water with depth

Below 30.0 cm, the isotopic content becomes depleted with the heavy isotopes. The depletion of the isotopic composition of this profile is not uniform because the $\delta^{18}O$ at 40.0 cm is – 4.61 ‰ vs VSMOW and that for 60.0 cm and 80.0 cm are – 3.06 ‰ vs VSMOW and – 3.52 ‰ vs VSMOW, respectively. This could be due to mixing water with different isotopic compositions. The net effect of evaporation is an enrichment of heavy isotopes ($\delta^{18}O$ ‰) near the soil surface.

Profile 3 (Fig 4.16) is also located at the upstream together with Profile 2 with an interval of 2.0 m between them (Fig 3.1). The isotopic composition for the profile ranged from – 3.82 ‰ vs VSMOW to– 0.24 ‰ vs VSMOW for $\delta^{18}O$ and – 26.99 ‰ vs VSMOW to–

15.67 ‰ vs VSMOW for δ^2H, whilst the mean for $\delta^{18}O$ was – 2.58 ‰ vs VSMOW and δ^2H is – 24.29 ‰ vs VSMOW.

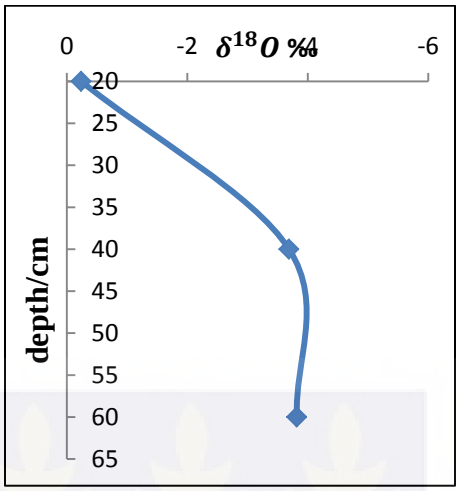

Fig. 4.16: Profile 3, vertical variation of $\delta^{18}O$ ‰ vs VSMOW of extracted water with depth

The profile showed isotopic enrichment (– 0.24 ‰ vs VSMOW) for $\delta^{18}O$ at the top (0.0 to 30.0 cm). This can be attributed to evaporation at the surface, because of vegetation cover found in the location which reduced the rate of evaporation. Below 30.0 cm, the isotopic content becomes depleted with the heavy isotopes. The depletion in isotopic composition of this profile is uniform, because $\delta^{18}O$ at 40.0 cm is – 3.69 ‰ and that for 60.0 cm is – 3.82 ‰. There are close and can be attributed to recent rainwater which shows a piston flow and pushes the existing water in the soil pores downwards.

Profile 4 (Fig 4.17) is also located at the intermediate stream. Profile 4 is located about 200.0 m from Profile 3. The isotopic composition for the profile ranged from – 5.02 ‰ vs VSMOW to + 1.04 ‰ vs VSMOW for $\delta^{18}O$ and – 28.72 ‰ vs VSMOW to– 10.91 ‰ vs VSMOW for δ^2H whilst the mean for $\delta^{18}O$ is – 3.06 ‰ vs VSMOW and δ^2H was – 21.50 ‰ vs VSMOW.

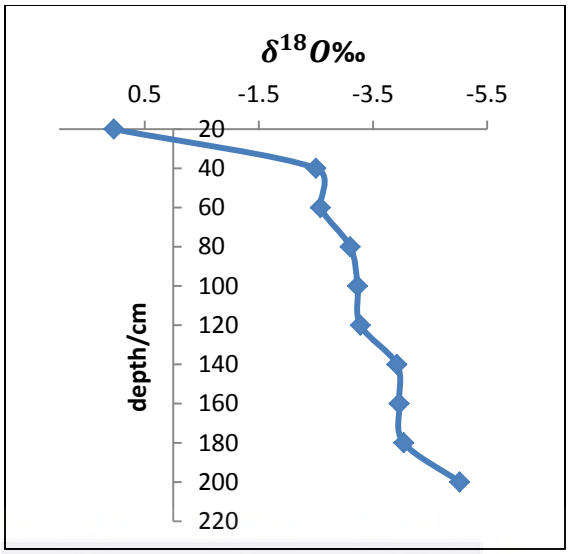

Fig. 4.17: Profile 4, vertical variation of $\delta^{18}O$ ‰ vs VSMOW of extracted water with depth

The profile showed isotopic enrichment (+1.04 ‰ vs VSMOW) for $\delta^{18}O$ at the top (0.0 to 30.0 cm) which suggests that high evaporation occurred near the surface. Below 30.0 cm, the isotopic content becomes depleted with the heavy isotopes. The depletion in isotopic composition of this profile along depth is non – linear. This suggests that, the infiltrated rainwater have different isotopic content and it is mixed with the existing water already in the soil and this gave rise to different and more depleted isotopic content of$\delta^{18}O$.

The net effect of evaporation is an enrichment of heavy isotopes ($\delta^{18}O$ ‰) near the soil surface.

Profile 6 (Fig 4.18) is also located at the intermediate stream together with Profile 4, with a distance of 4.0 m between them. The isotopic composition for the profile ranges from – 4.42 ‰ vs VSMOW to + 0.04 ‰ vs VSMOW for $\delta^{18}O$ and – 25.87 ‰ vs VSMOW to –

10.27 ‰ vs VSMOW for δ^2H. Whilst the mean for $\delta^{18}O$ is – 3.24 ‰ vs VSMOW and δ^2H is – 22.09 ‰ vs VSMOW.

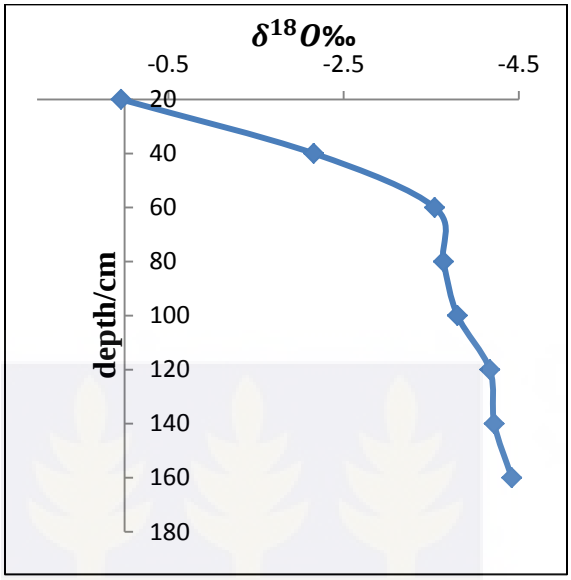

Fig. 4.18: Profile 6, vertical variation of $\delta^{18}O$ ‰ vs VSMOW of extracted water with depth

The profile shows isotopic enrichment (+0.04 ‰ vs VSMOW) for $\delta^{18}O$ at the topsoil (0.0 to 30.0 cm) which shows a little evaporation within the soil. Below 30.0 cm, the isotopic content becomes depleted with the heavy isotopes. The isotopic composition of $\delta^{18}O$ ‰ within the profile decreased along the profile as the depth increases.

This shows either piston flow of infiltrated rainwater with different isotopic content or mixing of recent rainwater with what was already in the soil because of the slow movement of water in the soil. Also from Appendix III, it can be seen that the moisture content started increasing after 60.0 cm.

This gave rise to different and more depleted isotopic content of$\delta^{18}O$. These can be attributed to the slow movement of water in the unsaturated zone and also evaporation has no effect on the soil water as the depth increases down the profile.

Profile 7 (Fig 4.19) was located at the lower/downstream. This profile is about 150 m from profile 6, as was shown in the Figure 3.2.

The isotopic composition for the profile ranged from – 4.26 ‰ vs VSMOW to – 2.66 ‰ vs VSMOW for $\delta^{18}O$ and – 28.45 ‰ vs VSMOW to – 20.33 ‰ vs VSMOW for $\delta^{2}H$. Whilst the mean for $\delta^{18}O$ is – 3.69 ‰ vs VSMOW and– 24.26 ‰ vs VSMOW for$\delta^{2}H$.

The profile shows isotopic enrichment of (– 2.66 ‰) for $\delta^{18}O$ at the topsoil (0.0 to 30.0 cm) which shows little evaporation within the soil. Below 30.0 cm, the isotopic content becomes more depleted.

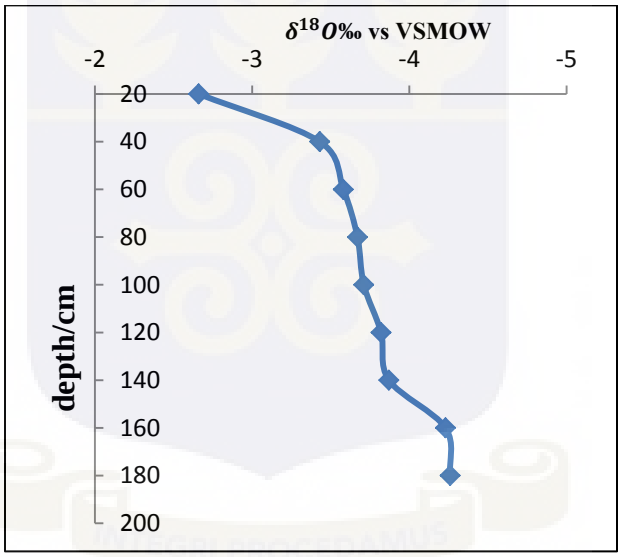

Fig. 4.19: Profile 7 vertical variation of $\delta^{18}O$ ‰ vs VSMOW of extracted water with depth

The isotopic composition of $\delta^{18}O$ ‰ within the profile decrease along the profile as the depth increases, suggesting infiltrated rainwater with different isotopic content and mixing of recent rainwater with the existing water in the soil because of the sluggish movement of water in soil most especially with clayey soil (Appendix IV) and also from (Appendix III), it can be seen that the profile shows both increasing and decreasing moisture content. These gave rise to different and more depleted isotopic content of$\delta^{18}O$.

Profile 8 (Fig 4.20) is also located at the lower/downstream together with Profile 7, but with a distance of 2.0 m between them, as shown in Fig. 3.1.

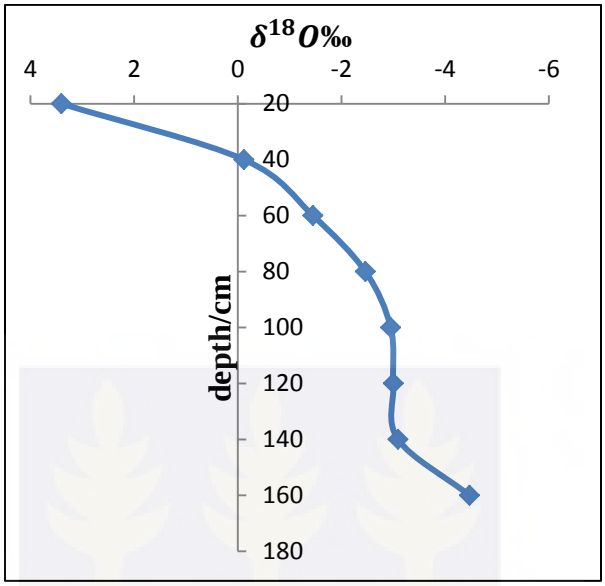

Fig. 4.20: Profile 8 vertical variation of $\delta^{18}O$ ‰ vs VSMOW of extracted water with depth

The isotopic composition for the profile ranged from – 4.47 ‰ vs VSMOW to + 3.40 ‰ vs VSMOW for $\delta^{18}O$ and – 24.94 ‰ vs VSMOW to – 8.16 ‰ vs VSMOW for$\delta^{2}H$. Whilst the mean for $\delta^{18}O$ for is – 1.77 ‰ vs VSMOW and – 16.47 ‰ vs VSMOW for$\delta^{2}H$.

The profile showed more isotopic enrichment (+3.40 ‰ vs VSMOW) for $\delta^{18}O$ at the top (0.0 to 60.0 cm) which suggests that, high evaporation have taken place near the surface, because there were no vegetative cover found in the location. Below 60.0 cm, the isotopic content becomes slightly depleted with the heavy isotopes, because water below this depth might have undergone small evaporation compared to the water above this depth.

The profile shows piston flow of infiltrated rainwater with different isotopic content which mixed with water already in the unsaturated zone below this depth, because

groundwater moves slow. These gave rise to different and depleted isotopic content of$\delta^{18}O$.

This profile recorded the most enriched isotopic content for the heavy isotopes ($\delta^{18}O$) in the study area because the isotopic value for $\delta^{18}O$ at the top (20.0 cm) is + 3.40 ‰ vs VSMOW, and an average of – 1.77 ‰ vs VSMOW. This suggests that, the percolating water in the profile has experienced evaporation as the water moves along the profile. The net effect of evaporation is an enrichment of heavy isotopes ($\delta^{18}O$ ‰) near the soil surface. It also indicates that the fractionation of water from the unsaturated zone caused by evaporate effect declines with depth.

The $\delta^{18}O$ ‰ of the upper layer of the profiles shows that, the rainfall infiltrated into the unsaturated zone in recent times suffered evaporation before infiltration. The effect of evaporation on oxygen – 18 isotopes in unsaturated zone showed that, evaporation at the surface of the unsaturated zone caused oxygen – 18 enrichment and decreases with depth along the profiles. This indicates that evaporation at the surface (prior to infiltration) and in the shallow depth in the unsaturated zone resulted in more enriched (positive values) isotopic composition values. However, these enrichment trends may come as a result of evaporation, change in isotopic composition of rainfall and mixing of recent and already existing water in the unsaturated zone.

The isotopic composition of water in the unsaturated zone will not be changed until the soil layer accepted the ‘‘new’’ water that had different isotopic composition. Generally, the values of $\delta^{18}O$ ‰ in soil water decrease with depth at the top layer below 40.0 cm in

all the profiles, because the vapour dominant transport near the surface is controlling the isotopic composition hence the shapes obtained from the study area in Figures 4.15 to 4.20. An enrichment of heavy isotopes in the subsurface may occur in the uppermost part of the soil column due to evaporation. These trends were also reported in other arid and semiarid regions (Zimmermann et al., 1967a; Barnes and Allison, 1983).

4.5 Recharge rate of soil water into groundwater

Recharge is the addition of water to an aquifer, generally from rainfall events that infiltrate downward through the unsaturated zone.

Qualitative estimates of relative recharge rates can be determined using chloride concentrations in groundwater or unsaturated zone pore water if rainfall and dry fallout are the only sources of chloride to the subsurface. In this case, chloride concentrations are inversely related to recharge rates.

Estimations of groundwater recharge rate in the study area were carried out using the chloride mass balance (CMB) technique (Allison and Hughes 1978; Edmunds et al. 1988) Eqn. 3.11. In this method, the degree of enrichment of Cl in moisture content is inversely proportional to the amount of recharge taking place. Chloride is assumed to be derived only from rainfall and to remain inert during the recharge process. It is also assumed that homogeneous moisture movement (piston flow) is taking place with no by – pass (matrix) flow. This assumption is also valid in this fine – grained and homogeneous unconsolidated material. It is also assumed that the wet deposition approximates to the

total deposition; it has been assumed that any dry deposition during the dry season will be in a steady state of movement with no net aerosol deposition to the surface.

Chloride concentrations generally increase through the root zone as a result of evapotranspiration and then remain constant below this depth.

Drainage is inversely related to Cl concentration in the unsaturated zone pore water (Eqn. 3.11). Figure 4.21 shows drainage rates at the study area with the individual piezometers and the corresponding individual drainage rate estimated from Eqn. 3.11 – 3.13 is shown in (Appendix VII).

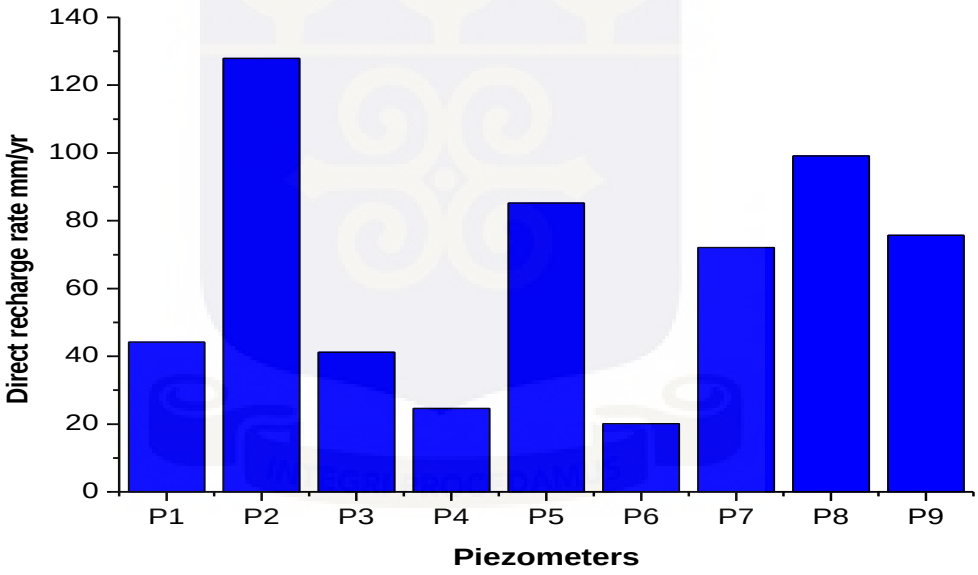

Figure 4.21: Drainage rate at study area averaged for three years

This inverse relationship results in the chloride mass – balance (CMB) approach being much more accurate at low drainage rates, because Cl concentrations change markedly over small changes in drainage.

The low chloride concentrations in Fig 4.21 indicate high recharge rates because chloride is flushed/leached out of the unsaturated zone by the percolating water towards the saturated zone (P4, P6, P3 and P1), whereas high chloride concentrations indicate low recharge rates because chloride accumulates as a result of evapotranspiration and this is evident in the chloride profiles (Fig 4.12 to 4.20).

Unsaturated zone sample analysis results provide estimates of downward water fluxes (drainage rates) below the root zone. However, in many cases the water has not reached the water table. If climate, vegetation, and soil conditions remain the same, it is assumed that the drainage rates will ultimately reach the aquifer and become groundwater recharge.

The amount of recharge is influenced by soil saturation status and water balance of soil mass at these depths to zero flux plane (ZFP) where the soil water will escape the evaporation effects and eventually reach to the groundwater table (Suarez 2001).

4.6 Origin of Salinity

In order to understand the origin of salinity (high chloride) in the groundwater systems in the study area, a plot of Cl^- concentration against $\delta^{18}O‰$ vs VSMOW was used. The plots are modified by (Akiti, 1981, and Akiti 1985) for Cl^- both in soil and water samples (ground water and unsaturated zone); and for $\delta^{18}O‰$ vs VSMOW, (Fig. 4.22).

Samples plotted in region 1 will be as a result of dissolution of soluble salts deposited and accumulated in the unsaturated zone. Water in the unsaturated zone will dissolve these soluble salts without causing any isotopic fractionation. The isotopic content of the percolating water will either remain the same or become more negative as the Cl concentration increases.

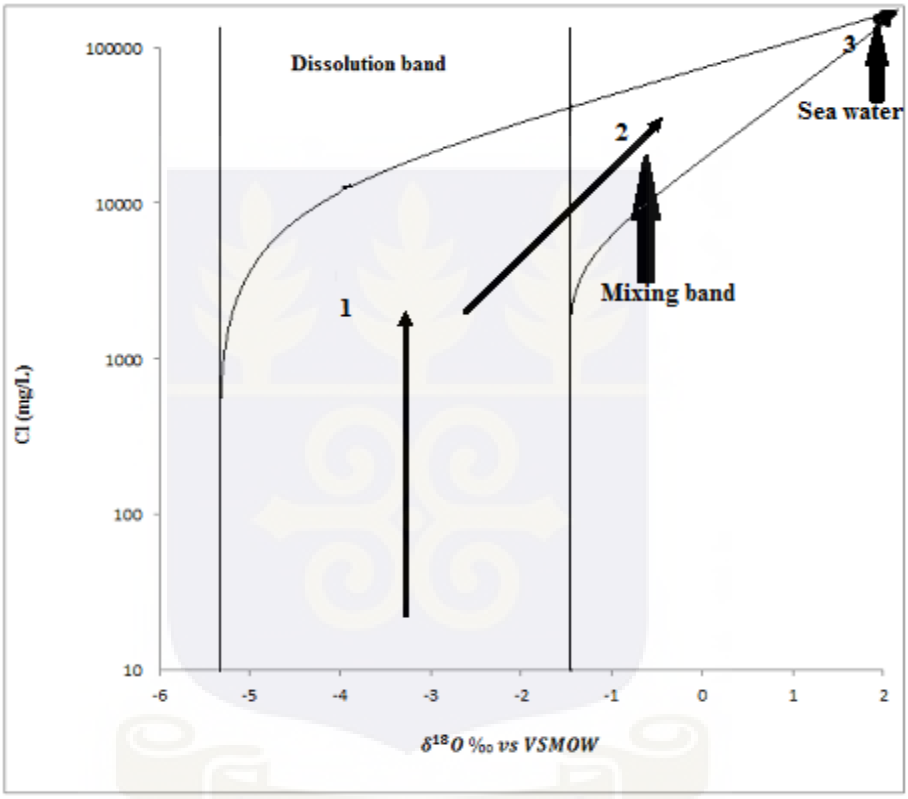

Fig 4.22 Relationship between Cl and$\delta^{18}O$ ‰ *vs VSMOW*, modified from Akiti, 1985

Samples plotted in region 2, will indicate mixing of water in the unsaturated zone with sea water and this will result in isotopic fractionation of the water, causing the water to be enriched (positive) with heavy isotopes as the Cl concentration increases (as indicated with an arrow). Those plotted in region 3 will have Cl concentration of the sea water,

which will indicate a direct sea water intrusion. The isotopic content of the water will be more positive. Cl concentration of sea water is > 19000 mg/L.

Figure 4.23 shows the relationship between chloride (Cl^-) and oxygen – 18; and chloride concentration with depth for profile 2.

The plot of Cl^- with oxygen – 18 shows no correlation, this suggests that evaporation is not the only dominant factor causing Cl^- content in the soil and there may be other sources. It could be as a result of seawater intrusion, halite dissolution or sea aerosol sprays. However, this can be proven with stable isotopes.

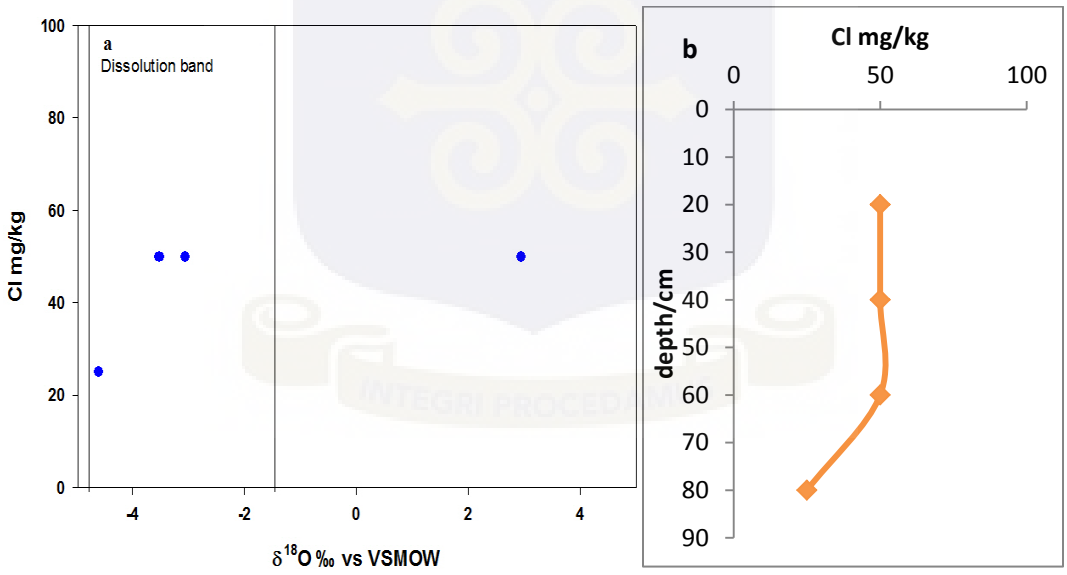

Fig. 4.23. Relationship between (a) Chloride and$\delta^{18}O‰$ $vs\ VSMOW$; and (b) Chloride vs depth

Three of the points plotted in the dissolution band region and one plotted outside this band. No point plotted in the mixing or sea water region. This suggests that, the soluble salts in the unsaturated zone are not as a result of direct sea water intrusion but can either

be halite dissolution or sea aerosol sprays which have been deposited in the soil in the past.

However, when sea water mixes with unsaturated zone water, there will be isotopic fractionation which will result in $\delta^{18}O‰$ becoming more positive and will tend to plot either in the mixing band or in the sea water region.

The salts are being dissolved by the percolating water in the unsaturated zone without any isotopic exchange. The Cl^- deposition of the profile is 49.98 mg/kg which remained constant within this depth (Fig 4.22 (b)). Also the rocks in the study area are not permeable to allow sea water to encroach and accumulate in the unsaturated zone.

Figure 4.24 shows the relationship between chloride (Cl^-) and oxygen – 18; and chloride concentration with depth for profile 3. The plot of Cl^- with oxygen – 18 shows no strong correlation, but suggests that evaporation may have contributed to the accumulation of Cl^- content in the unsaturated zone. Other sources of salts may be as a result of direct seawater intrusion, halite dissolution, and ancient sea water flooding or sea aerosol sprays. However, these can however, be proven with isotopes.

Two of the points plotted in the dissolution band region and one plotted outside this band, but no point plotted in the mixing or sea water region. This suggests that, the soluble salts in the unsaturated zone are not as a result of direct sea water intrusion but can be halite dissolution; and or ancient seawater flooding or sea aerosol sprays which have been deposited in the soil in the past.

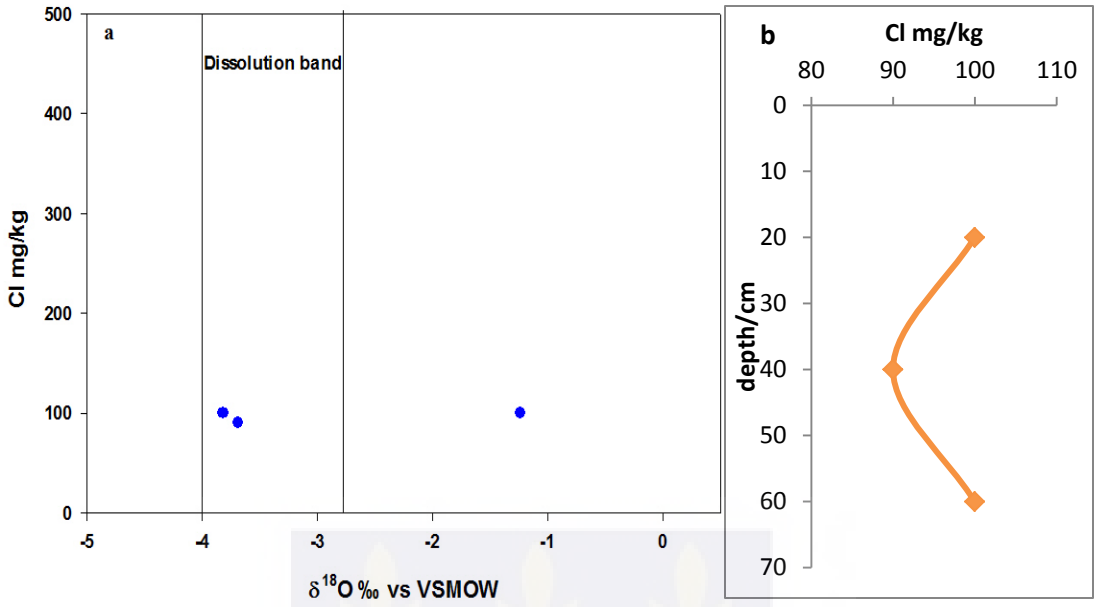

Fig. 4.24. Relationship between (a) Chloride and$\delta^{18}O‰$ $vs\ VSMOW$; and (b) Chloride vs depth

However, when sea water mixes with unsaturated zone water, there will be isotopic fractionation which will result in $\delta^{18}O‰$ becoming more positive and will tend to plot either in the mixing band or in the sea water region. However, as the concentration of Cl^- increases from 89.99 mg/kg at 20.0 cm to 99.97 mg/kg at 60.0 cm Fig 4.23 (b), stable isotopic content of the percolating water remains depleted (becomes more negative) instead of enriched (more positive). This suggests that, the salts are being dissolved by the percolating water in the unsaturated zone without any isotopic exchange, ruling out sea water intrusion.

Also the rocks in the study area are not permeable to allow sea water to encroach and accumulate in the unsaturated zone (section 3.1.2).

Figure 4.25 shows the relationship between chloride (Cl^-) and oxygen – 18; and chloride concentration with depth for profile 4. The plot of Cl^- with oxygen – 18 shows no strong

correlation, but suggests that evaporation has contributed to the accumulation of Cl^- content in the soil in the past. It could be as a result of seawater intrusion, halite dissolution; and ancient seawater flooding or sea aerosol sprays. However, this can be proven with stable isotopes.

Nine (9) out of ten (10) of the points plotted in the dissolution band region and one plotted outside this band, but no point plotted in the mixing or sea water region. This suggests that, direct sea water intrusion is not the cause of soluble salts' accumulation in the unsaturated zone but can either be halite dissolution; and or ancient seawater flooding or sea aerosol sprays which have been deposited in the soil in the past.

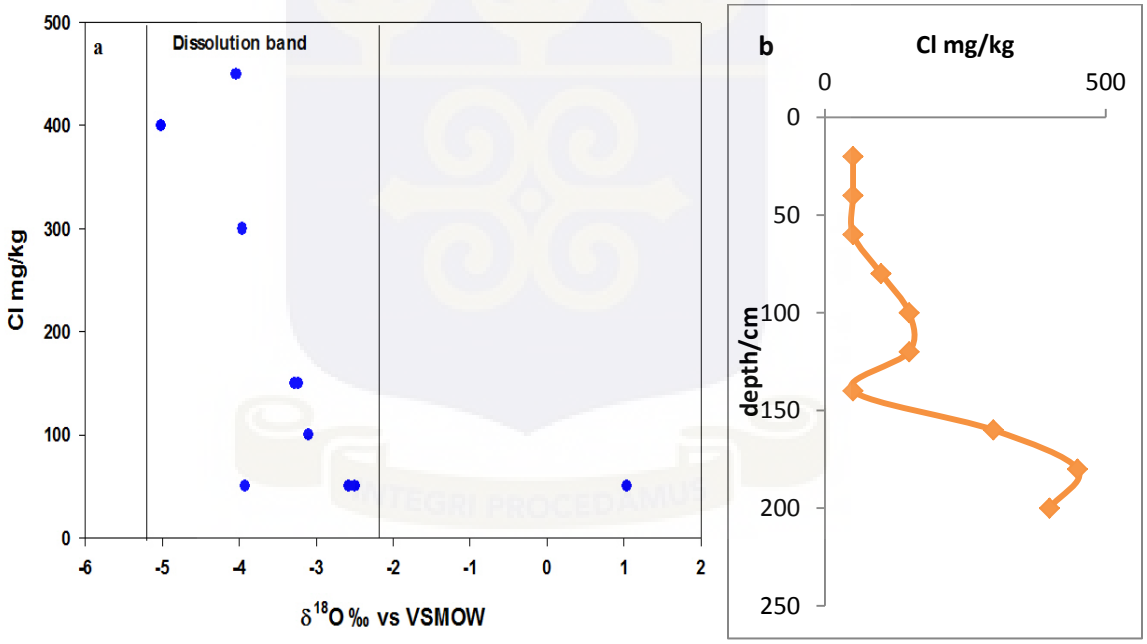

Fig. 4.25. Relationship between (a) Chloride and$\delta^{18}O‰$ *vs VSMOW*; and (b) Chloride vs depth

However, when sea water encroaches and mixes with unsaturated zone water, there will be isotopic fractionation which will result in $\delta^{18}O‰$ becoming more positive and will tend to plot either in the mixing band or in the sea water region. As Cl^- concentration increases from 49.99 mg/kg at 50.0 cm to 149.95 mg/kg at 120.0 cm and 449.86 mg/kg at

180.0 cm (Fig 4.24 (b)), the stable isotopic content of the percolating water remains depleted (becomes more negative) instead of enriched (more positive). This suggests that, the percolating water in the unsaturated zone is dissolving the accumulated salts without any isotopic exchange.

And also, the rocks in the study area are not permeable to allow sea water to encroach and accumulate in the unsaturated zone (section 3.1.2).

Figure 4.26 shows the relationship between chloride (Cl^-) and oxygen – 18; and chloride concentration with depth for profile 6. The plot of Cl with oxygen – 18 shows no linear correlation, but suggests that, evaporation may have contributed to the accumulation of Cl^- content in the soil. Other sources may be as a result of seawater intrusion, halite dissolution; and or ancient seawater flooding or sea aerosol sprays. This can however, be proven with isotopes.

Seven (7) out of eight (8) of the points plotted in the dissolution band region and one plotted outside this band. No point plotted in mixing or sea water region. This suggests that, sea water intrusion is not the source of soluble salts accumulation in the unsaturated zone but can be halite dissolution; ancient seawater flooding and or sea aerosol sprays which has been deposited in the soil in the past.

However, when sea water encroaches and mixes with unsaturated zone water, there will be isotopic fractionation which will results in $\delta^{18}O‰$ becoming more positive and will tend to plot either in the mixing band or in the sea water region.

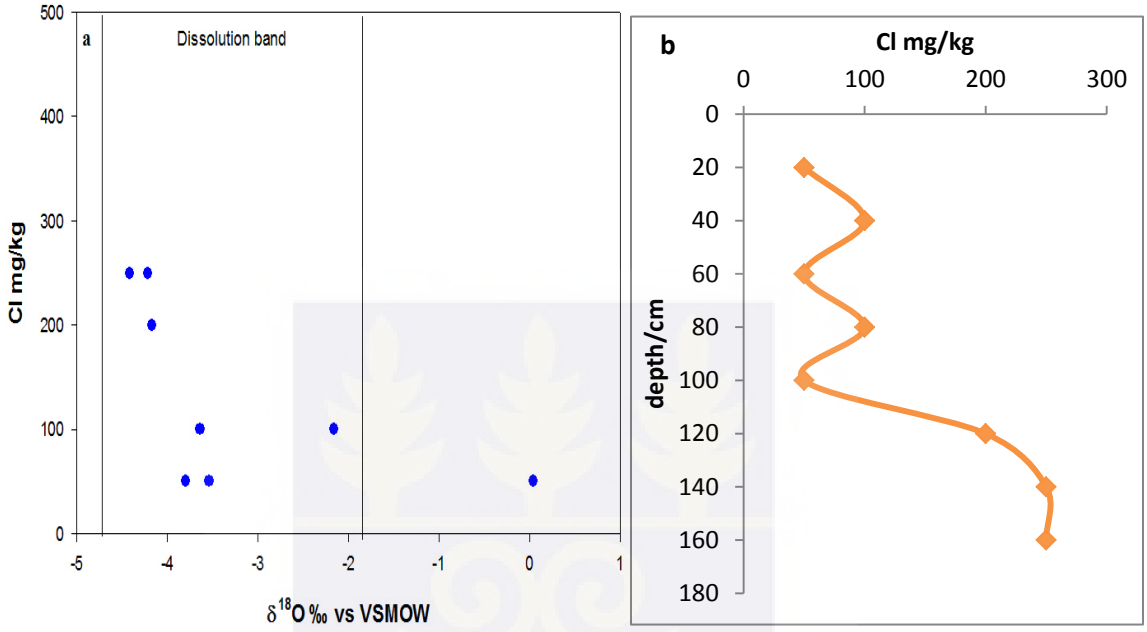

Fig. 4.26. Relationship between (a) Chloride and$\delta^{18}O‰$ *vs VSMOW*; and (b) Chloride vs depth

However, as Cl^- concentration increases from 49.99 mg/kg at 20.0 cm to 99.97 mg/kg at 80.0 cm and 249.92 mg/kg at 140.0 cm Fig 4.25 (b), the stable isotopic content of the percolating water remains depleted (becomes more negative) instead of being enriched (more positive). This suggests that, the percolating water in the unsaturated zone is dissolving the accumulated salts without any isotopic exchange.

The rocks in the study area are not permeable to allow sea water to encroach and accumulate in the unsaturated zone (section 3.1.2).

Figure 4.27 shows the relationship between chloride (Cl^-) and oxygen – 18; and chloride concentration with depth for profile 7. The plot of Cl^- with oxygen – 18 shows no strong

correlation but suggests that evaporation is a contributing factor to the accumulation of Cl^- content in the soil. It could be as a result of seawater intrusion, halite dissolution and or sea aerosol sprays. Stable isotopes can be used to delineate between sea water, halite dissolution and aerosol sprays.

All the nine (9) points plotted in the dissolution band, and none of the points plotted in mixing or sea water region. This suggests that, there is no mixing of sea water with the waters in the unsaturated zone, and is not responsible of soluble salts that have being accumulated in the unsaturated zone. However, other sources such as halite dissolution, ancient seawater flooding or sea aerosol sprays may have been the cause of deposition and accumulation in the soil in the past.

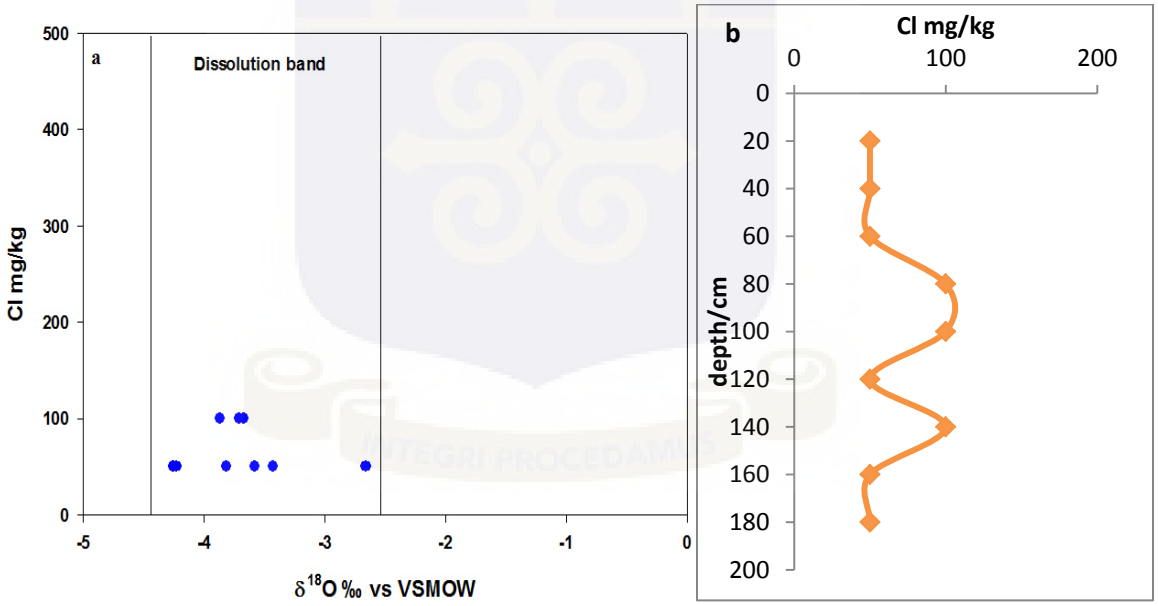

Fig. 4.27. Relationship between (a) Chloride and$\delta^{18}O‰$ $vs\ VSMOW$; and (b) Chloride vs depth

When sea water intrude and mixes with unsaturated zone water, there will be isotopic fractionation which will result in $\delta^{18}O‰$ becoming more positive rather than negative and this will plot either in the mixing band or in the sea water region. But as Cl^- concentration increases from 49.99 mg/kg at 20.0 cm to 99.97 mg/kg at 80.0 cm and at

140.0 cm (Fig 4.26 (b)) the stable isotopic content of the percolating water remains depleted (becomes more negative) instead of being enriched (more positive) Fig 4.27(a). This suggests that, the percolating water in the unsaturated zone is dissolving the accumulated salts without any isotopic exchange.

And also, the rocks in the study area are not permeable to allow sea water to encroach and accumulate in the unsaturated zone (section 3.1.2).

Figure 4.28 shows the relationship between chloride (Cl^-) and oxygen – 18; and chloride concentration with depth for profile 8. The plot of Cl^- with oxygen – 18 shows strong correlation but suggests that evaporation contributing factor to the accumulation of Cl^- content in the soil. It could be as a result of seawater intrusion, halite dissolution; ancient seawater flooding and or sea aerosol sprays. Stable isotopes can be used to delineate between sea water, halite dissolution and aerosol sprays.

Five (5) out of eight (8) points plotted in the dissolution band and none of the points plotted in mixing or sea water region. Three (3) points were plotted outside the dissolution band, mixing band and sea water region, which cannot be accounted for but needs further studies.

Points that plotted in the dissolution band suggest that, the percolating water in the unsaturated zone is dissolving the accumulated salts without any isotopic exchange. There is no mixing of sea water with the waters in the unsaturated zone, and is not responsible of soluble salts that have accumulated in the unsaturated zone, but other

sources such as halite dissolution; ancient seawater flooding and or sea aerosol sprays may have been the cause of deposition and accumulation in the soil in the past.

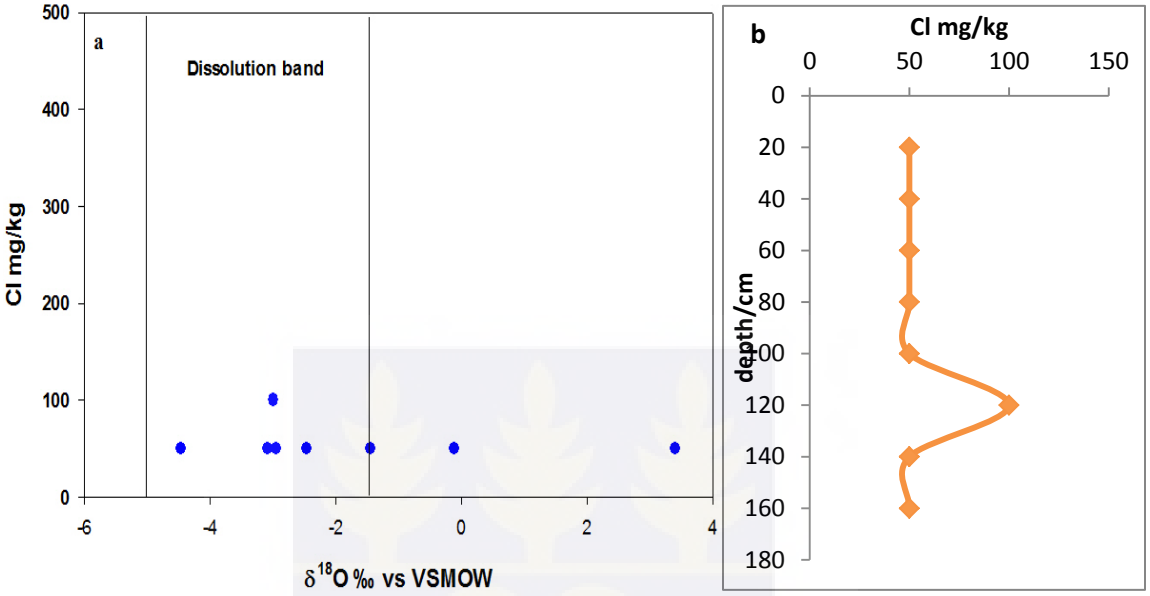

Fig. 4.28. Relationship between (a) Chloride and$\delta^{18}O‰$ $vs\ VSMOW$; and (b) Chloride vs depth

However, when sea water intrudes and mixes with unsaturated zone water, this will cause be isotopic fractionation which will result in $\delta^{18}O‰$ becoming more positive rather than negative and this will plot either in the mixing band or in the sea water region. However, as Cl^- concentration increases from 49.99 mg/kg at 20.0 cm to 99.97 mg/kg at 120.0 cm (Fig 4.28 (b)), the stable isotopic content of the percolating water remains depleted (becomes more negative) instead of being enriched (more positive) Fig 4.28 (a).

The rocks in the study area are not permeable to allow sea water to encroach and accumulate in the unsaturated zone (section 3.1.2).

Figure 4.29 shows the relationship between chloride (Cl^-) and oxygen – 18 for the six (6) profiles sampled and analysed for oxygen – 18. The plot shows poor correlation between the individual points. Most of the samples fall in the dissolution band confirming dissolution of soluble salts as the major process controlling groundwater salinity in the study area, ruling out a possible association with direct sea water intrusions in the study area.

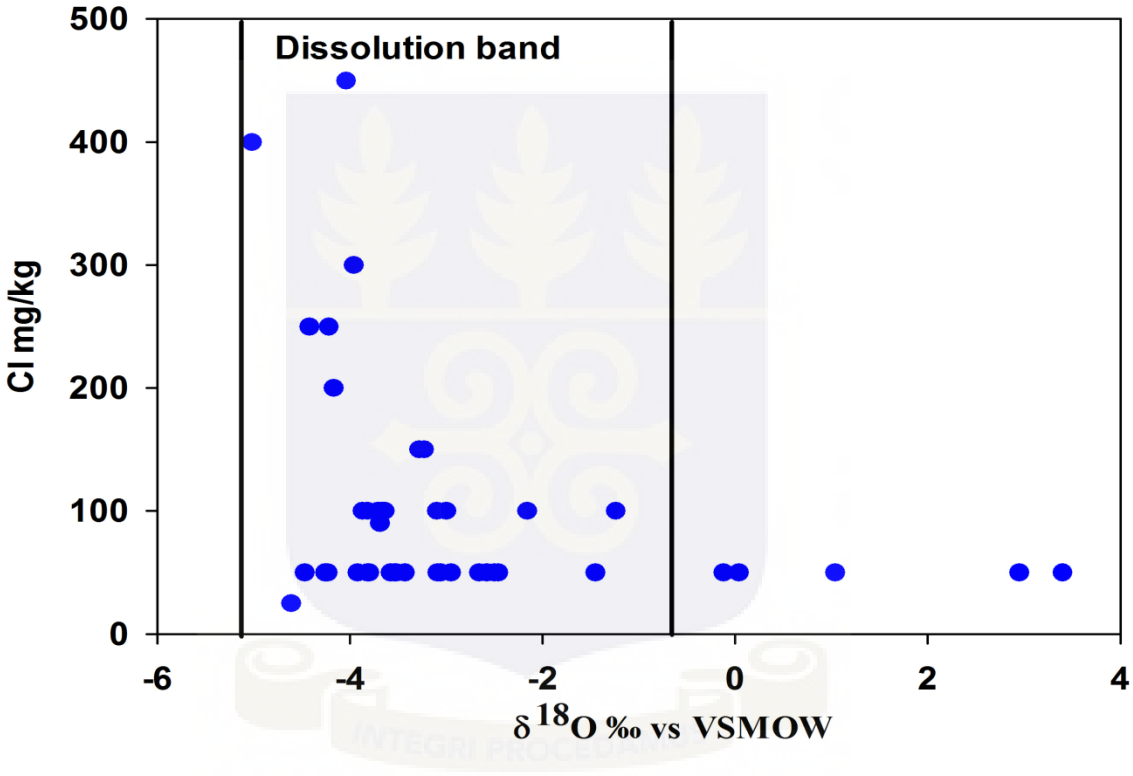

Fig. 4.29. Relationship between Chloride and $\delta^{18}O$‰ $vs\ VSMOW$ in the unsaturated zone

When water in the unsaturated zone passes through the soluble salts, it dissolves the salts accumulated at the depth of 80 cm and 120 cm, without any isotopic exchange with the salt. However, as Cl^- concentrations become high, the isotopic content of the percolating water in the unsaturated zone remains depleted. This suggests that, the salts accumulated at these depths in the unsaturated zone are not as a result of sea water mixing with the

unsaturated zone water at a point. However, if sea water mixes with the water in the unsaturated zone, there will be isotopic fractionation which will result in $\delta^{18}O‰$ becoming more positive as the Cl^- concentration increase.

Figure 4.30 shows a plot of Cl^- as against $\delta^{18}O‰$ VSMOW for water samples (groundwaters and unsaturated zone). All the samples fall in the dissolution band confirming dissolution of soluble salts in the unsaturated zone as the major process controlling groundwater salinity.

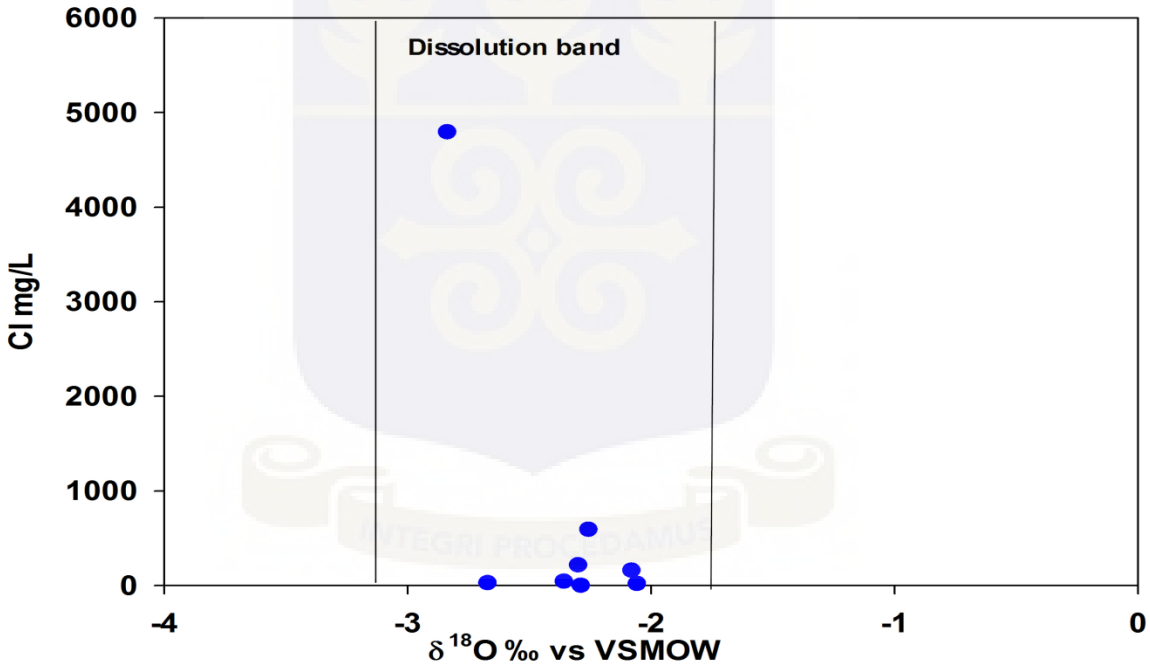

Fig. 4.30. Relationship between Chloride and $\delta^{18}O‰$ *vs VSMOW* for water samples

The $\delta^{18}O‰$ of water sample remain depleted whilst Cl^- content in the water samples increases, ruling out a possible association with direct seawater intrusion. This confirms the results from the soils from the unsaturated zone. It follows that, Cl^- in the

groundwater originates from washing/leaching of soluble salts that have been deposited and accumulated in unsaturated zone.

Moreover, the depletion of $\delta^{18}O$ ‰ and $\delta^{2}H$ ‰ is clearly associated with the increase in Cl^{-}, suggesting that, the salinity in the groundwaters in the study area, originated from dissolution of soluble salts by infiltrated rainwater as it passes through the salts. During the processes of leaching/dissolution of salt formations or mineral dissolution, the stable isotope content of the water is not affected (remains depleted) while the salinity (Cl^{-}) of water increases. This is a unique feature which will enable identification of such processes based on isotopic and chemical data.

From the results obtained from this study, it is found out that, the high chloride concentration found in groundwaters in the coastal aquifers (Armah, 2004; and Ganyaglo (personal comm., 2012)), is as a result of leaching/dissolution of Cl^{-} deposited and accumulated in the unsaturated zone as a result of marine transgression in the past; could be due to severe climatic change such as isostatic adjustment or tectonics events such as orogenies; as a result of aerosol deposition and not direct sea water intrusion. However, it was not possible to determine how the salt was accumulated in the unsaturated zone; radiocarbon dating of the soil is needed to solve this. This will help known the time (age) of deposition of these salts in the unsaturated zone of the study area.

However, those that fall outside the dissolution band, mixing band and sea water intrusion region could not be accounted for and needs further studies.

Chapter Five

Conclusions and Recommendations

5.1 Conclusions

The physico – chemical analysis of the soil in the study area showed that the soil is generally moderately acidic (range value of pH 5.3 – 7.0) with the mean of 6.48 pH units suggesting acidity resulting from carbonic acid derived from the dissolution of CO_2 both from atmosphere and the soil zone.

The redox potential (Eh) of the soil ranged from – 1.2 (pe = - 20.34) to + 101.7 (+ 1723.73) mV with the mean Eh been + 30.84 mV (pe = + 522.74) mV. This suggested that the soil is anaerobic with reducing conditions.

Soil moisture content showed that the soils were slightly moist with volumetric moisture content average of 17.4 % due to majority of the soil type being clayey.

Electrical conductivity values in the soil ranged from 35.1 $\mu S/cm$ to 1276 $\mu S/cm$ with the mean been 261.99 $\mu S/cm$ whilst total dissolved solids (TDS) ranged from 17.6 mg/L to 636.0 mg/L with mean being 130.83 mg/L. Electrical conductivity values for the water in the unsaturated zone ranged from ranged from 193.2 $\mu S/cm$ to 987.5 $\mu S/cm$ with the mean been 441.7 $\mu S/cm$ whilst total dissolved solids (TDS) ranged from 96.6 mg/L to 494 mg/L is and the mean being 220.03 mg/L and for groundwater from 1965 $\mu S/cm$ to

17000 $\mu S/cm$ with mean 9482.5 $\mu S/cm$ whilst total dissolved solids (TDS) also ranged from 983 mg/L to 8490 mg/L and the mean been 4736.5 mg/L.

The high values of EC, TDS and pH of the water from the unsaturated zone and the groundwater suggests that, water percolation in the unsaturated zone is dissolving the accumulated salt in the unsaturated zone as it moves from the surface and makes its way to the underlying aquifer.

The concentrations of major ions (Na, K, Ca, Mg, Cl, SO4, HCO3, NO3 and PO4) were measured in the soil, unsaturated zone water and groundwater with the dominant ions being Na, K, Ca, Cl, SO_4 and HCO_3 in the soil, water from the unsaturated zone and groundwater. The correlation between these ions showed an increasing trend from the soil surface down to the groundwater system in the area and this is evident in the groundwater sampled near the study area. These constitute the major soluble ions of the soils in the unsaturated zone in the study area, and increasing in trend with increasing depth in the study area to the groundwater.

The concentration of heavy metals (As, Cd, Cr, Cu, Fe, Mn, V, Pb, Co, Ni and Zn) measured in the soil, unsaturated zone water and groundwater were higher in the soil than in the water sample (piezometers and groundwater). This can due to natural variability such as weathering, sea aerosol and or as a result of agrochemicals which have being adsorbed on the soil and has become less mobile as water moves through the soil down to the groundwater system, hence their concentrations in the lower in the groundwater as measured as found in the study area.

The range of chloride (Cl) concentrations recorded in the study area 24.99 mg/kg to 449.86 mg/kg. It was assumed that the Cl in the study area is derived from aerosol deposition from the sea and no other source or sinks are available in the study area. The area receives equal amount of Cl deposition of the aerosol spray from the sea. Chloride concentrations along the profiles were varying as the depth increases down the profile. Also both larger and smaller Cl peaks shown on Cl – depth plots, which is typical of many chloride profiles in arid regions under different climatic change or non – piston movement of chloride as found. The combination of low chloride at depth and significant differences in stored chloride, within the individual profiles and the presence of secondary bulges suggests a series of recharging events to which the soil profiles have responded in varying ways.

The chloride mass balance (CMB) approach was used to estimate recharge in the flushed portion of profiles which was (mean 65.56 mm/yr., 9 profiles). Heavy/intense rainfall can result in downward movement of salts that had accumulated near the surface of the soil.

Stable isotope data were used to find out the relationship between rainfall, water from the unsaturated zone and groundwater in the study area. The slope and intercept of the unsaturated zone water was lower than that of GMWL, indicating an evaporation effect of rainfall. Comparing the $\delta^{18}O$ values in water from unsaturated zone, it was found that the high evaporation occurs in the top soil water. Due to the effect of evaporation, isotopes in soil water are enriched near the surface, causing departure to the right – side of GMWL. Water from the unsaturated zone shows a mixture of recent rainfall and water already in the unsaturated zone. It appears that rainfall mixes with existing water in the

unsaturated zone to some degree and moves downwards in a piston flow manner. This is indicated by a broad correlation between $\delta^{18}O$ values in the rainfall time series, and in the soil water versus depth profile. And, also coupling the isotopic composition in the rainfall with water from the unsaturated zone and groundwater in the study area, it is evident that the groundwater is being recharged by rainfall.

In order to understand the origin of salinity (high chloride) in the groundwater systems in the study area, a plot of Cl^- concentration against $\delta^{18}O‰$ vs VSMOW is used for Cl^- both in soil and water samples (ground water and unsaturated zone). The salinity (high chloride) in the groundwaters originated from dissolution of soluble salts by infiltrated rainwater as it passes through the salts and not as a result of direct sea water intrusion.

Based on this study, it can be concluded that, the high chloride concentration found in groundwaters in the coastal aquifers is (a) as a result of dissolution of salts (Cl^-) deposited and accumulated in the unsaturated zone as a result of marine transgression in the past; (b) could be due to severe climatic change such as isostatic adjustment or tectonics events such as orogenies; (c) as a result of aerosol deposition at a depth of 80.0 cm and 120.0 cm, (d) but not direct sea water intrusion. Movement of water through the unsaturated zone dissolves these salts and discharges them into the groundwater system leading to groundwater salinization. However, it was not possible to determine how the salt was accumulated in the unsaturated zone; radiocarbon dating is needed to solve this.

5.2 Recommendations

For future studies, it is recommended that samples should be taken during different seasons (i.e. wet and dry) in order to assess the seasonal variations of chloride and oxygen – 18.

Further studies are also recommended to investigate the zones of high salinity which were observed in the unsaturated zone by the use of radiocarbon dating.

This research work used only chloride and oxygen – 18 variations with depth; however, other tracer techniques should be used such as chlorine 36, strontium 87/86 ratio.

REFERENCES

Akiti T. T. 1980. Etudé géochimique et isotopique de quelqués aquifers du Ghana. (PhD Thesis) Univeristé Paris-Sud. 232 pp.

Akiti, T.T. 1985. Environmental Isotopes study of the groundwaters of the Island of Santiago. Mission report to the UNDP for the government of Cape Verde.

Akiti T. T. 1987. Environmental isotope study of groundwater in crystalline rocks of the Accra Plains, Ghana. Proceedings of the 4th Working Meeting, Isotopes in Nature, Leipzig, September 1986.

Allison, G.B., Bames, C.J. and Hughes, M.W., 1983. The distribution of deuterium and oxygen-18 in dry soils: II. Experimental. J. Hydrol. 64: 377-397.

Allison, G. B. 1998. Stable isotopes in soil and water studies. In : Causse C. (ed.), Gasse F. (ed.) Hydrologie et géochimie isotopique. Paris: ORSTOM, 1998, p. 23-38. (Colloques et Séminaires). Hydrology and Isotope Geochemistry: International Symposium in Memory of Jean-Charles Fontes, Paris (FRA), 1995/06/01-02.

Allison G. B. and Hughes M. W. 1978. The use of environmental chloride and tritium to estimate total recharge in an unconfined aquifer. Aust. J. Soil Res. 16: 181–195.

Allison, G. B., Stone, W. J. and Hughes, M. W. 1985. Recharge in karst and dune elements of a semi – arid landscape as indicated by natural isotopes and chloride./. Hydro. 76, 1-25.

Alloway, B.J. 1995. Heavy metals in soils, Blackie Academic and Professional, an imprint of Chapman & Hall, London.

APHA. 1992. Standard methods for the examination of water and waste water, 18th. Ed. American Public Health Association Washington, DC, USA, APHA-AWWWA-WEF.

Appelo, C.A.J. and Postma, D. 1993. Geochemistry, Groundwater and Pollution. A. A. Balkema. Rotterdam. (4th Ed.). Brookfield: Rotterdam.

Araguas-Araguas, L., Froehlich, K., Rozanski, K. 2000. Deuterium and oxygen-18 isotope composition of precipitation and atmospheric moisture. Hydrological Processes, 14, 1341-1355.

Araguas-Araguas, L., Rozanski, K., Gonfiantini, R., and Louvat, D., 1995. Isotope effects accompanying vacuum extraction of soil water for stable isotope analyses. Journal of Hydrology 168, 159–171.

Armah, T.E.K. 2004. Hydrochemical and Geophysical studies of groundwater salinity, Central Region Ghana, PHD Thesis, Department of Geology University of Ghana.

Ashraf, M. 2000. Water movement through soil in response to water – content and temperature gradients: evaluation of the theory of Philip and de Vries (1957). J. Engin. Appl. Sci., 19: 37-51.

Association of Official Analytical Chemists (Anon, 2007)

Bam, E.K.P., Akiti, T.T., Osae, S., Ganyaglo, S.Y., Adomako, D., Abass, A .G., Ahialey, E., and Ayanu, G. 2011. Major ions and trace elements partitioning in unsaturated zone

profile of the Densu river basin, Ghana and the implications for groundwater. African Journal of Environmental Science and Technology Vol. 5(6), pp. 427-436

Barnes C.J. and Allison G.B. 1988. Tracing of water movement in the unsaturated zone using stable isotopes of hydrogen and oxygen. J. Hydrol. 100: 143–76.

Barnes, C.J. and Allison, G.B. 1983. The distribution of deuterium and oxygen – 18 in dry soils: I. Theory, J. Hydrol. 60: 141 – 156.

Barnes, C.J., and Turner, J.V. 1998. Isotopic exchange in soil water. In: Isotope tracers in catchment hydrology, C. Kendall, and McDonnell, J.J., ed., Elsevier, Amsterdam, 137-162.

Benneh, G., and Dickson, B.K., 2004. A New Geography of Ghana, Pearson Education Limited, England, pp24-27.

Blake, G.R., and Hartge, K.H. 1986. Bulk density. In: Methods of soil analysis, Part 1. Physical and mineralogical methods, A. Klute, ed., American Society of Agronomy - Soil Science Society of America, Madison, WI, 363-375.

Borggaard O. K., Elberling B. 2004. Pedological Biogeochemistry. Paritas, Brøndby.

Breit, G. N., Goldstein, H. L., Reynolds R. L., and Yount, J. C. 2009. Distribution of Major Anions and Trace Elements in the Unsaturated Zone at Franklin Lake Playa, California, USA. ISSLR 10th International Conference & FRIENDS of Great Salt Lake 2008 Forum. NREI Volume XV 2009

Cattlet, K.M, Heil, D. M., Linday, W. L., and Ebinger, M. H. 2002. Soil chemical properties controlling Zn^{2+} activity in 18 Colorado soils. Soc. Soil Am. J. 66, 1182 – 1189.

Chapelle, F.H., 2001, Ground-water microbiology and geochemistry (2 ed.): New York, NY, John Wiley & Sons, Inc., 477 p

Chapman, H.D. and Pratt, P.F. 1961. Methods of Analysis for Soils, Plants and Waters. Univ. California Div. Agr.Sci., Riverside, CA.

Clark, I.D., and Fritz, P. 1997. Environmental isotopes in hydrogeology. Lewis, New York.

Cook, F.J., and D.W. Rassam 2002. An analytical model for predicting water table dynamics during drainage and evaporation. Journal of Hydrology 263, 105-113.

Cook, P.G, Edmunds. W.M., and Gaye, C.B. 1992. Estimating paleorecharge and paleoclimate from unsaturated zone profiles. Water Resour Res 28:2721–2731.

Craig, H. 1961. Isotopic Variation in Meteoric Water, Science, 133, pp. 1702-1703

Cramer, V.A., and Hobbs, R.J. 2002. Ecological consequences of altered hydrological regimes in fragmented ecosystems in southern Australia: Impacts and possible management responses. Austral Ecology 27 (5), 546-564.

Dalvi, R.R., and Robbins, T.J. 1978. Comparative studies on the effect of cadmium, cobalt, lead, and selenium on hepatic microsomal monooxygenase enzymes and glutathione levels in mice. Journal of Environmental Pathology and Toxicology, 1:601–607.

Dansgaard, W., 1964. Stable isotopes in precipitation. Tellus 16,436–468.

Dzombak, D. A., and Morel, F.M.M. 1990. Surface complexation modelling- Hydrous ferric oxide, John Wiley, New York.

Edmunds, W.M., Darling, W.G., and Kinniburgh, D.G. 1988. Solute profile techniques for recharge estimation in semi – arid and arid terrain. In: Estimation of natural groundwater recharge. NATO ASI Series. Reidel, Dordrecht, pp 139–158.

Fipps, Guy. 2003. Irrigation Water Quality Standards and Salinity Management. Fact Sheet B – 1667. Texas Cooperative Extension. The Texas A&M University System, College Station, TX

Fitzpatrick RW, Boucher SC, Naidu R,Fritsch E. 1994. Environmental consequences of soil sodicity. *Aust. J. Soil Res* **32**, 1069-1093

Fitzpatrick R. W., Merry R., and Cox J. 2000. What are saline soils and what happens when they are drained? J. Austral. Assoc. Nat. Res. Manage. (AANRM) 6, 26–30.

Flowers, T.J. 1988. Chloride as a nutrient and as an osmoticum. Adv. Plant Nutr. 3, 55-78.

Fontes, J. C., Yousfi, M., and Allison, G. B., 1986. Estimation of long – term, diffusegroundwater discharge in the Northern Sahara using stable isotope profilesin soil water. J. Hydrol., 86: 315-327.

Foster, S.S.D., Chilton, P.J., Moench, M.K., Cardy, F., and Schiffler, M. 2000. Groundwater in rural development: Facing the challenges of resource sustainability. World Bank Technical Paper No. 463. Washington D.C.: World Bank.

Gardner, W.R. 1958. Some steady state solutions of the unsaturated moisture flow equation to evaporation from a water table. Soil Sci. 85: 228-232.

Gazis, C., and Xiahong F. 2004. A stable isotope study of soil water: evidence for mixing and preferential flow paths. Geoderma 119 (2004) 97–111.

Ghassemi, F., Jakeman, A.J., and Nix, H.A. 1995. Salinization of land and water resources. Human causes, extent, management and case studies. Sydney: University of New South Wales Press Ltd.

Gibbs, R.J. 1970. Mechanisms controlling world water chemistry. Science 17:1088–1090.

Gonfiantini, R. 1986. Environmental isotopes in lake studies. In Handbook of Environmental Isotope Geochemistry: Vol 2, The Terrestrial Environment, A. P. Fritz and J.C. Fontes (Eds.),Elsevier, Amsterdam, The Netherlands. 113–168.

Gouhua Xu, Hillel Magen, Jorge Tarchitzky and Uzi Kafkafi. 2000. Advances in Chloride Nutrition of Plants. Advances in Agronomy, volume 68. Academic Press.

Hadas, A., and Hillel, D. 1968. An experimental study of evaporation from uniform soil columns in the presence of a water table. Trans. Ninth Int. Congress Soil Sci., pp. 67-74.

Hassan, F.A. and Ghaibeh, A.S. 1977. Evaporation and salt movement in soils in the presence of water table. Soil Science Society of America Journal 41: 470–478.

Hem, J.D. 1989. Study an Interpretation of the Chemical Characteristics of Natural Water. 3rd Edition. U.S Geological Survey Water – Supply Paper 2254.

Hillel, D. (1982). Introduction to soil physics, Academic Press, London.

International Atomic Energy Agency. 2008. Field Estimation of Soil Water Content A Practical Guide to Methods, Instrumentation and Sensor Technology. IAEA, VIENNA, 2005 IAEA-TCS-30 ISSN 1018–5518.

IAEA. 2009. Application of Isotopes to the Assessment of Pollutant Behaviour in the Unsaturated Zone for Groundwater Protection Final report of a coordinated research project 2004 –2005. IAEA, VIENNA, IAEA-TECDOC-1618.

Ibe, A. C. and Kullenberg G. 1995. Quality assurance quality control (QA/QC) regime in marine pollution monitoring programmes: The GIPME perspective. Marine Pollution Bulletin 31: 4-12, 209 – 213.

IPCS. 1991. Environmental Health Criteria 108: nickel. Geneva: WHO, International Programme on Chemical Safety.

Izbicki, J.A., Radyk, J., and Michel, R.L. 2000. Water movement through a thick unsaturated zone underlying an intermittent stream in the western Mojave Desert, Southern California, USA. J. Hydrol. **238** (2000) 194–217.

Jalili, S., Moazed, H., Boroomand Nasab, S., and Naseri, A. A. 2011. Assessment of evaporation and salt accumulation in bare soil: Constant shallow water table depth with saline ground water. Scientific Research and Essays Vol. 6(29), pp. 6068-6074. Academic Journals.

Jolly, I. D., Cook, P. G. Allison, G. B., and Hughes, M. W. 1989. Simultaneous water and solute movement through an unsaturated soil following an increase in recharge, J. Hydrol., 111, 391– 396.

Jury, W. A. and Horton, R., 2004. Soil Physics, Sixth ed, John Wiley and Sons, Inc., New York.

Kaufman, W. J. and Orlob, G. T. 1956. Measuring ground water movement with radioactive and chemical tracers: American Water Works Association Journal, v. 48, p. 559 – 572.

Kendall, C. and McDonnell, J. J. 1998. Isotope Tracers in Catchment Hydrology. Elsevier Science B.V., Amsterdam. pp. 51-86.

Kesse, G.O. 1985. The mineral and rock resources of Ghana. A. A. Balkema, Rotterdam pp.25-26.

Kuroda, P. K. and Sandell, E. B. 1953. Chlorine in igneous rocks: Geological Society of America Bulletin, v. 64, p.879 – 896.

Mallants, D., Van Genuchten, M Th., Šimunek, J., Jacques, D., and Seetharam, S. 2011. Leaching of Contaminants to Groundwater. F.A. Swartjes (ed.), Dealing with Contaminated Sites, Springer Science. DOI 10.1007/978-90-481-9757-6_18.

Marei, A., Khayat, S., Weise, S., Ghannam, S., Sbaih, M. and Geyer, S. 2010. Estimating groundwater recharge using the chloride mass – balance method in the West Bank, Palestine. Hydrol. Sci. J. 55(5), 780–791.

Marie, A. and Vengosh, A. 2001. Sources of salinity in groundwater from Jericho Area, Jordan Valley. Groundwater 39, no. 2: 240 – 248.

Maskall, J. E., and Thornton, I. 1998. Chemical partitioning of heavy metals in soils, clays and rocks at historical lead smelting sites. Water, Air Soil Pollut. 108, 391–409.

Mazor, E. 1991. Chemical and Isotopic Groundwater Hydrology, 2nd edn. Marcel Dekker, New York.

Mazor, E. 2004. Chemical and Isotopic Groundwater Hydrology, 3rd edn. Marcel Dekker, New York.

McBride, M.B. 1994. Environmental chemistry of soils, Oxford University Press, Inc., New York.

Mcgrath, S. P. 1995. Nickel. In Heavy Metals in Soils (2nd edn.) (ed. Alloway, B.J). London: Blackie Academic and Professional.

Merlivat, L. and Jouzel, J. 1979. Global climatic interpretation of the deuterium – oxygen – 18 relationships for precipitation. J. Geophysi. Res., 84, 5029–5033.

Mook, W. G., Klaus, F., and Rozanski, K. 2000. Environmental Isotopes in the Hydrological Cycle Principles and Applications. International Hydrological Programme. 1 Technical Documents in Hydrology No. 39, Vol. III.

Nayaka, S.B.M. Ramakrishna, S. Jayaprakash and Delvi, M.R. (2009). Impact of heavy metals on water, fish (Cyprinus carpio) and sediments from a water tank at Tumkur, India, Oceanol. Hydrobiol. Stud., 38(2): 17-28

Newman, B.D., Campell, R.A., and Wilcox, B.P. 1997. Tracer – based studies of soil water movement in semi – arid forest of New Mexico. Journal of Hydrology 196 (1997) 251 – 270.

Nielsen, DR., van Genuchten, MTh, Biggar, J.W.1986. Water flow and solute transport processes in the unsaturated zone. Water Resour Res 22(9):89–108

Nimmo, J.R., Deason, J.A., Izbicki, J.A., and Martin, P. 2002. Evaluation of unsaturated zone water fluxes in heterogeneous alluvium at a Mojave Basin site, Water Resour. Res,. 38, 10 (2002).

Pavelic, P., Dillon, P.J., Narayan, K.A., Herrmann, T.N., and Barnett, S.R. 1997. Integrated groundwater flow and agronomic modelling for management of dryland salinity of a coastal plain in southern Australia. Agricultural Water Management 35, 75-93.

Phillips, F. M., Mattick, J. L., and Duval, T. A. 1988. Chlorine 36 and tritiumfrom nuclear weapons fallout as tracers for long – term liquid movement indesert soils. Water Resource. Res., 24: 1877-1891

Qayyum, M.A. and Kemper, W.D. 1962. Salt – concentration gradients in soils and their effects on moisture movement and evaporation. Soil Science 93: 333–324.

Rengasamy, P. 2006. World salinization with emphasis on Australia. *Journal of Experimental Botany* **57**(5), 1017-1023.

Reynolds, R.L., Yount, J.C., Reheis, M., Goldstein, H., Chavez P. Jr., Fulton, R., Whitney, J., Fuller, C., and Forester, R.M. 2007. Dust emission from wet and dry playas in the Mojave Desert, USA. Earth Surface Processes and Landforms 32: 1811–1827.

Rose, D.A., Konukcu, F., and Gowing, J.W. 2005. Effect of water-table depth on evaporation and salt accumulation from saline ground water. Australian Journal of Soil Research 43: 565–573.

Rozanski, K.,Araguas – Araguas, L. and Gonfiantini, R. 1993. Isotopic patterns in modern global precipitation. In: Climate Change in Continental Isotopic Records, Geophysical Monograph 78, American Geophysical Union, 1–36.

Sadiq, M. 1997. Arsenic chemistry in soils: an overview of thermodynamic predictions and field observations. Water, Air and Soil Pollution, 93, 117-136.

Salama, R.B., Otto, C.J., and Fitzpatrick, R.W. 1999. Contributions of groundwater conditions to soil and water salinization. Hydrogeology Journal 7: 46–64.

Saravanapavan, T., and Saluvucci, G.D. 2000. Analysis of rate – limiting processes in soil evaporation with implications for soil resistance models. Adv. Water. Resour., 23:493-502.

Scanlon, B.R. 1991. Evaluation of moisture flux from chloride data in desert soils. J. Hydrol., 128: 137-156.

Scanlon, B. R., Jolly, I., Sophocleous, M., and Zhang, L. 2007. Global impacts of conversions from natural to agricultural ecosystems on water resources: Quantity versus quality. WATER Resources Research, VOL. 43, W03437, doi:10.1029/2006WR005486.

Sharma, M. L., and Hughes, M. W., 1985. Groundwater recharge estimation using chloride, deuterium and oxygen – 18 profiles in the deep coastal sands of western Australia. J. Hydrol., 81: 93-109.

Shimojima E., Yoshioka R. and Tamagawa, I. 1996. Salinization owing to evaporation from bare-soil surfaces and its influences on the evaporation. Journal of Hydrology 178: 109–136.

Strobel, B.W. (2004): Influence of humic substances on phosphate adsorption by aluminium and iron oxides. Geoderma 127: 270– 279.

Szabolcs, I. 1994. Soils and salinization. Handbook of Plant and Crop stress. M Pessarakli. New
York, Marcel Dekker**:** 3-11.

Tanji , K.K. 1990. Nature and extent of agriculture salinity. Agricultural salinity assessment and management, Manual and Report on Engineering Practice. KK Tanji. New York, American Society of Civil Engineers**:** 1-17

Tyler, G., and Olsson, T. 2001. Concentration of 60 elements in the soil solution as related to the soil acidity. Eur. J. Soil Sci. 52, 151–165.

van Weert, F., van der Gun, J. and Reckman, J. 2009. Global overview of saline groundwater occurrence and genesis. International groundwater resources assessment centre. Report nr. GP 2009-1.

Vengosh, A. 2003. Salinization and Saline Environments. Treatise on Geochemistry, Volume 9. Elsevier, p.333-365.

Walker, G.R., Hughes, M.W., Allison, G.B., and Barnes, C.J. 1988. The movement of isotopes of water during evaporation from a bare soil surface. J Hydrol 97:181–197

Walworth, J. L. 2006. Salinity Management and Soil Amendments for Southwestern Pecan Orchards. Arizona cooperative Extension. www.cals.arizona.edu/pubs.

Wehrli, B., and Stumm, W. 1989. Vanadyl in Natural-Waters - Adsorption and Hydrolysis Promote Oxygenation. Geochimica Et Cosmochimica Acta, 53(1), 69-77.

White, D. E., Hem, J. D. and Waring, G. A.1963. Chemical composition of subsurface waters, in Data of geochemistry (6th ed.): U.S. Geological Survey Professional Paper 440 – F, p. Fl – F67.

Windhorst, D., Waltz T., Frede, H.G., and Breuer, L. 2012. Impact of elevation and weather patterns on the isotopic composition of precipitation in a tropical montane rainforest. Hydrol. Earth Syst. Sci. Discuss., 9, 8425–8453, 2012

YongQin CUI, Jian, M.A.Y., and Sun W. 2011. Application of stable isotope techniques to the study of soil salinization. Journal of Arid Land. Science press doi: 10.3724/SP.J.1227.2011.00285

Young C, Wallender W, Schoups G, Fogg G, Hanson B, Harter T, Hopmans J, Howitt R, Hsiao T, Panday S, Tanji K, Ustin S, and Ward K (2007). Modelling shallow water table evaporation in irrigated regions. Irrig. Drain. Syst., 21: 119-132.

Zimerman, U., Ehhalt, D., and Munnich, K.O. 1967. Soil – water and evapotranspiration: changes in the isotopic composition of the water. IAEA Symposium. Isotope. Hydrology., IAEA, Viema, pp. 567-584.

Appendix I: Trace element concentration in soil along the profiles in the unsaturated zone

		Concentration in (mg/kg dry mass)										
Profiles	Depth/cm	As	Fe	Mn	Cu	Pb	Zn	Cr	V	Cd	Ni	Co
	20.0	75.91	164.03	49.61	3.96	4.32	1.17	110.15	1.55	0.16	27.09	1.77
P1	40.0	70.92	167.09	61.49	5.35	8.53	1.40	111.78	1.91	0.09	34.37	2.61
	60.0	53.16	168.53	54.51	5.32	0.17	1.35	109.36	2.05	0.40	31.73	2.26
	20.0	38.77	164.97	48.52	5.35	<0.001	1.63	71.96	1.89	0.44	30.19	2.20
P2	40.0	43.67	164.09	57.44	5.53	<0.001	1.69	108.94	1.93	0.33	29.81	1.72
	60.0	26.52	166.54	60.21	4.92	1.053	1.47	120.33	1.84	<0.002	28.85	1.48
	80.0	54.67	170.41	58.47	3.93	1.147	1.51	88.64	0.25	0.05	28.39	1.35
	20.0	27.68	170.31	59.23	4.29	2.05	1.52	102.72	1.83	<0.002	28.72	1.00
P3	40.0	38.62	169.37	51.04	4.27	2.65	1.57	108.48	1.96	<0.002	29.72	1.05
	60.0	52.96	168.98	56.25	4.23	2.11	1.40	101.42	2.12	<0.002	26.80	2.11
	20.0	41.16	162.15	2.12	5.27	<0.001	0.17	18.28	0.20	<0.002	33.35	0.63
P4	40.0	78.03	42.27	42.87	4.76	<0.001	0.76	22.72	1.21	0.13	7.51	3.45
	60.0	58.89	158.90	28.31	0.16	<0.001	0.69	27.97	1.52	0.40	8.83	2.59

Appendix I: Trace element concentration in soil along the profiles in the unsaturated zone, contd.

		Concentrations of Trace Metals in soil (mg/kg dry mass)										
Profiles	Depth/cm	As	Fe	Mn	Cu	Pb	Zn	Cr	V	Cd	Ni	Co
	80.0	60.12	158.84	29.71	2.01	<0.001	0.51	18.49	1.33	0.08	8.41	2.19
	100.0	45.64	159.77	18.88	3.39	<0.001	1.53	39.12	1.88	0.11	15.49	2.32
P4	120.0	30.09	165.51	25.33	3.20	<0.001	0.89	57.84	1.27	<0.002	9.03	2.76
	140.0	64.04	154.67	29.69	4.17	<0.001	1.51	44.93	1.69	<0.002	12.09	2.73
	160.0	78.48	109.67	20.44	2.04	0.79	1.96	31.78	2.23	<0.002	12.00	2.47
	180.0	74.84	13.92	30.15	3.72	0.40	1.92	30.34	2.21	0.21	12.09	3.24
	200.0	91.72	155.39	34.81	4.81	<0.001	1.85	27.26	2.16	<0.002	12.25	2.81
	20.0	84.97	57.68	16.09	4.13	<0.001	0.38	21.46	0.80	<0.002	6.05	1.37
P5	40.0	71.73	66.14	33.39	1.89	<0.001	0.60	22.25	1.11	<0.002	7.21	2.75
	60.0	33.2	162.01	38.92	2.44	<0.001	1.03	28.53	1.24	0.2267	7.79	1.81
	20.0	33.97	60.16	18.75	2.84	<0.001	0.53	36.56	8.80	0.04	5.55	1.25
	40.0	45.09	15.24	25.03	1.53	<0.001	0.49	32.99	0.95	<0.002	7.47	1.79
P6	60.0	60.19	156.97	33.56	3.25	<0.001	0.99	36.84	1.27	<0.002	9.21	1.75
	80.0	30.84	158.79	48.43	1.68	<0.001	0.96	49.76	1.29	<0.002	10.11	2.32

Appendix I: Trace element concentration in soil along the profiles in the unsaturated zone, contd.

Profiles	Depth/cm	Concentrations of Trace Metals in soil (mg/kg dry mass)										
		As	Fe	Mn	Cu	Pb	Zn	Cr	V	Cd	Ni	Co
	100.0	48.99	158.53	46.28	2.79	<0.001	0.99	34.70	1.37	<0.002	10.49	2.16
	120.0	57.05	195.62	22.44	2.92	<0.001	1.08	43.21	1.37	<0.002	9.03	2.36
P6	140.0	69.36	162.20	10.16	3.20	0.667	1.55	22.86	1.77	<0.002	10.59	2.41
	160.0	93.00	165.88	12.44	4.52	<0.001	1.93	25.13	1.97	0.04	10.80	2.12
	20.0	86.35	164.40	27.92	1.81	<0.001	2.00	7.62	1.24	0.12	6.4	1.85
	40.0	79.20	167.67	44.51	4.24	<0.001	1.89	14.17	1.75	<0.002	8.91	2.05
P7	60.0	71.72	162.73	40.72	3.99	<0.001	1.37	18.54	1.73	<0.002	7.64	1.79
	80.0	73.39	159.69	41.72	3.88	<0.001	1.49	17.38	1.71	<0.002	6.65	1.68
	100.0	55.85	158.73	39.87	3.00	<0.001	1.15	8.73	1.52	<0.002	5.68	3.00
	120.0	77.85	157.69	53.91	3.47	<0.001	1.12	12.36	1.23	<0.002	5.53	3.17
	140.0	103.95	159.50	30.00	2.73	<0.001	1.13	7.02	1.25	<0.002	4.92	2.65
	160.0	106.61	162.28	18.53	2.96	<0.001	1.03	16.31	1.11	<0.002	4.52	1.76
	180.0	118.96	165.88	27.91	2.73	<0.001	0.67	17.89	0.99	<0.002	3.83	1.33

Appendix I: Trace element concentration in soil along the profiles in the unsaturated zone, contd.

		Concentrations of Trace Metals in soil (mg/kg dry mass)										
Profiles	Depth/cm	As	Fe	Mn	Cu	Pb	Zn	Cr	V	Cd	Ni	Co
	20.0	132.60	162.00	41.83	3.40	<0.001	1.53	16.03	1.13	0.16	6.72	1.97
	40.0	12.95	162.34	76.46	5.23	<0.001	1.07	17.79	1.59	<0.002	8.61	2.59
P8	60.0	58.80	163.67	44.16	3.75	<0.01	1.37	19.47	2.00	<0.002	8.72	2.00
	80.0	67.05	159.66	71.31	0.09	<0.001	0.12	12.22	<0.010	<0.002	2.29	0.76
	100.0	5.52	152.88	59.17	4.29	<0.001	1.07	4.46	1.45	<0.002	4.68	2.01
	120.0	<0.001	151.95	48.71	2.16	<0.001	1.23	5.48	1.31	0.21	5.03	1.45
	140.0	<0.001	160.40	31.60	3.31	<0.001	1.41	10.55	1.23	0.43	5.27	0.88
	160.0	<0.001	161.91	31.31	4.88	<0.001	1.15	12.27	1.37	0.52	4.95	1.68
	20.0	31.17	157.57	3.05	0.23	<0.00	0.05	18.82	<0.001	0.40	0.25	0.27
	40.0	135.08	154.46	54.96	4.17	<0.001	1.23	5.06	1.24	0.41	4.96	1.57
P9	60.0	167.33	155.03	33.84	3.79	<0.001	1.32	9.71	1.56	0.20	6.51	1.31
	80.0	146.64	82.40	28.61	3.75	<0.001	1.48	11.48	1.67	0.20	8.44	2.08
	100.0	142.61	156.44	48.64	5.56	<0.001	1.07	10.50	1.69	0.11	5.57	2.43

Appendix II: Major ion concentration in the soil along the profiles in the unsaturated zone

		Major ions concentration of in soil (mg/kg dry mass)								
Profiles	Depth/cm	Na^+	K^+	Ca^{2+}	Mg^{2+}	Cl^-	SO_4^{2-}	NO_3^-	PO_4^{2+}	HCO_3^-
	20.0	332	484	561.12	10.60	24.99	183.52	3.01	0.54	975.35
P1	40.0	232	38	400.80	28.60	249.92	20.48	0.48	1.58	975.35
	60.0	208	22	32.64	87.60	99.9.7	35.42	0.36	1.70	1463.02
	20.0	554	344	240.48	101.52	49.99	1221.49	2.06	1.24	1950.69
P2	40.0	358	246	200.00	101.00	49.99	2841.75	0.26	0.77	2072.61
	60.0	560	164	280.56	56.80	49.99	2734.15	0.71	1.08	2682.20
	80.0	888	144	400.80	42.80	24.99	911.37	1.74	0.77	1706.85
	20.0	508	484	400.80	21.80	99.97	72.76	1.58	4.34	2438.36
P3	20.0	430	294	320.64	11.80	89.99	221.49	0.38	0.77	1463.02
	60.0	392	146	160.32	39.20	99.97	126.56	0.59	0.30	1463.02
	20.0	542	482	240.48	65.8	49.99	47.44	1.16	0.03	1706.85
P4	40.0	728	90	721.44	19.6	49.99	94.91	0.28	1.31	1463.02
	60.0	768	80	320.64	16.6	49.99	518.96	4.82	2.48	1706.85
	80.0	918	262	480.96	19.2	99.97	499.98	2.33	8.77	1463.02

Appendix II: Major ion concentration in the soil along the profiles in the unsaturated zone, Contd.

		Major ions concentration of in soil (mg/kg dry mass)								
Profiles	Depth/cm	Na^+	K^+	Ca^{2+}	Mg^{2+}	Cl^-	SO_4^{2-}	NO_3^-	PO_4^{2+}	HCO_3^-
	100.0	1778	18	561.12	63.8	149.95	2588.58	0.80	38.74	1463.02
	120.0	3940	12	480.96	22.8	149.95	215.47	0.53	1.39	1463.2
P4	140.0	3360	28	400.8	38.0	49.99	183.52	1.82	1.00	2438.36
	160.0	8720	20	480.96	62.6	299.90	291.91	0.39	0.62	1219.18
	180.0	12820	40	240.48	20.4	449.86	36.56	0.62	1.47	1463.02
	200.0	13080	2	240.48	18.6	399.88	113.90	2.21	0.54	1463.02
	20.0	494	162	100.2	48.2	49.99	107.57	0.29	1.39	2438.36
P5	40.0	378	104	240.48	18.4	49.99	620.23	5.68	2.56	2682.20
	60.0	486	118	240.48	14	49.99	734.15	6.83	3.18	2926.04
	20.0	324	152	320.64	47.40	49.99	132.89	0.42	1.39	2194.53
	40.0	448	68	240.48	35.40	99.97	94.91	3.27	1.31	1950.69
P6	60.0	506	164	160.32	12.00	49.99	835.42	3.41	2.94	1219.18
	80.0	554	218	240.48	51.20	99.97	297.44	10.80	5.20	1463.02
	100.0	910	220	160.32	52.00	49.99	202.51	12.13	11.45	2194.53

Appendix II: Major ion concentration in the soil along the profiles in the unsaturated zone, Contd.

		Major ions concentration of in soil (mg/kg dry mass)								
Profiles	Depth/cm	Na^+	K^+	Ca^{2+}	Mg^{2+}	Cl^-	SO_4^{2-}	NO_3^-	PO_4^{2+}	HCO_3^-
	120.0	1678	442	400.80	127.42	199.94	1727.82	17.02	22.98	1950.69
P6	140.0	6620	160	320.64	119.81	249.92	240.48	1.91	1.91	975.35
	160.0	862	38	240.48	83.2	249.92	2120.23	1.08	4.26	1219.18
	20.0	362	318	240.48	39.60	49.99	159.24	5.64	0.69	1950.69
	40.0	420	80	400.80	28.40	49.99	2183.52	5.46	0.77	1950.69
P7	60.0	622	544	320.64	100.80	49.99	980.52	9.94	16.61	2682.20
	80.0	644	578	240.68	27.60	99.97	702.51	4.74	16.99	3169.87
	100.0	738	544	320.64	11.60	99.97	632.89	13.89	10.94	2438.36
	120.0	870	972	320.64	30.60	49.99	5310.10	16.90	11.64	1706.85
	140.0	1048	1244	400.80	113.84	99.97	936.68	9.55	19.40	1950.69
	160.0	1268	286	400.80	6.00	49.99	1462.00	3.07	3.81	1219.18
	170.0	1286	1080	400.80	9.00	49.99	1006.30	9.72	14.36	1950.69

Appendix II: Major ion concentration in the soil along the profiles in the unsaturated zone, Contd.

		Major ions concentration of in soil (mg/kg dry mass)								
Profiles	Depth/cm	Na^+	K^+	Ca^{2+}	Mg^{2+}	Cl^-	SO_4^{2-}	NO_3^-	PO_4^{2+}	HCO_3^-
	20.0	846	276	360.72	31.80	49.99	24.66	0.69	12.65	1706.85
	40.0	410	308	440.88	22.80	49.99	1848.08	9.55	3.64	975.35
	60.0	552	982	400.80	12.00	49.99	2898.71	13.09	14.67	2194.53
	80.0	586	1098	320.48	20.20	49.99	1696.18	2.97	19.56	1950.69
P8	100.0	558	406	240.78	39.60	49.99	575.92	15.08	10.48	1950.69
	120.0	850	1004	240.48	155.30	99.97	1626.56	18.23	13.66	1463.02
	140.0	1038	1064	400.80	37.80	49.99	1784.78	19.05	14.98	1706.85
	160.0	1304	1226	320.64	22.40	49.99	936.68	11.56	16.45	2438.36
	20.0	852.00	306.00	160.32	14.80	49.99	227.82	0.43	1.55	1463.02
	40.0	608.00	838.00	320.64	44.20	49.99	3025.29	16.72	13.81	2194.53
P9	60.0	436.00	358.00	480.96	18.40	99.97	2088.58	10.12	10.48	1463.02
	80.0	388.00	364.00	400.80	23.20	49.99	3360.73	17.35	5.18	1706.85
	100.0	846.00	822.00	240.48	24.40	49.99	1791.11	18.23	12.18	1219.18

Appendix III: Moisture content (MC), Bulk density (Bd), Electrical conductivity (EC), Salinity (Sal), Total dissolve solids (TDS), pH and electrical potential (Eh) along the soil profiles

Profiles	Depth	MC	Bd	EC	Sal	TDS	pH	Eh	Porosity
	cm	%	(gcm^{-3})	(µS/cm)	(‰)	(mg/L)		mV	
	20.0	21.41	1.14	287.0	1.2	143.7	6.9	7.9	0.57
P1	40.0	21.45	1.17	160.3	0.9	80.1	6.9	7.3	0.56
	60.0	21.42	1.12	176.3	1.0	88.1	6.7	20.4	0.58
	20.0	24.98	1.17	529.0	1.5	264.0	6.0	58.0	0.56
P2	40.0	20.43	1.17	447.0	1.2	223.0	6.5	28.7	0.56
	60.0	21.40	1.06	596.0	1.3	298.0	6.5	28.6	0.60
	80.0	20.07	1.05	677.0	1.2	339.0	6.8	6.9	0.60
	20.0	15.47	1.14	1001.0	1.9	500.0	6.4	33.9	0.57
P3	40.0	15.51	1.16	562.0	1.6	281.0	6.6	22.9	0.56
	60.0	15.41	1.13	519.0	1.5	259.0	6.8	22.0	0.57
	20.0	13.58	1.10	249.0	1.5	124.7	6.0	57.7	0.59
P4	40.0	15.28	1.14	145.9	1.4	72.6	5.8	69.9	0.57
	60.0	16.11	1.19	106.0	1.2	53.0	6.0	61.7	0.55

Appendix III: Moisture content (MC), Bulk density (Bd), Electrical conductivity (EC), Salinity (Sal), Total dissolve solids (TDS), pH and electrical potential (Eh) along the soil profiles, contd.

Profiles	Depth	MC	Bd	EC	Sal	TDS	pH	Eh	Porosity
	cm	%	(gcm^{-3})	(µS/cm)	(‰)	(mg/L)		mV	
	80.0	19.04	1.23	113.6	1.3	56.8	6.4	35.1	0.54
	100.0	17.73	1.02	185.0	1.1	92.5	6.9	4.2	0.62
P4	120.0	14.45	1.01	343.0	1.5	171.5	6.7	16.2	0.62
	140.0	16.14	1.02	308.0	1.6	153.9	6.6	21.5	0.62
	160.0	15.97	1.08	821.0	1.8	410.0	6.5	28.9	0.59
	180.0	15.45	1.03	1276.0	1.9	636.0	6.4	37.3	0.61
	200.0	16.30	1.01	1137.0	2	569.0	6.5	31.1	0.62
	20.0	17.33	1.22	147.0	0.9	73.5	5.3	101.7	0.54
P5	40.0	17.35	1.19	42.7	0.8	21.3	6.1	56.3	0.55
	60.0	17.32	1.21	35.1	0.5	17.6	6.3	40.7	0.54
	20.0	9.64	1.14	165.7	1.3	82.9	5.9	63.5	0.57
P6	40.0	8.91	1.09	86.2	0.5	43.1	6.0	59.0	0.59
	60.0	10.74	1.13	60.4	0.3	30.2	6.1	51.4	0.60
	80.0	9.53	1.06	48.8	0.2	24.4	6.4	33.2	0.59

Appendix III: Moisture content (MC), Bulk density (Bd), Electrical conductivity (EC), Salinity (Sal), Total dissolve solids (TDS), pH and electrical potential (Eh) along the soil profiles, contd.

Profiles	Depth	MC	Bd	EC	Sal	TDS	pH	Eh	Porosity
	cm	%	(gcm^{-3})	(µS/cm)	(‰)	(mg/L)		mV	
	100.0	10.57	1.10	70.9	0.6	35.5	6.6	25.7	0.58
	120.0	11.48	1.11	18.4	1.2	69.2	7.0	-1.2	0.58
P6	140.0	10.98	1.11	740.0	1.4	370.0	7.0	-0.1	0.58
	160.0	10.13	1.11	843.0	1.6	421.0	6.9	5.8	0.58
	20.0	18.74	1.05	242.0	1.6	121.4	6.1	51.9	0.60
	40.0	23.43	1.34	76.3	1.3	38.2	6.3	43.7	0.49
P7	60.0	23.52	1.33	43.4	0.9	21.6	6.6	23.7	0.50
	80.0	21.99	1.34	69.4	0.6	34.7	6.2	47.1	0.49
	100.0	20.04	1.33	48.9	0.7	24.5	6.5	32.4	0.50
	120.0	15.24	1.33	52.9.0	0.5	26.5	6.5	28.1	0.51
	140.0	18.99	1.29	70.1	0.8	34.2	6.5	27.3	0.53
	160.0	13.25	1.24	138.0	1.1	69.3	6.2	47.5	0.55
	180.0	12.65	1.19	69.4	0.8	34.6	6.7	18.8	0.56

Appendix III: Moisture content (MC), Bulk density (Bd), Electrical conductivity (EC), Salinity (Sal), Total dissolve solids (TDS), pH and electrical potential (Eh) along the soil profiles, contd.

Profiles	Depth	MC	Bd	EC	Sal	TDS	pH	Eh	Porosity
	cm	%	(gcm^{-3})	(µS/cm)	(‰)	(mg/L)		mV	
	20.0	25.0	1.32	241.0	1.6	120.3	6.4	33.3	0.50
	40.0	26.9	1.33	69.9	1.1	30.5	6.6	21.4	0.50
	60.0	25.47	1.27	39.8	1.0	19.9	6.7	19.6	0.52
	80.0	20.77	1.27	37.8	0.8	18.9	6.7	16.3	0.52
P8	100.0	20.05	1.25	43.0	0.9	21.5	6.8	13.3	0.53
	120.0	20.05	1.25	51.1	1.0	25.5	6.8	12.8	0.53
	140.0	17.78	1.24	49.6	0.8	24.8	6.8	13.0	0.53
	160.0	17.07	1.10	82.6	0.7	41.3	6.7	20.3	0.59
	20.0	17.62	1.23	231.0	1.9	115.7	6.4	20.5	0.54
	40.0	17.65	1.24	46.4	0.8	23.2	6.9	5.9	0.53
P9	60.0	17.64	1.23	43.2	0.6	21.6	6.5	28.9	0.54
	80.0	17.63	1.22	64.6	0.7	32.4	6.1	52.7	0.54
	100.0	17.61	1.21	57.8	0.8	28.9	6.7	19.9	0.54

Appendix IV: Soil characteristics with depth – wise

Profiles	Depth/cm	Soil Texture	Profiles	Depth/cm	Soil Texture
	20.0	Greyish loose soil		80.0	Greyish clayey soil
P1	40.0	Greyish clayey soil		100.0	Greyish clayey soil
	60.0	Greyish clayey soil and pebbles	P4	120.0	Yellowish moist sandy soil
				140.0	Yellowish moist sandy soil
	20.0	Greyish loose soil		160.0	Yellowish moist sandy soil
P2	40.0	Greyish clayey soil		180.0	Yellowish clayey soil (partly sandy and lateritic)
	60.0	Greyish clayey soil		200.0	Yellowish soil partly clayey
	80.0	Greyish clayey soil, Lateritic soil and rocky			
P3	20.0	Greyish lose soil		20.0	Greyish top soil
	40.0	Greyish lose soil	P5	40.0	Greyish moist sandy soil
	60.0	Greyish clayey soil, impermeable rock (pebbles)		60.0	Greyish clayey soil
	20.0	Greyish soil		20.0	Sandy soil
P4	40.0	Greyish moist sandy soil	P6	40.0	Sandy clayey soil
	60.0	Greyish clayey + sandy soil		60.0	Sandy clayey soil

Appendix IV: Soil characteristics with depth – wise contd.

Profiles	Depth/cm	Soil Texture	Profiles	Depth/cm	Soil Texture
	80.0	Yellowish clayey soil		20.0	Black agricultural soil
	100.0	Yellowish clayey soil		40.0	Sandy clayey soil
	120.0	Yellowish clayey soil		60.0	Sandy clayey soil
P6	140.0	Yellowish clay soil, partly rocky with gravels	P8	80.0	Clayey soil
	160.0	Yellowish clayey soil		100.0	Clayey soil
				120.0	Clayey soil
	20.0	Brownish sandy soil		140.0	Clayey soil + rocky
	40.0	Sandy clayey soil		160.0	Clayey soil +rocky
P7	60.0	Brownish clayey soil			
	80.0	Brownish clayey soil		20.0	Black agricultural soil
	100.0	Brownish clayey soil		40.0	Brownish clayey soil
	120.0	Rocky + brownish clayey soil	P9	60.0	Brownish clayey soil
	140.0	Brownish clayey soil		80.0	Brownish clayey soil
	160.0	Brownish clayey soil and lateritic		100.0	Brownish clayey soil
	180.0	Brownish clayey soil and lateritic			

Appendix V: Stable Isotopes composition of soil pore water

Profiles	Depth/cm	δ^2H‰	$\delta^{18}O$‰	Profiles	Depth/cm	δ^2H‰	$\delta^{18}O$‰	Profiles	Depth/cm	δ^2H‰	$\delta^{18}O$‰
	20.0	-6.08	2.95	P4	180.0	-24.35	-4.04	P7	120.0	- 22.56	-3.82
P2	40.0	-24.05	-3.06		200.0	-28.72	-5.02		140.0	- 25.81	-3.87
	60.0	-22.05	-3.52						160.0	- 23.67	-4.23
	80.0	-29.06	-4.61		20.0	- 10.27	0.04		180.0	- 28.45	-4.26
					40.0	- 19.23	-2.16				
	20.0	-15.67	-024	P6	60.0	- 23.05	-3.54		20.0	- 8.16	3.40
P3	40.0	- 30.2	-3.69		80.0	- 25.38	-3.64	P8	40.0	- 10.05	-0.12
	60.0	- 26.99	-3.82		100.0	- 23.47	-3.80		60.0	- 12.51	-1.45
					120.0	- 24.58	-4.17		80.0	- 16.20	-2.46
	20.0	- 10.91	1.04		140.0	- 25.83	-4.22		100.0	- 19.37	-2.95
	40.0	- 17.09	-2.50		160.0	- 24.87	-4.42		120.0	- 19.07	-3.00
P4	60.0	- 18.28	-2.58						140.0	- 21.48	-3.09
	80.0	- 20.19	-3.10		20.0	- 25.59	-2.66		160.0	- 24.94	-4.47
	100.0	- 23.51	-3.23		40.0	- 23.29	-3.43				
	120.0	- 22.20	-3.28	P7	60.0	- 24.05	-3.58				
	140.0	- 26.40	-3.92		80.0	- 24.63	-3.67				
	160.0	- 23.32	-3.96		100.0	- 20.33	-3.71				

Appendix VI: Concentrations of major ions in mg/L and stable isotopes (VSMOW) in water samples (groundwater and unsaturated zone)

Sample ID	Na^+	K^+	Ca^{2+}	Mg^{2+}	Cl^-	SO_4^{2-}	NO_3^-	PO_4^{2-}	HCO_3^-	δ^2H‰	$\delta^{18}O$‰
EABH	1845	55.5	93.00	204	4798.50	58.00	0.64	1.24	231.80	- 9.76	- 2.84
OREA	21.1	20.4	0.16	0.23	35.99	7.98	0.57	0.01	224.33	2.13	1.12
EAHDW	519.0	78.4	4.13	2.39	595.00	109.11	2.1	0.00	320.00	- 9.99	- 2.26
P2	15.0	8.0	80.16	0.73	4.00	75.06	1.17	0.96	165.81	- 16.15	- 2.29
P4	245.0	0.7	19.24	0.98	163.95	53.29	0.32	0.15	292.60	- 10.38	- 2.08
P6	285.0	7.0	12.83	1.14	219.93	88.99	0.42	1.02	273.10	- 15.01	- 2.30
P9	98.0	5.0	6.41	0.61	23.99	62.86	0.61	0.79	146.30	- 12.03	- 2.06
P8	90.1	0.1	9.62	0.21	31.99	28.86	0.72	0.42	146.30	- 9.05	- 2.67
P7	98.8	2.2	6.41	0.40	47.99	40.00	0.84	0.11	121.92	- 9.82	- 2.36

EABH = Ekumfi Akwakrom Borehole

EAHDW = Ekumfi Asokwa hand dug well

OREA = Osumpunu river Ekumfi Abeka

P2, P4, P6, P7, P8, P9 are the piezometers

Appendix VII: Distribution of sampling intervals, mean rainfall, GPS locations and mean recharge rate in the study area

Profiles	Sampling Interval (cm)	No. of samples (n)	Mean rainfall (mm year^{-1})	Mean Cl in profile (mg/L)	Mean recharge (mm year^{-1})	GPS Locations		
						North (N ^{o})	West (W ^{o})	Elevation (ASL)
P1	0.0 – 60.0	3	23.21	5.83	44.16	5.26233 ^{o}	0.97958 ^{o}	24
P2	0.0 – 80.0	4	23.21	2.01	127.89	5.26230 ^{o}	0.97978 ^{o}	24
P3	0.0 – 60.0	3	23.21	6.25	41.21	5.26228 ^{o}	0.97980 ^{o}	24
P4	0.0 – 200.0	10	23.21	10.47	24.59	5.26134 ^{o}	0.98098 ^{o}	20
P5	0.0 – 60.0	3	23.21	3.02	85.22	5.26132 ^{o}	0.98102 ^{o}	20
P6	0.0 – 160.0	8	23.21	12.80	20.11	5.26133 ^{o}	0.98103 ^{o}	20
P7	0.0 – 180.0	9	23.21	3.57	72.07	5.26111 ^{o}	0.98325 ^{o}	14
P8	0.0 – 160.0	8	23.21	2.60	99.09	5.26109 ^{o}	0.98323 ^{o}	14
P9	0.0 – 100.0	5	23.21	3.40	75.69	5.26118 ^{o}	0.98330 ^{o}	14

Ion concentrations are also expressed as mg/L of pore water (mg/kg divided by gravimetric water content and multiplied by water density)
mg/L = $\frac{mg/kg}{\theta}\rho$, ρ is the density of water Mg/cm^{-3}, θ is the water content
The mean annual Cl in the rain water is 11.10 mg/L

ASL = Above sea level

Appendix VIII: Physical parameters and trace element in the piezometric water and ground water

Sample ID	EC (µS/cm)	TDS (mg/L)	pH	Eh (mV)	T (°C)	Fe	Mn	Cu	As	Ni	Cr
EABH	17000.0	8490	6.15	55.3	25.4	3.144	0.060	0.056	0.264	0.060	<0.001
OREA	114.6	57.3	6.48	-10.0	24.7	0.960	0.048	0.048	0.264	0.030	0.044
EAHDW	1965.0	983	7.84	-36.6	25.6	0.348	0.128	0.064	0.264	0.112	0.056
P2	193.2	96.6	7.00	10.0	25.3	3.512	0.240	0.068	0.264	0.184	0.080
P4	694.0	347.0	7.02	-43.0	25.3	4.048	0.284	0.040	26.40	0.044	0.096
P6	987.5	494.0	7.00	-41.0	25.3	1.624	0.312	0.020	0.272	0.060	0.016
P9	277.0	133.6	6.69	-23.0	26.6	9.552	0.292	0.056	0.268	0.200	0.108
P8	226.0	113.0	6.73	-25.0	25.7	1.536	0.112	0.032	0.260	0.080	0.108
P7	272.5	136.0	6.73	-14.0	24.7	5.696	0.180	0.044	0.264	0.084	0.028

Appendix IX: Mean rainfall amount and Cl^- concentration in rainwater for the period 2010 – 2012 in the study area

Year	Mean rainfall amount mm/yr	Mean Cl^- in rainwater mg/L
2010	17.69	9.68
2011	33.55	7.54
2012	18.38	16.08

Appendix X

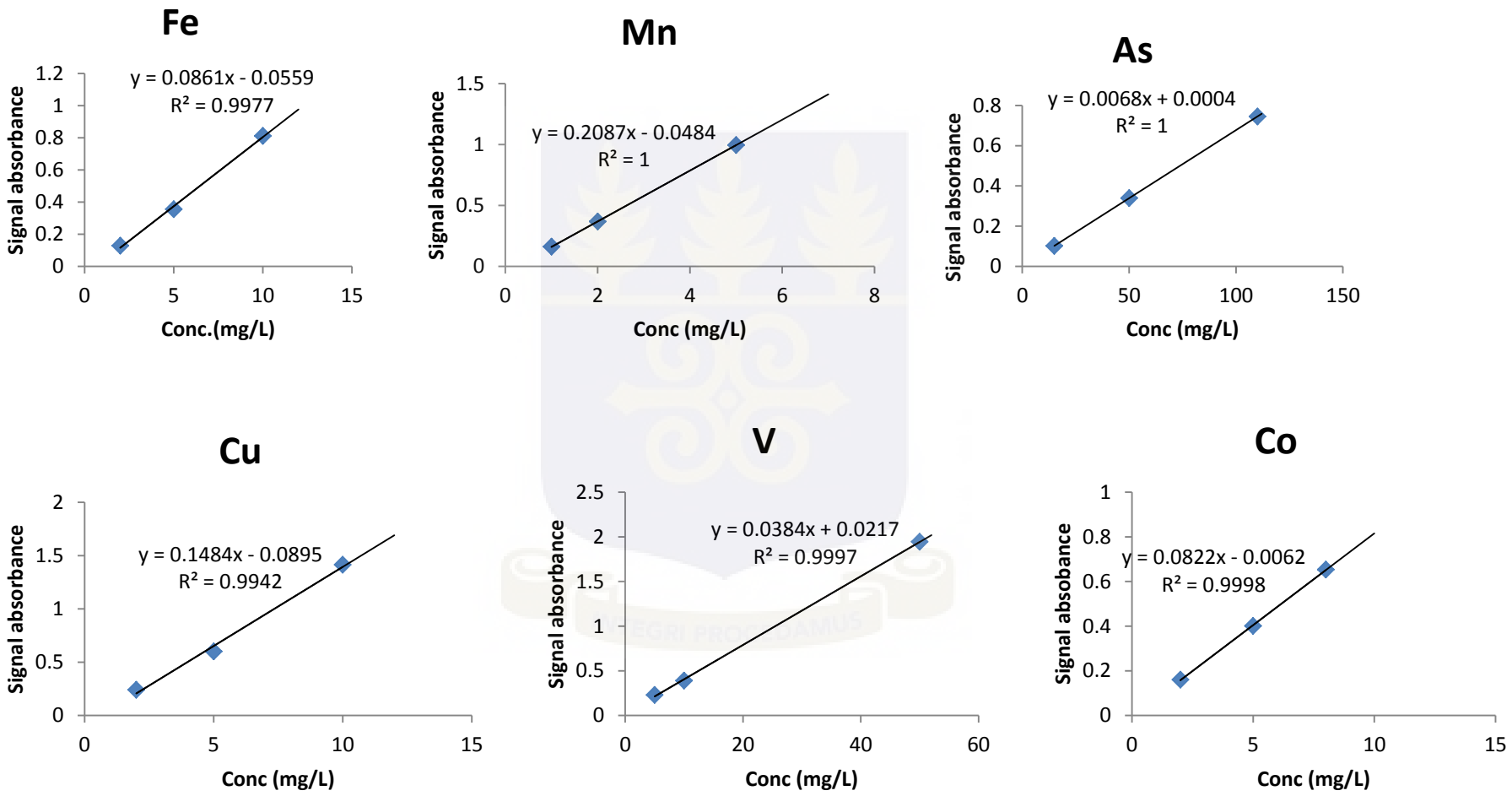

Rgression line for signal absorbance against element concentration of FAAS for trace elements: Fe, Mn, As, Cu, V and Co

Appendix X cont'd.

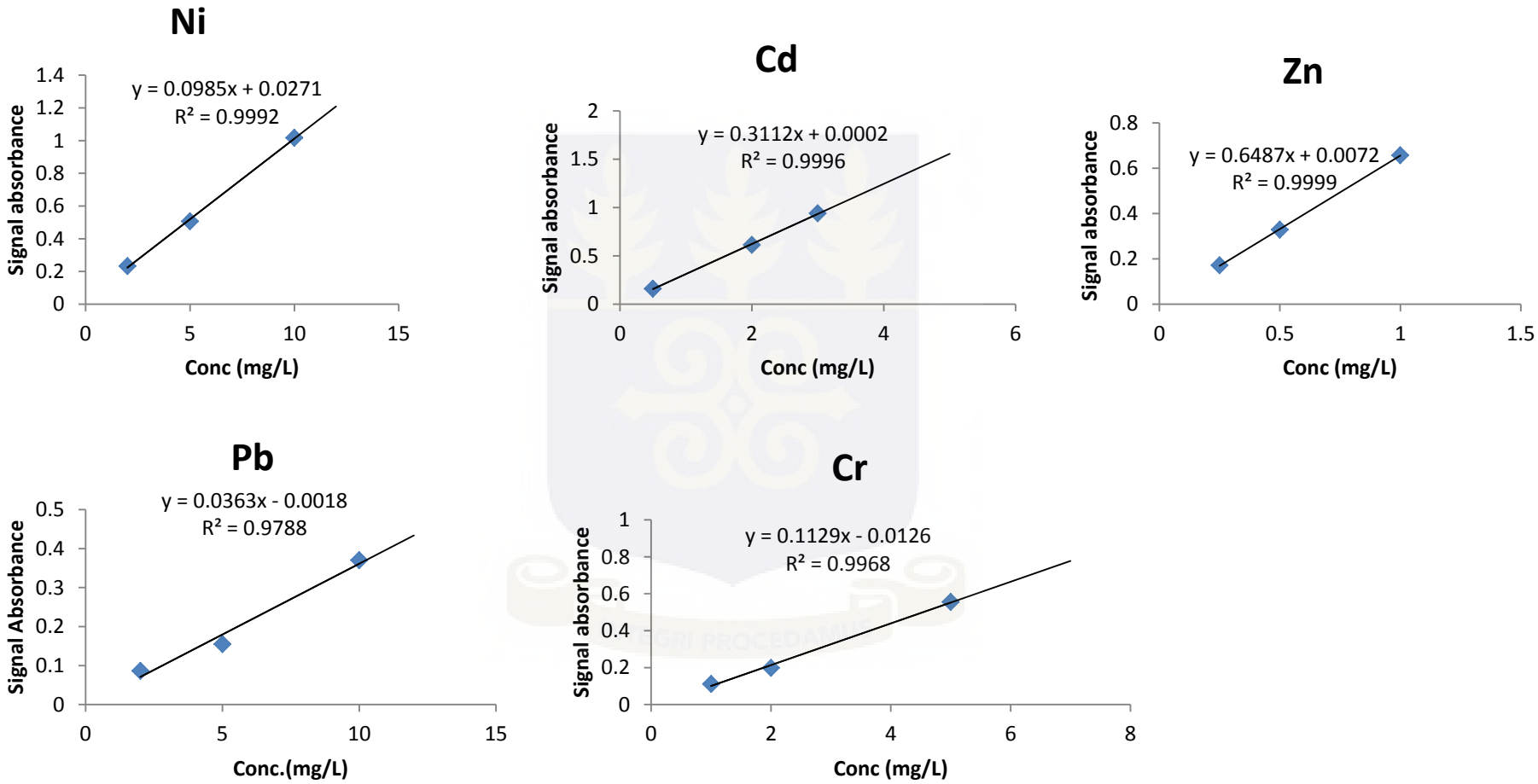

Rgression line for signal absorbance against element concentration of FAAS for trace elements: Ni, Cd, Zn, Pb and Cr